

Anna Ådnøy

An Expansion of *Aspergillus niger*'s Promoter Library

Promoter strength screening via CRISPR-Cas9-mediated genomic integration of luciferase expression constructs

Master's thesis in Chemical Engineering and Biotechnology

Supervisor: Dr.-Ing. Jochen Schmid

July 2020

Anna Ådnøy

An Expansion of *Aspergillus niger*'s Promoter Library

Promoter strength screening via CRISPR-Cas9-mediated genomic integration of luciferase expression constructs

Master's thesis in Chemical Engineering and Biotechnology
Supervisor: Dr.-Ing. Jochen Schmid
July 2020

Norwegian University of Science and Technology
Faculty of Natural Sciences
Department of Biotechnology and Food Science

Preface

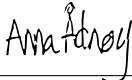
This master's thesis was carried out from February until July of 2020 as a collaboration between the Norwegian University of Science and Technology (NTNU) and the Technical University of Berlin. The two universities have since 2012 been official strategic partners, a prime example of global cooperation in the scientific community. As a student at NTNU's Faculty of Natural Sciences (NV), in the Department of Biotechnology and Food Science (IBT), I have been performing research for this thesis at TU Berlin's Institute for Biotechnology, in the Department of Applied and Molecular Microbiology (AMM). My exchange has in part been financed by the Erasmus+ Traineeship Program.

I would like to thank my main supervisor Dr.-Ing. Habil Jochen Schmid, working at NTNU, who supported my somewhat sudden choice to do research abroad, at what happened to be his alma mater. He has previously been a good teacher for me when learning laboratory techniques and considerations, and has been available digitally during my entire stay in Berlin. Further, I am very grateful to AMM's head of department Prof. Dr. Vera Meyer for being open to a foreign student coming into her lab. Her leadership and presence in the AMM group impresses me, especially in light of the special circumstances of the 2020 spring.

In guiding my research, my AMM advisors Dr.-Ing. Carsten Pohl and Dr.-Ing. Tabea Schütze have been invaluable. Thank you both so much for your patience with my experimental work and sometimes slow understanding, and for useful inputs and corrections to my writing. Also, many thanks to Tom Morris for added help in learning the MoClo system and my way around the AMM lab.

This research is part of a larger project titled "Mind the Fungi", where fungal biotechnology, bioprocess development and science communication come together thanks to a TU Berlin and Art Laboratory Berlin collaboration. As part of this project, a goal of being more able to perform genomic manipulations in the filamentous fungus *Fomes fomentarius* is being pursued, and my research into expanding the genetic toolbox for another filamentous fungus could in the end benefit this goal. Even though the direct links between my work and "Mind the Fungi" are not strong, it has been inspiring to take part in this project.

Due to the outbreak of COVID-19, the AMM laboratory facilities were closed to students for ten weeks. My research was halted in a very early phase, and the prospects of completing the project in time were uncertain, leading to a temporary shift in objective to a more literature-based thesis. In the end, I was able to resume experiments for a month, and therefore present my results here. They are slightly limited, but I think that the current alternative was the best solution to the given challenges.

Berlin	17.07.2020	
Place	Date	Signature, Anna Ådnøy

Abstract

Filamentous fungi are increasingly being exploited as industrial production organisms, and *Aspergillus niger* is currently the most significant and studied species among them. Natural products, including secondary metabolites and organic acids, can be collected in high-yield titers from these cellular biofactories. However, production of non-native compounds, such as high-value recombinant proteins, remains limited by an incomplete understanding of relevant cellular mechanisms as well as an underdeveloped genetic engineering toolbox. In order to optimize heterologous production in these hosts, a range of constitutive promoters with characterized strengths needs to be readily available. Therefore, this research aimed to expand the genetic toolbox of *A. niger* by augmenting the promoter library.

Here, 19 candidates for novel constitutive promoters were selected and cloned into convenient modules, before 4 of the putative promoter sequences were screened in a reporter assay. Using the MoClo method for cloning and CRISPR-Cas9 technology for genome editing, expression cassettes putting luciferase reporter genes under the control of alternate promoters were constructed and integrated in a pre-defined genomic locus. Bioluminescence was then monitored to quantify the enzyme activity of luciferase, which is expected to correspond to promoter strength. Also an alternative reporter, the fluorescent protein DsRed, was briefly tested for functionality in a pre-experiment. It was found that the luciferase assay was a reliable indicator of relative promoter strengths, showing the same results in two separate assays. Furthermore, these results were comparable to promoter strength predictions that were made based on a previously published meta-analysis of the *A. niger* transcriptome.

This research initiates a much-needed expansion of *A. niger's* promoter library. Although the four promoters that were studied here still require further analysis to complete their characterizations, and a greater quantity than these four constitutive promoters should still be added to the library, what was found here provides valuable starting ground for future research with similar objectives as this.

Sammendrag

Muggsopp utnyttet i økende grad som industrielle produksjonsorganismer, og *Aspergillus niger* er for tiden den mest betydningsfulle og studerte arten blant dem. Naturlige produkter, inkludert sekundære metabolitter og organiske syrer, produseres med høye utbytter og titere i disse cellulære biofabrikkene. Derimot er fremstilling av ikke-naturlige produkter, som rekombinante proteiner med høy verdi, begrenset på grunn av ufullstendige forståelser av de relevante celledynamikkene, samt en underutviklet verktøykasse for genteknologi (“genetic toolbox”). For å optimalisere heterolog produksjon i disse vertene, må det være tilgjengelig et utvalg av konstitutive promotorer med karakteriserte styrker. Derfor tok denne forskningen sikte på å ekspandere den genetiske verktøykassen til *A. niger* ved å utvide promotorbiblioteket.

Her ble 19 kandidater for nye konstitutive promotorer valgt ut og klonet inn i praktiske moduler, før 4 av de antatte promotorsekvensene ble studert ved hjelp av reporter-basert analyse. Ved å bruke MoClo-metoden til kloning og CRISPR-Cas9-teknologi til genomredigering, ble ekspresjonskassetter som plasserte luciferase-reportergenene under kontroll av varierende promotorer konstruert og integrert i et forhåndsdefinert genomisk lokus. Bioluminescens ble deretter overvåket for å kvantifisere enzymaktiviteten til luciferase, noe som forventes å svare til promotorens styrke. Også en alternativ reporter, det fluorescerende proteinet DsRed, ble testet for funksjonalitet i et pre-eksperiment. Det ble funnet at den luciferase-baserte analysen var en pålitelig indikator på relative promotorstyrker, fordi den viste de samme resultatene i to separate eksperimenter. Videre var disse resultatene sammenlignbare med forutsigelser om promotorstyrker, som ble gjort basert på en tidligere publisert meta-analyse av *A. niger*-transkriptom.

Denne forskningen har iverksatt en særdeles nødvendig utvidelse av *A. nigers* promotorbibliotek. Selv om de fire promotorene som ble studert her fortsatt krever ytterligere analyse for å bli fullstendig karakterisert, og flere enn disse fire konstitutive promotorene fortsatt bør legges til biblioteket, gir det som ble funnet her et verdifullt utgangspunkt for fremtidig forskning med lignende mål.

Abbreviations

AMA, autonomous maintenance in *Aspergillus*; bp, basepairs (of DNA); Cas, CRISPR-associated protein; CLSM, confocal laser scanning microscopy; CM, complete medium; CRISPR, clustered regularly interspaced repeats; DIC, differential interference contrast (microscopy); DSB, double-strand break; ER, endoplasmic reticulum; GFP, green fluorescent protein; GRAS, generally regarded as safe; HDR, homology-directed repair; HR, homologous recombination; HS, high-stringency; kb, kilobasepairs (of DNA); LB, lysogeny broth (medium); LCPS, luminescent counts per second; LS, low-stringency; MM, minimal medium; MoClo, modular cloning; MQ-H₂O, milli-Q purified water; NC, negative control; NHEJ, non-homologous end-joining; nt, nucleotides; OD, optical density; PAM, protospacer-adjacent motif; PC, positive control; PCR, polymerase chain reaction; PEG, polyethylene glycol (polymer); Pol, RNA polymerase; PS, physiological saline solution; qPCR, quantitative PCR; RNP, ribonucleoprotein; RT-qPCR, reverse transcription quantitative PCR; sgRNA, single guide RNA; SOC, super-optimal broth with catabolite repression (medium); SPdb, signal peptide database; TM, transformation medium; TMTC, too many to count (grown colonies); UTR, untranslated region; WT, wild-type.

Table of Contents

Preface	i
Abstract	iii
Sammendrag	v
Abbreviations	vii
1 Introduction	1
1.1 Background	1
1.1.1 Filamentous Fungi in Biotechnology	1
1.1.2 The Cellular Biofactory <i>Aspergillus niger</i>	2
1.1.3 Assaying Promoter Strengths	3
1.1.4 CRISPR-Cas Editing of Fungal Genomes	5
1.1.5 Modular Cloning - MoClo	8
1.2 Objectives	9
2 Materials and Methods	11
2.1 Strains, Media and Cultivation Conditions	11
2.2 Plasmid Construction by the MoClo System	11
2.2.1 Cloning Design	12
2.2.2 Part Synthesis	12
2.2.3 Golden Gate Assembly	12
2.2.4 Chemical <i>E. coli</i> Transformation	12
2.2.5 Diagnostic Colony PCR	13
2.2.6 Plasmid Isolation and Verification	13
2.2.7 Expanding a Collaborative MoClo Library	14
2.3 Working with <i>A. niger</i>	14
2.3.1 Preparation of Spore Suspensions	14
2.3.2 Extraction of Genomic DNA	14
2.3.3 Preparation of Protoplasts	14
2.3.4 PEG-Mediated Genetic Transformation	15
2.4 Screening of Genome-Edited <i>A. niger</i> Strains	15
2.4.1 Confirmation of Genomic Integration by Colony PCR	15
2.4.2 Copy Number Determination by Quantitative PCR	15
2.5 Microscopy	16
2.6 Luciferase Assay	16

3	Results	17
3.1	MoClo Plasmids	17
3.1.1	Promoter Modules	17
3.1.2	Plasmids for Expression of Fluorescent Proteins	17
3.1.3	Reporter Constructs for Promoter Assay	17
3.2	Localization Targeting of Fluorescent Proteins	18
3.2.1	Experimental Design	18
3.2.2	<i>A. niger</i> Transformation	18
3.2.3	Fluorescence Microscopy	18
3.3	CRISPR-Cas9 System Functionality	19
3.3.1	Experimental Design	19
3.3.2	<i>A. niger</i> Transformation and Editing Efficiency	20
3.4	Promoter Assay	21
3.4.1	Experimental Design	21
3.4.2	<i>A. niger</i> Transformation and Editing Efficiency	22
3.4.3	Luciferase Reporter Assay	24
4	Discussion	27
4.1	How the MoClo System Allowed for Expedited Research	27
4.2	Suitable Reporters for Promoter Assays in <i>A. niger</i>	28
4.3	Precise Genome Editing Using CRISPR-Cas9 Technology	32
4.4	An Expansion of <i>A. niger</i> 's Promoter Library	36
5	Conclusions	41
	Literature	43
	Appendices	47
A	Supplementary Tables	47
A.1	Primers	47
A.2	Promoters	49
A.3	Plasmids	50
A.4	PCR Products	52
A.5	Details of Transformation Experiments	52
B	Supplementary Figures	55
B.1	Plasmid Maps	55

C	Supporting Results	59
C.1	Diagnostic Colony PCR	59
C.2	Sequencing of MoClo Level 0 Plasmid	60
C.3	Plasmid Restriction Analysis	62
C.4	Spore Phenotypes	62
C.5	Microtiter Cultivation During Luciferase Assay	63
C.6	Luciferase Assay Raw Data	63
D	Experimental Protocols	67
D.1	Agarose Gel Electrophoresis	67
D.2	Golden Gate Restriction and Ligation	67
D.3	DNA Polymerase Protocols	67
D.4	Kit Manuals	69
E	Buffers and Media	73
E.1	Buffers	73
E.2	LB: Lysogeny Broth	73
E.3	SOC: Super-Optimal Broth with Catabolite Repression	73
E.4	Stock Solutions for <i>A. niger</i> Media	74
E.5	MM: Minimal Medium	74
E.6	CM: Complete Medium	74
E.7	TM: Transformation Medium	74

1 Introduction

1.1 Background

1.1.1 Filamentous Fungi in Biotechnology

Filamentous fungi are abundant and diverse organisms that impact natural ecosystems both positively and negatively. The growth of these multicellular eukaryotes appears as mycelia, web-like structures consisting of tubular hyphae (filaments) that extend and branch to their surroundings. These hyphae facilitate nutrient uptake, protein secretion and reproduction. Each filament of the network consists of multiple end-to-end cells that are separated by internal cross-walls called septa, and is surrounded by a cell wall matrix composed of various interlinked compounds, most prominently glucans, glycoproteins and the fungi-characteristic polysaccharide chitin. This wall functions as a physical barrier for nutrient uptake and excretion, as well as providing structural integrity to the cell [1]. A range of enzymes secreted from the hyphal tips are responsible for pre-digestion of organic matter and polymeric substances in the surroundings. This makes nutrients available in more basic molecular forms that can be transported back through the cell wall matrix and over the cell membrane by transporter proteins [2], which results in a multitude of symbiotic relationships. An example is *mycorrhiza*, associations between fungi and plant roots, where the rhizosphere's soil nutrient availability and transport is improved by various filamentous fungi's decomposition of biomass [3]. In contrast to this, filamentous fungi can also be detrimental to their ecosystems. Their growth can infect and deteriorate their surroundings, causing parasitic diseases in plants and humans, or otherwise cause disease by release of harmful secondary metabolism products such as mycotoxins [4]. For humans, this has a negative effect on both global health and food production [5]. However, filamentous fungi also contribute positively to humans. Many medically relevant compounds, including several antibiotics, were discovered in filamentous fungi, and they are increasingly proving to have enormous worth as industrial production platforms. Fungal biofactories are being employed for bulk manufacturing of a range of products, including organic acids, proteins, enzymes, plant growth regulators, alkaloids, pigments, mycotoxins, antibiotics and active pharmaceutical ingredients [5, 6], often yielding product qualities and production titers that are superior to alternative biofactory platforms, such as bacteria and yeasts [7, 8].

Particularly advantageous to the fermentation in-

dustry is filamentous fungi's powerful secretion machinery. Because of their saprophytic nature, degradative enzymes are constantly secreted from the hyphal tips to the environment in high levels to ensure sufficient nutrition, an ability which has been exploited in protein production processes. When the protein is released from the cell, downstream processing can be simplified, and the risks of feedback inhibition and protease-driven product degradation are minimized [6, 9]. Currently, filamentous fungi are the most important source of enzymes used industrially, and this sector of the fermentation industry is still growing rapidly [10]. Enzymes are marked for secretion by information carried in their genes, so that once the peptide starts being synthesized, a segment of 13-30 amino acids at the N-terminal, known as the signal sequence, recruits the peptide expression to ribosomes at the endoplasmic reticulum (ER), where the enzyme is inserted past the membrane into the lumen [6, 11]. The protein is then fully formed by various post-translational processes, including removal of the signal sequence from the main chain. From the ER, the protein is transported to the Golgi, where vesicles bud off and are transported along microtubules and actin filaments inside the hyphae, forming clusters known as Spitzenkörper before finally attaching to the plasma membrane via SNARE complexes near the apical region of the hyphae. Here, the cargo is released on the other side of the cell membrane [12]. The cell wall presents a final barrier to the exterior, and will trap a certain ratio of the secreted protein, dependent on the porosity of the cell wall [6], but release the rest into the environment. In an industrial fermentation, this means that the product can be harvested directly from the medium without need for cellular disruption.

As the number of sequenced filamentous fungi genomes and the available genome editing tools have increased in later years, the biotechnological possibilities for strain improvements and expanded product portfolios seem endless. There is still a vast reservoir of native secondary metabolites with high potentials that are not yet explored [13], both in previously studied fungi and in novel strains. Further, recombinant technology allows for production of non-fungal compounds in these biofactories, for example high-value therapy proteins such as human antibodies [14, 15]. However, we are yet unable to reach maximum production potentials in filamentous fungi, particularly of non-native proteins, because of incomplete understanding of the metabolic pathways involved. The molecular and cellular basis of filamentous growth

and the links to secretion patterns is still highly relevant to research, and until we have a more complete understanding of these mechanisms, our ability to rationally engineer cost-effective, hyper-producing and hypersecreting filamentous fungi will remain problematic [6, 12].

1.1.2 The Cellular Biofactory *Aspergillus niger*

The most significant and versatile filamentous fungal species for industrial processes is *Aspergillus niger* [6, 16, 17]. Production of citric acid in *A. niger* is said to mark the age of industrial biotechnology 100 years ago, and citric acid is still the fungus' main product with a current annual production of over 1 million tons [17]. However, also a wide array of other compounds are being manufactured in this fungus. This includes industrially important enzymes, for example β -galactosidase which is used in dairy industry [18], and a wide array of secondary metabolites and mycotoxins. Further, as more and more products derived from *A. niger* are qualified GRAS (Generally Regarded As Safe) by the U.S. Food and Drug Administration, the fungus itself gets recognition as a safe and reliable host. It is mesophilic and acidogenic, can grow in submerged cultures on most carbon sources, and can adapt to varied growth morphologies depending on process requirements, from compact pellets of hyphae to more homogeneous mycelium suspensions. The first full sequencing of an *A. niger* genome was published in 2007 [19], and the availability of this knowledge made the organism the focus of much wide-spread research in fungal gene function, gene regulation and metabolism, leading to increased genetic tractability [20]. As a consequence of its dependable safety and considerable genomic information, *A. niger* is also often favored as the host for development of new products [8].

A. niger biofactories are known to exhibit excellent natural secretion capabilities. In comparison to yeast, *A. niger* can secrete up to 10 times more protein [7], with the most abundantly secreted protein being glucoamylase A (GlaA) [21]. Due to the advantages of secreting products during industrial fermentations mentioned in the previous section, the secretion machinery is often sourced in recombinant technology. Non-native proteins or proteins that are naturally intracellular can be manipulated to be recognized as secreted proteins by supplementing the gene with a signal sequence from a naturally secreted peptide [9]. An organism's native signal sequences can for example be viewed in the freely accessible, manually curated signal peptide database (SPdb) that was created

in 2005 [22, 23]. Using this database, appropriate native signals can be selected and subsequently fused to the N-terminal of a recombinant protein to target it for secretion. However, production rates of recombinant proteins in *A. niger* are unsatisfactorily low. This is assumed to be due to a combination of incorrect processing/folding and proteolytic degradations of the proteins prior to product harvesting [6]. For non-fungal proteins produced in *A. niger*, the titers can be 100-fold lower than native proteins [24], and also native proteins expressed homologously on plasmids often have limited titers.

A. niger's secretion machinery is very complex, making it difficult to predict how a secretion signal will function together with a recombinant protein. A 2009 study proved that increasing the secretion of GlaA upregulated over 90 genes [25], indicating a vast network of secretion-linked genes that determine the release of enzymes. This gene network is regulated in time and space according to substrates available, the condition of the fungus during development or in response to stress [7, 12], and is not yet fully understood. Therefore, several secretion signals often have to be tested before they can be used in an organism. In a 2020 study that involved improving production of *A. niger* lipase, Zhu *et al.* (2020) tested three different signal sequences to optimize secretion [8]. They found that transformants with the gene of interest fused to a signal sequence taken from a glucanase (*cbhI* gene) exhibited higher levels of the lipase than those with GlaA's signal or with the lipase's native secretion signal. Further, Zhu *et al.* found that increased lipase titers could be achieved by expressing the gene as close as possible to its native form. By including natural introns and adding a Kozak sequence, the production was boosted because the recombinant protein was treated as a native protein by the cell. This shows that when it comes to "tricking" the cells to increase secretion, some trial and error will likely be necessary.

Alternatively to this camouflaging of recombinant proteins as native proteins, efforts to improve recombinant production are often focused on engineering superior host strains, either by creating more forgiving hosts to foreign proteins or hosts with unbiased hypersecretion capabilities [10, 12, 26]. However, as described in the previous section, any rational establishment of hypersecreting fungal strains is hampered by limited genetic understanding and tractability. Since protein secretion mainly is restricted to hyphal tips, a positive correlation between hyphal growth and secretion has been postulated [12, 27]. This is still debated, but if true it should follow that an increase

in hyphal branching would improve the yields of enzyme secretion [6]. In *A. niger* this has been indicated by results of a hyperbranching strain secreting four times more GlaA than the wild-type (WT) [26]. Another study on *A. nidulans* showed that mutating a specific gene related to vesicle trafficking and glycosylation (*podB*) increased protein secretion ability in comparison to the wild-type, and indicated this gene "as a target when engineering fungal strains for enhanced secretion of valuable biomolecules" [24]. In general, there is no single rational approach that will improve filamentous fungi's secretory capabilities using genome editing technology [12, 26].

Despite *A. niger* arguably being the most researched filamentous fungus, its use as a microbial cell factory remains limited by an under-developed genetic tractability. The available genome editing tools are not extensively explored, and experimental strategies often vary largely between different research groups [28]. For genetic transformations, an approach using protoplasts (generated by enzymatically removing cell walls from raw material of hyphae and spores) mediated by polyethylene glycol (PEG) is most common, being generally reliable and time-efficient once competent protoplasts have been prepared. However, also *Agrobacteria* [8], electroporation, biolistics and shock-waves are used in some *A. niger* transformations, with varying efficiencies depending on a multitude of factors [28, 29]. Further, the genetic toolbox of *A. niger* has been quite limited. In metabolic engineering, a broad choice of vectors, markers, signal sequences, regulatory elements etc. should be available for any given purpose [30], and for *A. niger* the available tools are currently insufficient. In fungi, most genetic manipulation studies have been focused on integrating genes in the host chromosome. The goal is to yield a transformant that stably expresses the introduced gene during cell division, but often the integration is ectopic at random sites in the genome, sometimes disrupting normal cell function and expression stability [31]. Plasmid-based expression is also available for many filamentous fungi, including *A. niger*, by AMA vectors. These plasmids carry the autonomously replicating sequence *AMA1*, and are kept in the cells by selection pressure. Typical markers for selection are based on antifungal resistance or auxotrophy, but availability and expense of these remains an issue. The toolbox should also contain a choice of well-characterized regulatory elements, such as promoters. With a set of defined promoters of variable strengths in the toolbox, expression levels can be fine-tuned by the user, giving the ability to tailor-make metabolic pathways to suit individual needs.

1.1.3 Assaying Promoter Strengths

Promoters are vital transcriptional regulators that control the binding of RNA polymerase (Pol) to DNA, thereby largely determining a gene's expression level. As such, promoters are important components in any organism's genetic toolbox. For many organisms, including *A. niger*, the established genetic toolbox mainly consists of strong promoters, intended on maximizing the expression of a target gene in protein production processes. For recombinant proteins in Aspergilli, the constitutive promoters *pgpdA* (from *A. nidulans*), *ppki* (from *Trichoderma reesei*) and *padhA* (from *A. niger*) [30, 32], all giving stable high-level gene expressions, are typically used. On the contrary, for rational establishment of industry-optimized strains, it can be advantageous to study how minor differences in promoter strengths can affect a metabolic network. Meyer *et al.* (2011) therefore introduced a tight, tunable expression system that is dependent on doxycycline concentration, known as the TetON system because the promoter is induced by tetracycline [33]. Such inducible systems are very advantageous for scientific development, but in industry the wish is often to use constitutive promoters. This is because inducer molecules are often expensive in the long run, and a stable metabolic network with defined and balanced enzyme activities is generally advantageous to expression systems relying on special components in the media. For this reason, the genetic toolbox of organisms used as a biofactories should include a range of well-characterized constitutive promoters with variable strengths, allowing reliable fine-tuning of any gene's expression levels [32].

Complete promoter characterizations necessitate uncovering both the promoter's intrinsic strength and how external effects, such as the host's growth rate and environmental conditions, influence the promoter's activity [34]. Direct measurements of a cell's transcriptome is possible with tools like RNA sequencing (RNA-seq) or quantitative reverse transcription PCR (RT-qPCR), giving indications for how much messenger RNA (mRNA) a promoter yields. RT-qPCR uses reverse transcriptases (copies RNA to DNA) to quantify a gene's mRNA transcripts in a cell lysate sample. This is a cheap way to investigate promoters, but RT-qPCR cannot distinguish between increased transcription and decreased removal of the mRNA (i.e. increased mRNA stability), and is therefore considered an imprecise and unreliable method for accurate determination promoter strength. On the contrary, reporter assays use *in vivo* models, revealing features about the proteome as an indirect approach to studying promoter strength.

Consequently, reporters can give more information about promoter activity over time and in different conditions. Ideally, both a direct and an indirect method should be used to get a clear picture of how a promoter functions. That is, both the actual transcription level and the effects of regulatory mechanisms, RNA degradation, etc., which are revealed only by *in vivo* studies, should be investigated.

As the term implies, a reporter gene's purpose is to report back to the scientist, qualitatively or quantitatively, giving indications of function, activity, structure or, in promoter assays, expression levels. Typically, promoter assays are comparative. By placing a reporter alternately under the control of different promoters of interest, expressing each individual cassette, and measuring some output from the reporter, the promoters' relative strengths can be compared [35]. To avoid multi-copy expression that would disturb the results, it is important that the expression cassette is stably integrated in one position of the genome. This has previously hampered the functionality of reporter assays in filamentous fungi, because introduced genes are often integrated randomly in the fungal chromosome with different copy numbers and at different positions among stable transformants [31]. Before promoter activity could be accurately determined, genetic validation was therefore necessary, which was a highly limiting requirement [36]. However, with emerging gene editing technologies such as CRISPR, these unwanted ectopic effects can be largely avoided [16].

Several reporter genes with different types of measurable outputs are available for use in promoter assays in filamentous fungi. Some reporter genes that are representative of different output formats in fungi are *gfp*, *luc*, *lacZ* and *gusA*, where the first encodes a green fluorescent protein (GFP) that is detectable fluorometrically, and the last three are encoding enzymes whose activities can be measured [36]. The four systems, and others like them, each have advantages and disadvantages that need to be taken into consideration when designing a promoter assay. Fluorescent proteins are quite cheap, requiring no substrate, and have long half-lives. However, low-intensity signals and minute changes in expression are hard to measure accurately using fluorescent proteins, both because their stabilities are too high, causing accumulation of signal, and because of wavelength interference caused by incoming photons that are used to excite the fluorophore [35]. On the contrary, *luc*, *lacZ* and *gusA* systems tend to be more costly, but often have higher precision at lower concentrations [36], i.e. if a promoter is giving weak expression levels. Also, the

lacZ reporter systems can be disadvantageous in fungi because endogenous fungal enzymes interfere with the activity reading of the reporter [36]. The most clear difference between fluorescent proteins and enzyme reporters is, perhaps, that the proteins are measured directly, while the enzymes are indirectly measured by their catalytic activity in a specific biological reaction, which can be thought to decrease the links between measurements and actual expression levels.

The first fluorescent protein to be isolated was GFP in 1994. This dramatically altered the nature and scope of issues that could be addressed by cell biologists because they could mark proteins to study localization and expression levels *in vivo* [21, 37]. Later, in 1999, six new fluorescent proteins were discovered in nonbioluminescent *Anthozoa* species. One of these is DsRed, a tetrameric protein complex named after its origin genus *Discosoma* and the red color it fluoresces when excited [37]. Since these discoveries, novel fluorescent protein derivatives have kept emerging, leading to a wide variety of fluorescent reporters being available today. The original wild-type GFP has largely been replaced with an enhanced, brighter derivative (eGFP), while DsRed, whose maturation time was too slow for many experiments, was improved by directed molecular evolution and random mutagenesis into DsRed-Express, with 10-15-fold shorter maturation time than wild-type DsRed [38]. Where eGFP has an excitation wavelength of 488 nm and emission wavelength of 507 nm [39], DsRed-Express excites at 558 nm and emits at 583 nm [40], giving red light rather than green. A remaining drawback to natural DsRed is its obligate tetrameric structure. This slight spacial bulkiness causes easy aggregation, which can be disruptive to localization experiments because natural fluxes inside the cells are prevented [38]. Furthermore, DsRed's structure makes it acid-sensitive. At pH levels between 4.5 and 7, the effects of pH on the protein's fluorescence and absorbance are negligible (<10 %), but at pH<4.5, the fluorescence of the protein drops significantly and abruptly [41]. This limits the use of this reporter in experiments where it is targeted to acidic environments, such as the lumen of lysosomes or secretory vesicles [42]. Monomer and dimer DsRed-derivatives have also been developed that are better optimized for these kinds of studies, but generally they are less bright and therefore less suited for promoter assays [42].

Another problem with fluorescent proteins as reporters in general is that low-intensity signals are often hard to measure because of background interference [36]. On the contrary, luciferase-based assays have shown to give very accurate

measurements at very low concentrations, detecting even low-abundance transcripts and certain minute changes in expression levels that cannot be measured by RNA-seq or RT-qPCR [43]. Luciferase is an umbrella term to describe enzymes that catalyze light-producing reactions, and can be derived from several bioluminescent organisms, including fireflies, certain beetles and photobacteria. Firefly-luciferase (from *Photinus pyralis*) is a monomeric protein that converts the substrate luciferin to oxy-luciferin in an ATP-dependent exothermic reaction [44], and a recombinant improved version of this enzyme is by far the most popular bioluminescent reporter today [35]. Each oxidation of luciferin releases energy converted to photons (wavelength 550-570 nm) in a burst of light that lasts approximately 15 seconds. Measurements can be taken over time using a luminometer, and the bioluminescence will be proportional to the enzyme activity. If the *luc* gene is placed under control of a promoter of interest, its activity level can thereby be linked to the promoter strength. Luciferase is a monomeric protein that does not require any post-translational modifications in order to be functional, meaning the reporter system has a rapid response rate and can easily be adapted for use in a variety of organisms, from bacteria to mammals [45]. Commercially available luciferase genetic reporters are enhanced from their native forms by codon optimization and minimized unintended transcription regulatory sequences, so that their expression suits the biological systems and the risks of anomalous expression are reduced. Today, a broad range of luciferases are available, designed to meet different experimental needs [35].

1.1.4 CRISPR-Cas Editing of Fungal Genomes

In nature, CRISPR is a bacterial defense system against viral attack. This is a three-step process of acquisition, expression and interference, which, similarly to humans' acquired immune systems, speeds up the cellular response against viral attacks if they are repeated [46]. First, the bacteria acquire pieces of DNA from an invading phage. These fragments are incorporated into the bacterial genome as spacers, and make up a sort of "archive" of intruders termed CRISPR, an acronym for *clustered, regularly interspaced short palindromic repeats*. Premature transcripts from these spacers are recognized and bound by effector complexes of one or more Cas proteins (CRISPR-associated proteins). Processing of the transcript occurs here, from pre-crRNA to crRNA (CRISPR RNA) and, in some cases, forming a molecular duplex with tracrRNA (trans-activating CRISPR

RNA) by base-pairing [47]. If a repeat viral attack happens, the bacteria's Cas proteins loaded with the crRNA-tracrRNA duplex are directed to the intruder and cleave the phage DNA with nuclease activity.

The CRISPR system was isolated from *Streptococcus pyogenes* and adapted as a genome editing tool in 2013, described as a revolutionary step in biotechnology because this is the first genuinely programmable tool to be employed for inducing double-strand breaks (DSBs) in DNA [48, 49]. Certain site-specific recombinases and nucleases have been reprogrammed to direct edits in specific user-defined loci of various genomes, but targeting a cut using CRISPR is generally far less cumbersome and has an accuracy and predictability that is unmatched by other approaches [49], such as Zinc-finger nuclease or Transcription Activator-Like Effector Nuclease (TALEN) [20]. Another major benefit to CRISPR over other genome manipulation tools is its versatility and easy adaptability to almost all organisms as long as their genome has been sequenced; prokaryotes and eukaryotes alike. Much of the CRISPR-related research is linked to curing human genetic diseases, but applications of this system in industrially relevant biological systems are also highly researched, including genome edits of fungal cell factories [16]. The first report on CRISPR-Cas being used in filamentous fungi came out in 2015, describing the development of a system to introduce highly specific, genome-wide mutations in different *Aspergillus* species [4], and since then the number of reports in fungal platforms has been on an exponential rise [50].

CRISPR technology can be employed to both mutate, delete or insert specific parts of fungi's chromosomal DNA, in order to create strains that are superior biofactories. Introducing smaller mutations can be beneficial for disrupting secondary metabolite clusters, either because their productions are pulling resources from the desired product or because they are directly detrimental to the industrial process, such as unwanted mycotoxins [50]. CRISPR has also been used to make deletions of entire clusters, generating minimal genomes devoid of unnecessary mechanisms and products [51]. Further, heterologous protein production can be improved from plasmid-based expression by using CRISPR to integrate the relevant genes in defined genomic loci, causing stable production and reduced need for selection markers over time [20]. Still, this new technology is definitely at an early stage in fungal biotechnology [51]. There are holes in our knowledge that need to be further investigated, such as the risks of unintended impacts of off-targeting and larger

chromosomal-scale rearrangements due to the induced DSBs [50].

Natural CRISPR-Cas systems present differently in different bacterial strains and are categorized by classes (1-2), types (I-VI) and subtypes (A, B, etc.) [46, 52], often simplified by denoting the signature Cas protein of a given system. For example, CRISPR type II is within class 2 and is characterized by the Cas9 protein. It is this CRISPR-Cas9 system that was first employed as a genetic tool in 2013, that was first reported for filamentous fungi in 2015 and that has since carried out the bulk of CRISPR genome edits [53]. The Cas9 protein has a dual function as both the crRNA effector complex and the nuclease that cuts target DNA, which means that a fully functional editing tool can be created consisting of only the two components Cas9 and a single chimeric guide RNA (sgRNA), which replaces the crRNA-tracrRNA duplex from the natural system. The sgRNA directs the Cas9-induced cut by forming an RNA-DNA hybrid at the target genomic locus, due to a 20 nucleotide homology between protospacer in the sgRNA and the region upstream of the desired cut site. Therefore, by careful design of the guide, a DSB can be user-defined virtually anywhere in the genome with high precision. The only prerequisite for placement of the DSB is the presence of a short and conserved sequence known as the PAM site (protospacer adjacent motif), 3-4 bp next to where the cut will be made. For the Cas9 isolated from *S. pyogenes*, SpCas9, the PAM sequence is 5'-NGG-3' where N is any nucleotide and GG are two sequential guanine bases [54]. Figure 1.1 illustrates how the CRISPR-Cas9 machinery induces a DSB in genomic DNA.

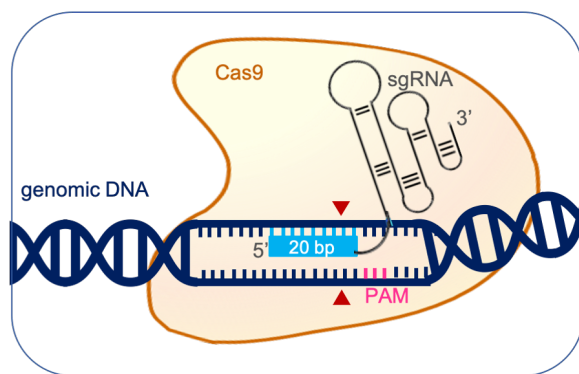


Figure 1.1: Illustration of CRISPR-Cas9 technology. The sgRNA molecule, consisting of a 20 bp guide sequence (bright blue) and scaffolding (gray), is loaded into the Cas9 nuclease (brown). The guide binds to genomic DNA (dark blue) next to the PAM site (pink), targeting Cas9 to induce a DSB (red triangles).

CRISPR-Cas technology is multi-faceted, with many alternative strategies for how to employ the tool. The previously mentioned SpCas9 is by no means the only available nuclease. In addition to Cas9, there are sev-

eral optional nucleases available, with differences regarding for instance the choice of PAM sequence and the placement of the DSB relative to PAM, as well as guide RNA requirements and how it is loaded into the protein. Cas9's dual functionality as both crRNA effector and genomic cut-inducer has made it a popular choice. However, other Cas proteins, for example Cas12a, may have higher sensitivity to mismatches, which limits off-target cleavage and may increase the overall efficiency and reliability of the system [53]. Both Cas9, Cas12a and other Cas nucleases have been successfully employed in CRISPR editing of filamentous fungi, and their respective advantages and disadvantages must be evaluated when an experiment is designed. Further, considerations have to be made for how to deliver the CRISPR machinery to the cells of interest. Two main routes are available here, where one is to express the *cas* gene and the sgRNA *in vivo*, and the other is to pre-assemble an active Cas protein with sgRNA *in vitro* and then transform this ribonucleoprotein (RNP) into the cells of interest. Again, no single approach is perfect. The gene-free RNP approach is typically more useful if the genome editing needs to occur quickly after transformation, because the nuclease's activity is not delayed by expression and subsequent protein maturation [13, 16]. On the other hand, *in vivo* expression makes it possible to achieve a certain stability over time when it comes to availability of the editing machinery, but will be somewhat delayed. Gene-based delivery is the norm for most applications of CRISPR-Cas in filamentous fungi [29]. Often, non-replicating plasmids lacking origins of replication and selectable markers are used, meaning the CRISPR components are only expressed early on after transformation, before cell division. This helps create stable transformants that are not subject to further unwanted edits by continuously expressed editing machinery. Alternatively, extrachromosomally replicating plasmids such as those harboring the *AMA1* gene, can be used to express the machinery, and keep producing it as long as selection pressure is maintained [29]. Only in rare cases, if the propagation of plasmids is unsatisfactory, are integrative plasmids used. This naturally complicates the removal of the machinery and is therefore not typically favored [4].

For efficient mutagenesis to be initiated by CRISPR, both the Cas protein and the sgRNA need to be present in the nucleus of the target organism. A bottleneck of CRISPR introduced in filamentous fungi has been the production and localization of functional sgRNA [20, 29]. Strong, native promoters are most reliable to ensure sufficient *in vivo* transcription, which means substitutions must be made for each strain being edited [4]. Further, the sgRNA transcript requires maturation by splicing mechanisms in order to be functional. In the first reported CRISPR-Cas platform in filamentous fungi, the sgRNA was embedded in the middle of a larger transcript synthesized by Pol II, and the sgRNA transcript was liberated from the larger transcript by the action of two self-splicing ribozyme sequences flanking the sgRNA [4]. However, sgRNA is more suitably synthesized by Pol III, recognizing different promoters. Pol III generates

transcripts that are retained in the nucleus because they lack cap structures and poly-A tails [29], which is typical for short non-coding sequences like sgRNA. Therefore, endogenous Pol III promoters, such as U6 and U3, as well as 5S rRNA promoters, have been applied in different *Aspergilli*, with moderate success in some cases and failing in others [1]. A 2018 study by Song *et al.* (2018) using tRNA promoters for expressing sgRNA in *A. niger* gave very high gene disruption rates [20]. Fungal tRNA genes are constitutively transcribed by Pol III, independent of carbon source and cultivation conditions, and include sequences with self-splicing capacity, making them ideal candidates as sgRNA expression promoters [20]. This research provides a list of highly efficient tRNA promoters with mutation rates in the range of 82-97%. The promoters contain the entire sequence of tRNA gene plus 100 bp upstream sequence, which is post-transcriptionally cleaved from the sgRNA at the 3'-end by RNase Z. This effectively matures the sgRNA transcript as shown in Figure 1.2.

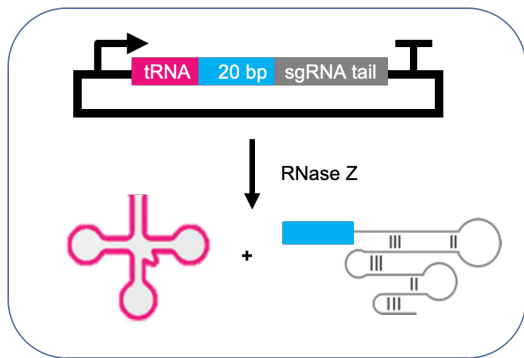


Figure 1.2: Illustration of plasmid-based transcription and maturation of sgRNA using a tRNA gene as promoter. Pink shows the tRNA gene, blue shows the 20 bp guide which will target the genome, and gray is showing the sgRNA tail, which functions as scaffolding when the RNA molecule is loaded into a Cas protein.

CRISPR-Cas technology's programmability comes from the ease of designing one or multiple sgRNAs that target defined genomic loci with high precision. Selecting a protospacer can be done manually, but homology search programs relying on genome sequences and algorithms are often used to automate and refine the process [29], available as online tools. These tools intend to minimize the risks of off-targeting, which increase with increasing genome size. In the *A. niger* genome (35.5-38.5 Mb), off-targeting risks should be near insignificant with proper guide design [4], but one also needs to consider that different loci might have different targetability [13]. It has been shown that CRISPR-Cas cutting efficiencies varied between different genomic loci of *Saccharomyces cerevisiae*, assumed to be due to limited DNA availability in some regions because of chromatin packing [50]. Therefore, several sgRNAs can be introduced to cut within the same region of interest, lowering the chances that no cuts will be made. This introduction of multiple sgRNAs for a

single targeted edit should not, however, be confused with multiplexing. The term multiplexing refers to the editing of more than one genomic site in an organism simultaneously, and can be achieved in CRISPR-Cas technology by inducing several DSBs in separated genomic loci [29]. As opposed to introducing several sgRNAs for a single edit, multiplexing in addition requires multiple repair templates to be introduced, allowing the desired combinations of edits to occur by multiple events of homologous recombination.

All genome modifications rely on endogenous repair pathways of the target organism. Homologous recombination (HR), manipulates the genome using fragments with sequence similarity (homology) to a target region, but is generally inefficient on its own in wild-type filamentous fungi [50]. However, with CRISPR, a DSB is created, causing the cell to initiate vital repair mechanisms that can be exploited to introduce edits. The cellular response to DSBs has two facets; homology-directed repair (HDR), which makes use of an intact copy of DNA as a repair template to fuse the broken strands, and non-homologous end-joining (NHEJ), where no template is needed, the broken ends are simply brought into contact and re-fused as is. NHEJ is highly error-prone, either by including new nucleotides in the fused region or deleting existing ones [47]. Therefore, it is used in gene editing as an inducer of random indels, for example disrupting a gene's function by introducing frame shifts [29]. On the contrary, the HDR pathway can be recruited to introduce larger edits, by using strategically designed DNA cassettes as repair templates, referred to as the donor DNA. In genomic insertions or replacements, the donor DNA will include homologous sequences to the target on either side of the induced DSB, flanking the mutation or marker being introduced [29]. These homology arms need to be long enough to ensure proper targeting, but their size will also limit the transformation efficiencies. For some fungi, it has been proven that the highest editing efficiencies are reached with homology flanks of 1 kb, but also flanks down to 30-60 bp have been functional in some studies, including several *Aspergilli* [13, 29]. A significant advantage of short flanks (<100 bp) is that they can be added to the donor DNA as primers in a PCR reaction [13], limiting the cloning efforts that are required.

In HDR-dependent genome modifications, efficiencies can be increased when the NHEJ pathway is defective. Filamentous fungi's repair machinery is often dominated by NHEJ [4], and suppressing this response can minimize the risk of unpredictable outcomes, such as unwanted deletions or ectopic integrations after the genome has been cut [1, 16]. The NHEJ process of eukaryotes is complex, involving versatile machinery for different steps, but can simply and efficiently be diminished or prevented by disrupting one component: Ku. The Ku heterodimer, consisting of the partner proteins Ku70 and Ku80, is responsible for recognizing the DSB and initiating successive repair mechanisms, and is therefore the typical target for NHEJ mutant construction [55]. *A. niger's* orthologous gene to *ku70* is called *kusA*, and is the typical NHEJ disruption tar-

get in this organism, with HR efficiencies having been proven to increase over 90% in $\Delta kusA$ strains over wild-type [56].

Gene targeting with CRISPR-Cas can be efficient enough in itself to have potential as a marker free approach, but often it still relies on integrative selection markers being introduced with the donor DNA [1]. The most common marker-dependent transformation systems in *A. niger* are based on *pyrG* (deletion hampers pyrimidine synthesis) or *amdS* (dominant nutritional marker), but also other dominant markers such as hygromycin or phleomycin, or use of amino acid auxotrophs is common. It used to be laborious to make the mutants used for counter-selection (e.g. $\Delta pyrG$ or *his*⁻ strains), but today this is relatively easy thanks to advances in genetic engineering tools [4]. Integrative markers have been known to be problematic because of so-called position effects. This means that if the marker is integrated somewhere in the genome where expression is unstable, it might not function properly. However, because of the CRISPR system's targeting ability, markers used with this technology can be forced to integrate at a previously determined location with known constitutive expression, so that position effects should be negligible.

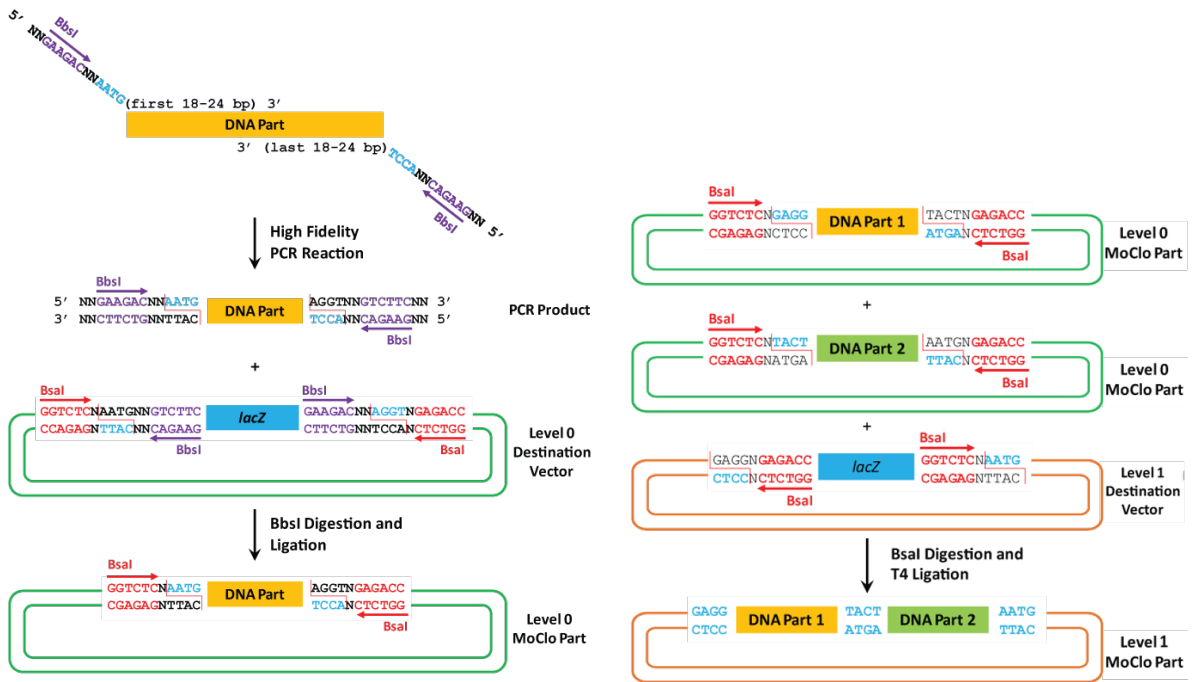
1.1.5 Modular Cloning - MoClo

Modular cloning, or simply "MoClo", is a method of combinatorial plasmid cloning based on Golden Gate technology [57]. The approach was developed and published by Weber, Engler, Gruetznier, Werner and Marillonnet in 2011 as a system in which complex DNA molecules encoding multiple genetic elements can be assembled in predefined arrangements. This is extremely useful for applications in eukaryotic synthetic biology, facilitating construction of large gene libraries that can be used for efficient pathway engineering. The authors draw on principles from more mature engineering technologies in developing standardization of the basic parts in a device, meaning validating and reusing genetic elements from one application to the next [57]. A toolkit in the form of a variety of plasmid destination vectors facilitates the establishment of MoClo in any lab. This MoClo toolkit, deposited in Addgene by the Marillonnet lab [58], is the basis for creating a library of genetic parts stored in plasmids that can easily be combined into a desired multigene construct with high efficiency. Figure 1.3 summarizes the ideas behind this system, which will be described in the following paragraphs.

The principle tool behind Golden Gate assembly technology is type IIS restriction enzymes, which characteristically cut outside of their recognition sites and leave 4 bp overhangs after the digestion. The resulting "sticky ends" of two DNA

fragments can be designed to be compatible with each other, in the end allowing for seamless ligation of the fragments in an orientation-specific manner. Regions where overhangs will appear are therefore referred to as fusion sites. Other restriction-dependent cloning methods, such as that used in BioBrick [60], similarly fuse by sticky ends, but use standard type II enzymes, leaving a construct with scar sequences and inability to assemble multiple fragments in one step [57]. In Golden Gate cloning, the relevant recognition sites are removed in the cleavage process so that a successfully assembled construct avoids repeated cuts. Therefore, in a one-pot reaction undergoing multiple temperature cycles for restriction and ligation to increase the amount of successful assemblies, very high efficiencies towards 100 % can be obtained even for very large constructs of up to at least 10 DNA fragments [57]. Some examples of type IIS restriction enzymes are BpiI (BbsI), BsaI (Eco31I), Esp3I and SapI [61]. In the case of MoClo, both a fragment (or multiple fragments) of interest and a destination vector are digested with one of these enzymes, namely BpiI or BsaI, which makes corresponding sticky ends to piece the module together in the desired order and orientation. The MoClo destination vectors, also known as receiver plasmids, are strategically equipped with appropriate recognition sites and fusion sites, which can also be added to the far 5' or 3' end of any DNA fragment of interest by oligonucleotide extension PCR. Further, cloning is facilitated by the receiver plasmids carrying antibiotic resistance markers and LacZ (β -galactosidase) or CRed (canthaxanthin biosynthesis operon cloned by Weber *et al.*) cassettes, allowing for color screening of transformed colonies [57].

By developing a hierarchical system in MoClo, Weber *et al.* could construct a 33 kb DNA molecule containing 11 transcriptional units from 44 individual modules using only three successive one-pot cloning steps. The most basic modules belong to level 0 and are one of five types; promoters, 5' untranslated regions (5'-UTRs), signal peptides, coding sequences or terminators. As shown in Figure 1.3a, level 0 plasmids can be made by Golden Gate assembly of a PCR product of interest into the level 0 destination vector. A high-fidelity oligonucleotide extension PCR adds the BpiI recognition sites and appropriate fusion sites, and the destination vector has BpiI sites flanking a LacZ cassette, so that the PCR product will be inserted in place of the *lacZ* gene. With the basic modules in level 0, a library of parts can be created, which can later be combined and mixed, for example for screening multiple signal peptides with a certain gene. Combination of multiple level



(a) A DNA part is adapted for MoClo by PCR. Then, it is incorporated in a level 0 destination vector by BpiI (BbsI)-restriction and ligation, replacing *lacZ* in the process.

(b) Two modules in level 0 plasmids are cloned into a level 1 plasmid using strategically placed BsaI restriction sites.

Figure 1.3: An overview of the principles of MoClo plasmid assemblies. Figures are copied without changes from the article “Modular Cloning DNA Assembly” by iGEM, Boston University 2013 (CC BY 3.0), downloaded from <http://2013.igem.org/Team:BostonU/MoCloChara> [59].

0 modules into a transcriptional unit creates a level 1 module, illustrated in Figure 1.3b. Level 1 construction is done similarly to the previous level, but using differently designed destination vectors and restricting with BsaI instead of BpiI. For level 2 constructs, BpiI is used again. The level 2 destination vectors again resemble those of levels 0 and 1, but harbor CRed as the color selectable marker instead of LacZ. This CRed cassette is also flanked by BpiI sites which will create corresponding fusion sites to modules from a digested level 1 module. Where there are five types of level 0 modules, and therefore five “positions” available in a level 1 module, there are seven different types of level 1 modules, and therefore seven positions in level 2. For combination of even more complex multigene constructs, such as the one mentioned containing 11 transcription units, specially designed end-linker constructs with additional, novel restriction sites can be added in one or two of the available positions, leading to a level 2-2 construct. Weber *et al.* (2011) conclude that the construction principle of MoClo theoretically could be repeated indefinitely to add more transcription units, but that the limitation lies in the constructs becoming too large for transformation and propagation in standard hosts such as *E. coli* [57].

1.2 Objectives

The central goal of this project was to address the lack of a significant choice of promoters in the *A. niger* genetic engineering toolbox. In order to tailor-make metabolic networks with fine-tuned expression levels in this industrially important fungus, its limited promoter library requires expansion with constitutive promoters of variable strengths. Prior to the start of the project, genes with stable expression levels across varying environmental conditions had been selected as candidates for novel constitutive promoters. This candidate selection was based on a published dataset by Paegle *et al.* (2016), consisting of RNA microarray results conducted in *A. niger* [62], and genomic regions 1 kb upstream of each gene were then chosen as this project’s promoters of interest. In total 19 of these putative promoter sequences were to be amplified from the *A. niger* genome and cloned into convenient MoClo modules. Subsequently, some of these promoters were selected for characterization in a promoter assay. This quantitative analysis was based on integrating a reporter gene under the control of a promoter of interest in *A. niger*’s genome and measuring the reporter’s output as an indicator of promoter strength. The six promoters that were selected

for this comparison are hereafter called p*ANC1*, p*prp115*, p*L34.B*, p*NDK1*, p*pleu2A* and p*rad24*. A hypothesis was formed that there would be a correlation between promoter strengths and average microarray signals for the genes they were derived from, as indicated by the RNA microarray analysis [62].

The intended reporter for this promoter assay was the improved version of DsRed with reduced maturation time, DsRed-Express. However, the previously described pH dependence of DsRed yielded uncertainty if this reporter could be used in *A. niger* cultures [41]. *A. niger* grows in acidic conditions, so it is possible that fluorescence from DsRed would not be functional. Therefore, an alternative approach with firefly luciferase as the reporter was prepared in parallel with the DsRed reporter, and investigations were launched into the usefulness of this fluorescent protein as a general reporter in *A. niger*. To this end, an experiment was set up where DsRed was expressed in the fungus with different localization signals fused. Due to the outbreak of COVID-19 and resulting time limitations, this path was not extensively explored. Initial experiments were conducted, but no conclusions were drawn based on these, and they were temporarily abandoned in favor of addressing the main project goal: assaying promoters.

The chosen promoter assay relies on single-copy chromosomal integration of reporter cassettes, and therefore requires an efficient genome editing tool. Due to its success in recent years in precisely editing fungal genomes [13, 16], CRISPR-Cas technology was selected for this purpose, and a strategy for its use in this project was developed. The resulting system involves *in vivo* expression of CRISPR machinery, consisting of the Cas9 nuclease and two sgRNAs, from separate, non-integrative

plasmids, designed to introduce DSBs in the *funA* locus of the *A. niger* genome. The fungus' HDR response will be recruited to integrate desired expression cassettes. These cassettes carry the reporter gene luciferase under control of a promoter of interest as well as a selectable marker, and are introduced as donor DNA with 100 bp homology flanks.

In summary, this project aims to:

- Expand *A. niger*'s genetic engineering toolbox with a set of 19 constitutive promoters cloned into MoClo modules.
- Investigate the usefulness of the fluorescent protein DsRed as a reporter in *A. niger*.
- Design a CRISPR-Cas system for the genome editing required to conduct a reporter assay in *A. niger* and briefly evaluate the system's efficiency.
- Assay six putative promoter sequences in *A. niger* by CRISPR-Cas-mediated genomic integration of luciferase reporter cassettes and subsequent bioluminescence measurements. The results should be compared to available transcriptomic data.

Throughout the project, MoClo provided rapid and simple construction of genetic components that were supplied to the fungi. Both the set of putative promoter sequences, the tagged DsRed fusions, the reporter assay expression cassettes and all components of the CRISPR-Cas9 machinery were efficiently cloned in MoClo plasmids, facilitated by the hierarchical setup of different levels, allowing increasingly complex vectors to be assembled.

2 Materials and Methods

2.1 Strains, Media and Cultivation Conditions

In this project, *Escherichia coli* TOP10 was the general cloning host for construction of recombinant plasmids. Chemically competent cells were supplied in the laboratory facilities (protocol for synthesis not shown), stored in glycerol aliquots at -80°C . *E. coli* cultures were grown at 37°C in liquid LB medium with 200 rpm shaking, and on LB agar plates. For selection, suitable antibiotics were added to the medium. The antibiotics used in this project were spectinomycin (Sigma-Aldrich product number S4014, final concentration $50\ \mu\text{g mL}^{-1}$), ampicillin (Sigma-Aldrich product number A9518, final concentration $100\ \mu\text{g mL}^{-1}$) and kanamycin (Roche product number 10106801001, final concentration $50\ \mu\text{g mL}^{-1}$). LB agar plates were also supplemented with IPTG (isopropyl thiogalactoside, final concentration $0.1\ \text{mM}$) and X-Gal (5-bromo-4-chloro-3-indoyl-beta-D-galactopyranoside, final concentration $20\ \mu\text{g mL}^{-1}$) to facilitate blue-white screening of *E. coli* transformants, based on disruption of the LacZ cassette.

Aspergillus niger strains employed in this project are presented in Table 2.1. The parental strain for all is *A. niger* N402, a densely sporulating strain with short conidiospores that is well-established in research. *A. niger* MF41.3 was used as genetic background for all performed genomic engineering, facilitated by a double auxotrophy (histidine and pyrimidine) that allowed for positive selection during transformations. Its *kusA* gene has previously been disrupted to limit the NHEJ repair pathway, and in the process of this gene disruption an AmdS selectable marker was integrated. The strains FH1.1, TS41.6 and TS41.13 were all used to create positive controls in experiments where fluorescence or luminescence were recorded, and MA169.4 was used as a control in a qPCR experiment.

Table 2.1: *A. niger* strains used in this work, the genotypes that are relevant to this project and a reference for the strain construction.

Name	Relevant Genotypes	Ref.
N402	WT	[63]
MF41.3	<i>hisB</i> ⁻ , <i>pyrG</i> ⁻ , <i>amdS</i> ⁺ , <i>disruKusA</i>	[64]
FH1.1	<i>pgpdA::glaA</i> ₅₁₄ - <i>dTomato</i>	[12]
TS41.6	TetON- <i>luc</i> ⁺ (multi-copy)	-
TS41.13	TetON- <i>luc</i> ⁺ (single-copy)	[65]
MA169.4	<i>amdS</i> ⁺	[55]

A. niger was cultivated at 37°C in minimal medium (MM), complete medium (CM) or transformation medium (TM) depending on the strain and experiment conditions. When auxotrophy selection was needed, MM was used, in some cases supplemented with uridine ($1\ \text{mM}$) to allow for single-auxotrophy selection of MF41.3 transformants. CM was used for rapid, non-selective fungal growth. Transformation plates were made with TM, a minimal medium with high osmolarity due to added sucrose ($1\ \text{M}$). This stabilizes transformed protoplasts until they regrow a proper cell wall. To activate expression of genes controlled by the TetON system, the inducer molecule doxycycline was added to the medium, to a final concentration of $10\ \mu\text{g mL}^{-1}$. Detailed compositions of all media and buffers used in this project can be found in Appendix E.

2.2 Plasmid Construction by the MoClo System

As described in section 1.1.5, the MoClo method is a combinatorial cloning approach that was developed by Weber *et al.* (2011), allowing for hierarchical plasmid assembly based on Golden Gate cloning [57]. MoClo was used in this project to construct plasmids of various complexities (levels 0, 1 and 2), through the experimental methods which will be described in this subchapter. Figure 2.1 outlines these methods in a flowchart.

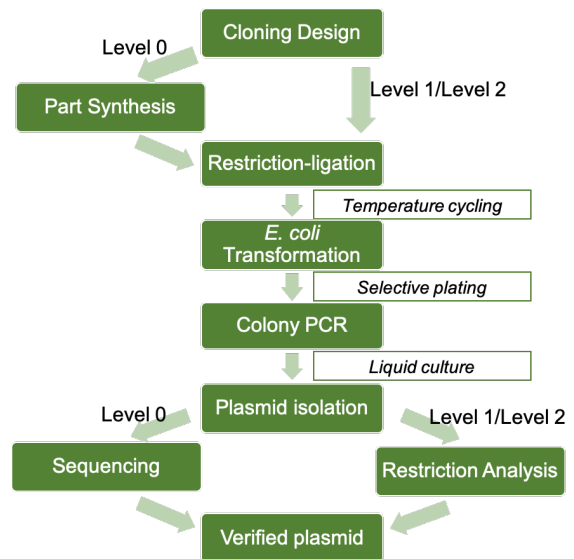


Figure 2.1: Flowchart presentation of how the experimental steps in the MoClo method are related.

2.2.1 Cloning Design

Each plasmid assembly was planned to completion *in silico* before any experimental steps were started. This was facilitated by following instructions from the two papers “A modular cloning system for standardized assembly of multigene constructs” and “Fast track assembly of multigene constructs using Golden Gate cloning and the MoClo system”, both by Weber, Engler, Gruetznier, Werner and Marillonnet [57, 66], and using the MoClo Toolkit (Addgene kit #100000004495) deposited by Sylvestre Marillonnet’s lab. The toolkit consists of 95 empty standardized genetic modules which were used as destination vectors (also called receiver plasmids) in this project. DNA sequence files were uploaded into SnapGene software (Insightful Science), where each cloning step could be simulated and analyzed. To make the parts for MoClo assembly compatible for use with restriction enzymes BpiI and BsaI, oligonucleotide extension PCR was done with precisely designed primers to give the correct overhangs. Primer design was also employed to remove unwanted internal restriction sites, while avoiding introduction of non-silent mutations in the process. Selected primers were ordered (Eurofins Genomics) with target melting temperatures between 57 °C and 62 °C, and can be studied in Table A.1.

2.2.2 Part Synthesis

Parts for level 0 modules belong to one of five categories: promoters, 5’-UTRs, signal peptides, coding sequences or terminators. These parts were synthesized either by ordering oligonucleotides and annealing them, or by PCR amplifying from appropriate template DNA, depending on the size of the part. If the part was less than 120 bp, it could be constructed by ordering oligos (Eurofins Genomics), annealing them and cleaning up the product using a kit with a size limit less than 100 bp (e.g. Oligo Clean & Concentrator, Zymo Research catalog number D4060). However, all parts required for this project exceeded 120 bp in length and were therefore amplified by PCR.

PCR amplifications were done on extracted genomic DNA from *A. niger* N402. The PCRs were set up in 15 μ L reactions with KAPA HiFi Polymerase (KAPA biosystems, product number KK2602), following the protocol for KAPA, which can be viewed in Appendix D.3.1. PCR products were subsequently cleaned up and a sample was analyzed by agarose gel electrophoresis, following the protocol in Appendix D.1. The product bands were compared to a DNA ladder (Invitrogen 1 kb Plus DNA Ladder, Thermo Fisher cata-

log number 10787018). If a single specific band appeared with the intended size of the part, the rest of the mixture was cleaned up directly, but if unspecific bands were visible, the entire remaining mixture was instead loaded on gel and separated by a new electrophoresis run. Then, appropriately sized bands were cut from the gel for subsequent clean up. A dual-usage column purification kit (innuPREP DOUBLEpure Kit, Analytic Jena product number 845-KS-5050250) includes reagents for clean-up process in both these scenarios. The kit allows for purifying amplification products from PCR reaction mixtures and also extracting DNA fragments from TAE agarose gel slices. Direct clean-up from the PCR mixture follows a simple 2-step procedure: a binding buffer was added to the mixture causing the PCR fragments to bind to a spin filter, and then the DNA fragments were eluted with 100 μ L of elution buffer. Gel extraction starts by solubilizing the gel, then the DNA is bound to a spin filter and washed with ethanol, and finally the DNA is eluted. The kit manufacturer’s protocols can be viewed in Appendix D.4.2.

2.2.3 Golden Gate Assembly

DNA parts were combined in destination vectors using the principle of Golden Gate cloning. The necessary volumes (V) of DNA parts in each reaction were determined following equation 2.1.

$$V[\mu\text{L}] = \frac{n[\text{fmol}] \times \text{size} [\text{bp}]}{1520 \frac{c[\text{ng } \mu\text{L}^{-1}]}{[\text{bp} \cdot \text{fmol ng}^{-1}]}} \quad (2.1)$$

Here, n is molecular amount of the part, size is the length of the fragment, and c is the sample concentration available of the part. The number 1520 is used as a conversion factor (1 μ g DNA with avg. length of 1000 bp is 1520 fmol [67]). For 15 μ L plasmid assembly reactions, 20 fmol destination vector and 40 fmol of each insert were used. The insert(s) and the destination vector were cut by a suitable restriction enzyme (BpiI for levels 0 and 2, BsaI for level 1; Thermo Scientific, catalog numbers ER0291 and ER1011) at 37 °C, and assembled by ligation using T4 DNA ligase (Thermo Scientific, catalog number EL0011) at 16 °C. This restriction-ligation was completed in 50 temperature cycles before the enzymes were inactivated by heating. A detailed pipetting protocol and thermocycler parameters is given in Appendix D.2.

2.2.4 Chemical *E. coli* Transformation

The assembled plasmids were grown in *E. coli* TOP10 cells. Chemically competent cells were

thawed on ice, before 50 μ L aliquots were taken out and combined with plasmid DNA (7.0 μ L MoClo assembly mixture) in a microcentrifuge tube. As a positive control for the transformation, the plasmid backbone was also introduced in one parallel, and a negative control consisted of cells with no added DNA. For increased transformation efficiency, the tubes were incubated on ice for 30 minutes before proceeding. Then, the cells were transformed by heat shock by placing the tube in a heating block set to 42 °C for 45 seconds. Subsequently, the cells were chilled on ice for 2 minutes and 950 μ L growth medium (either LB or SOC were used with similar results) was added to the tube for regeneration at 37 °C for 1 hour (heating block with 200 rpm shaking). Finally, different aliquots were plated on selective LB agar plates. Plating of the transformed cells was done in two 50 μ L aliquots, one with ~5 % cells (supernatant after pelleting by centrifugation), and one with ~95 % concentrated cells (pellet). LB-agar plates were used, supplemented with IPTG and X-Gal to allow for blue-white screening of transformants (due to LacZ cassette in levels 0 and 1) and with added antibiotics depending on the selectable marker in the MoClo plasmid level being transformed. For transformations of level 0 plasmids the antibiotic was spectinomycin, for level 1 ampicillin and for level 2 kanamycin. The plates were incubated overnight at 37 °C.

2.2.5 Diagnostic Colony PCR

For an initial screen of the transformants, colony PCR was performed on white colonies. A mastermix was prepared using Phire Green HotStart II DNA Polymerase Mix (Thermo Scientific catalog number F126) and screening primers for the appropriate MoClo level (see Table A.1), with sufficient volume for the number of colonies being screened. Typically, 2-8 white colonies of each transformant were tested simultaneously. This was then distributed into 10 μ L reactions and template DNA was added directly from the plate to each reaction tube by dipping a sterile pipette tip into a colony and swirling the tip in the reaction mixture to release some cells. The protocol shown in Appendix D.3.2 details reaction composition and parameters of temperature cycles. The colonies being screened were continuously marked on the plates by numbering for future reference.

After amplification, the entire 10 μ L reaction mixture was run on 1.0 % agarose in 0.5 \times TAE buffer, following the protocol in Appendix D.1, except without the need to add loading dye (present in DNA Polymerase Mix). The colony PCR products could then be compared to a DNA ladder (In-

vitrogen 1 kb Plus DNA Ladder, Thermo Fisher catalog number 10787018) to verify appropriate size of amplicon, depending on size of insert(s) assembled in the plasmid. Upon identification of a likely correctly assembled plasmid, the corresponding colony (previously marked) was grown overnight in liquid growth medium (LB with antibiotic corresponding to MoClo level) at 37 °C with 200 rpm shaking.

2.2.6 Plasmid Isolation and Verification

Plasmid DNA was isolated from 2 mL liquid *E. coli* cultures. A column purification kit (innuPREP Plasmid Mini Kit 2.0, Analytik Jena product number 845-KS-5040250) was used following the manufacturer's manual (Appendix D.4.3), with overall steps being as follows: cell lysis by alkaline conditions, centrifugation to clear supernatant, binding of plasmid DNA onto spin filter, washing with ethanol (repeated twice) and finally elution of the DNA.

The plasmid product was then analyzed to verify that the correct assembly had occurred. For level 0 plasmids containing only a single module, verification entailed controlling that the module's DNA had remained entirely error-free throughout amplification and restriction-based insertion processes. Therefore, these plasmids were sequenced (LGC Genomics, Biosearch Technologies Genomic Analysis) and thereafter aligned *in silico* to a reference DNA file. For plasmids in levels 1 and 2, verification was done by performing a trial digestion with suitable enzymes. The restriction mixture was composed of 0.5 μ L restriction enzyme(s), 1.5 μ L enzyme buffer, ~500 ng plasmid DNA and MQ-H₂O to make the final volume 12 μ L. After mixing, the reaction was left in a heating block at 37 °C for 1 hour, before analysis on agarose gel (protocol in Appendix D.1). The electrophoresis results could then be compared to an *in silico* simulation of the digestion, showing expected band sizes.

Given positive confirmation of the isolated plasmid, a glycerol stock was created for the *E. coli* colony harboring correct plasmids. Thereby, the plasmid could easily be extracted again if necessary. If a need for large quantities of a certain plasmid arose, liquid *E. coli* cultures of 50 mL or more were made, allowing for larger-scale plasmid isolation. This was also a column-based purification, but using a vacuum set-up with columns and solutions provided in a midiprep kit (PureYield Plasmid Midiprep System, Promega product number A2496) following the protocol as indicated in Appendix D.4.4. Ultimately, the isolated

and verified plasmids were analyzed in a Nano-Drop spectrophotometer, giving DNA concentrations and indications of plasmid purity.

2.2.7 Expanding a Collaborative MoClo Library

This project was, in part, contributing to a larger project by several persons collaborating in the same laboratory facilities. Therefore, many of the plasmids were designed, constructed and employed by different people, requiring effective methods of communicating up-to-date data regarding available MoClo plasmids. This was facilitated by shared online spreadsheets, creating an archive where plasmids were given numbers and descriptive names, so that their assembly progress, current status, concentrations, sizes, positions in freezers etc. could easily be tracked. The same strategy was also used to catalog ordered primers and for an overview of the destination vectors from the MoClo toolkit. All the recombinant plasmid constructs that were used in this project were part of this MoClo library, and only some were created specifically for this project.

2.3 Working with *A. niger*

2.3.1 Preparation of Spore Suspensions

To prepare spores, a fresh medium plate was inoculated with the desired strain. Depending on the strain source, a sterile cotton swab was either dipped in spore suspension or gently rubbed over grown mycelium to harvest spores, before streaking the spores on a plate in squares. After incubation at 30 °C for at least 3 days, the grown mycelium was rinsed with 10 mL sterile physiological saline solution (PS, 0.9 % NaCl), and spores were released into the solution by gentle but thorough rubbing with a sterile cotton swab. Then, the spore solution was pipetted directly from the plate into a sterile tube. If a cleaner spore suspension was required, the solution was filtered through Miracloth before proceeding. The tube was vortexed for 30s and the concentration of spores was determined by triplicate counting in a Thoma chamber. Stored spore suspensions were refrigerated until needed, or used to create glycerol stocks for long-term storage in freezer.

2.3.2 Extraction of Genomic DNA

Genomic DNA was extracted from *A. niger* strains either using a kit or following a protocol for phenol-free extraction using a DNA extraction

buffer. First, a fungal sample was prepared for extraction by freeze-drying. Biomass was generated by inoculating spores from suspension in 1-3 mL CM in a 15 mL tube. Incubation was done with tubes placed horizontally, at 37 °C overnight. Mycelium could then be harvested using tooth picks and put into 2 mL reaction tubes, which were sealed with caps that had small holes. Samples were frozen at -80 °C or liquid nitrogen and dried overnight in a freeze-dryer. The employed kit was EZNA HP Fungal DNA Kit (Omega Bio-Tek product number D3195-01). The manufacturer's protocol was followed as it is shown in Appendix D.4, based on HiBind matrix spin column technology to remove polysaccharides, phenolic compounds and enzyme inhibitors from the fungal sample. For a higher yield of extracted DNA, the following method was instead used:

The dried samples were pulverized by grinding using a pipette tip, resuspended in 500 μ L DNA extraction buffer and heated at 65 °C for 15 min. After cooling the tubes on ice for 5 min, 100 μ L 8 M potassium acetate was added and mixed in with the sample by inverting the tube 8-10 times. A supernatant was yielded by centrifugation (13,000 \times g for 15 min), and transferred to fresh 1.5 mL tubes. If the supernatant appeared bright yellow, 100 μ L 8 M potassium acetate was added anew and the centrifugation was repeated. Then, 300 μ L isopropanol was mixed in and the samples were again centrifuged (13,000 \times g for 15 min). Pellets were washed without resuspension with 500 μ L 70 % ethanol, spun down again (13,000 \times g for 15 min), and dried by removing the supernatant and putting the tubes at 42 °C. Finally, the DNA pellet was resuspended in 50-100 μ L H₂O with 2 μ L RNase A (10 mg mL⁻¹) added to completely dissolve the DNA and degrade RNA. This mixture was incubated at 65 °C for 30 min. The yielded genomic DNA was studied on an agarose gel to verify the presence of a product band over 10 kb in size.

2.3.3 Preparation of Protoplasts

Protoplastation was done by subjecting *A. niger* biomass to a lysing enzyme. First, 1 · 10⁸ spores (from a spore suspension) were inoculated in 100 mL CM overnight (16-18 hours) at 30 °C with 100 rpm shaking. After incubation, biomass could be harvested from the medium using a sterile Miracloth filtration material. A washing step with SMC buffer was done before the mycelium was ready for use (does not need to dry).

The protoplastation solution composed 2 % lysing enzyme (Glucanex from *Trichoderma harzianum*,

Sigma-Aldrich product number L1412) in SMC, with a pH adjusted to the enzyme's optimal pH of 5.6 by added NaOH/HCl. This solution was then filtered through a syringe-fitted filter into a 50 mL tube, where ~ 0.5 g mycelium from the Miracloth filter was added per 10 mL SMC. The tube was then incubated lying horizontally in a 37 °C shaker at 80 rpm. At the start, after 1 hour of incubation and thereafter with 30 minute intervals, the mycelium was studied microscopically for signs of protoplasts. The reaction was stopped within 1.5-2.5 hours, when ~ 20 protoplasts could be seen with 250 \times magnification.

Protoplasts could be released from clumps of mycelium by pipetting an additional 10 mL SMC up and down in the solution. Filtering through a sterile Miracloth filter then allowed protoplasts to remain in solution while removing biomass. The solution was subsequently centrifuged at 2000 \times g for 10 min. The supernatant was discarded, while the protoplast pellet was resuspended in 1 mL STC. By centrifuging (3000 \times g for 5 min) and resuspending again twice, the protoplasts were washed. The protoplasts could then be stored on ice or in a freezer until use.

2.3.4 PEG-Mediated Genetic Transformation

A. niger strains were transformed with donor DNA mediated by PEG. First, frozen protoplasts in 2 mL aliquots were thawed on ice and transferred to 15 mL tubes, where they were washed with 10 mL STC. The protoplasts were then spun down (1500 \times g for 5 min), the supernatant was decanted and the pellet was resuspended in the necessary volume STC. The final concentration of protoplasts should be around $1 \cdot 10^7$ protoplasts/mL, which was taken into consideration when adding the last STC. Then, 200 μ L of the protoplast solution, 200 μ L 20 % PEG and donor DNA (maximum 100 μ L, depending on experiment) were added and left on ice for 30 minutes. 1.5 mL 60 % PEG was added and gently but thoroughly mixed into the transformation solution by rotating the tube at a tilt. This was left at room temperature for 25 minutes before 1.2 M sorbitol was added to stop the reaction, increasing the total volume to 11 mL. A pellet was again formed by centrifugation (2770 \times g for 5 min) and the supernatant was decanted. Finally, the pellet was resuspended in 1 mL 1.2 M sorbitol, and 200 μ L aliquots of this was plated on TM agar plates.

The transformants were grown on TM agar plates at 37 °C until spore phenotypes were evident. Images were then taken of the plates to document

colony sizes and numbers, as well as coloring of mycelium and spores.

2.4 Screening of Genome-Edited *A. niger* Strains

2.4.1 Confirmation of Genomic Integration by Colony PCR

Transformants were studied by diagnostic colony PCR facilitated by Phire Plant Direct PCR Kit (Thermo Scientific, catalog number F130WH). The fungal DNA was made available by dissolving mycelium scraped from colonies on TM plates in a DNA dilution buffer. After spinning down the biomass, 0.5 μ L of the supernatant was used directly as template DNA in a 20 μ L PCR reaction. The protocol in Appendix D.3.3 details reaction composition and parameters of temperature cycles. As a positive control for each transformant, actin was amplified using suitable primers.

2.4.2 Copy Number Determination by Quantitative PCR

To determine the number of integrations that had been made in transformants' genomic DNA, qPCR was done. Primers were designed to amplify a region of interest in an insert and an intercalating dye was used as an indicator of double-stranded DNA molecules, corresponding to the copy number of a target region. A pipetting robot (OT-2 Liquid Handler, Opentrons) was used to set up the reactions. For each set of primers, a master mix was set up by hand, consisting of DNA polymerase (2x Blue S'Green qPCR Mix, Biozym product number 331416), forward and reverse primers and MQ-H₂O, as described in the protocol in Appendix D.3.4. Extracted genomic DNA was subsequently diluted 1:1000 before being used as template DNA for the qPCR. Then, the OT-2 robot was used to pipette the master mix and samples of genomic DNA from different strains into wells on a 96 well plate, which was afterwards sealed with tape and centrifuged to spin samples down. Temperature cycles (see Appendix D.3.4) were set up in a qPCR thermocycler (BioRad CFX96 Real-Time PCR Detection System) and the results were exported and interpreted using *Microsoft Excel*.

2.5 Microscopy

Different microscopy techniques were used according to need. A standard optical microscope was used to study protoplastation and for counting spore concentrations in suspension, whereas confocal laser microscopy (CLSM) techniques were used to study *A. niger* strains expressing fluorescent proteins. For initial viewing of fluorescence in transformants, the fungi were dilution streaked on MM plates and grown for 2 days at 37 °C. The resulting colonies were studied directly from the plates using a confocal Leica TCS SP8 microscope (Leica, Germany). An appropriate region dense with hyphae was found using DIC imaging at 40× magnification, before this area was recorded by fluorescence imaging. For each sample, at least 2-3 regions were documented. To facilitate viewing of secreted fluorescence proteins, strains were cultivated in accordance with a similar experiment by Fiedler *et al.* (2018) [12]. In brief, a spore suspension of the relevant strain was used to inoculate cover slides. This was done in a Petri dish containing 15 mL MM, adding $1 \cdot 10^5$ spores/ml and placing a sterile cover glass at the bottom. Cultivation was then completed overnight at 25 °C, before cover slides were extracted from the solution, and viewed under the microscope.

2.6 Luciferase Assay

Promoter strengths were investigated in a luciferase assay as indicated by previous publications [33, 68]. A master mix containing medium (CM) and the substrate luciferin (Beetle Luciferin Potassium salt, Promega catalog number E1605) was made, where the luciferase was diluted to a final concentration of 0.34 mM. 200 µL aliquots were pipetted into wells in a microtiter plate (Cellstar 96 well plates, Greiner BIO-ONE product number 655098). The wells had translucent, flat bottoms and white scaffolds to avoid signal interference. Inoculations were then made of the strains of interest, transferring 10 µL Mira cloth-filtered spore suspension previously diluted to concentration $1 \cdot 10^6$ spores/mL to each well with medium. Control parallels included one non-inoculated well, one inoculated with a strain not expressing luciferase, and one with a strain known to show luminescence. Measurements were recorded at intervals in a microplate reader (Victor Multilabel Plate Reader X3, Perkin Elmer part number 2030-0050), at room temperature and with plate shaking. Optical density (OD) was measured by absorbance at wavelength 595 nm to determine growth rate, and luminescence (luminescent counts per second, LCPS) was measured with 2 seconds exposure time to quantify luciferase activity. The results were exported and evaluated in *Microsoft Excel*.

3 Results

3.1 MoClo Plasmids

The following subchapter presents results obtained during MoClo plasmid assemblies. Other MoClo plasmids than the ones described here were also used in this project, but the following only details the construction of plasmids created directly for use in this project. An overview of all plasmids that are used can be found in Appendix A.3, and representative plasmid maps for all MoClo levels are shown in Appendix B.1. Results indicating correct assembly (colony PCR and sequencing or restriction analysis readouts) are not presented here, but example results showing how these verifications were done can be seen in Appendix C.

3.1.1 Promoter Modules

19 putative promoter sequences were successfully amplified from *A. niger* N402 genome by PCR. Each promoter was 1 kb long, from the upstream region of genes with stable expression levels, as indicated by an RNA microarray meta-analysis conducted by Paegge *et al.* (2016) [62]. The selected promoters are presented in the appended Table A.2. Oligonucleotide extension PCR created suitable overhangs for MoClo assembly on the promoter fragments. Simultaneously, 4 terminators were similarly prepared, with fragment lengths roughly half of the promoters'. The primers used for synthesis of these MoClo parts can be studied in Table A.1 as numbers 2442 to 2491. Promoters with unwanted internal restriction sites were synthesized in two parts in order to remove these sites by primer design.

Once the PCR products had been verified on gel and cleaned up, they were assembled into level 0 MoClo destination vectors, resulting in plasmids named pMC_0.46 to pMC_0.68 (Table A.3). The appended Figure B.1 shows an *in silico* assembly to exemplify the strategy of MoClo level 0 construction. Most *E. coli* transformants screened by colony PCR indicated correct assemblies immediately. The appended Figure C.1 shows the agarose gel readout from colony PCR screening of twelve level 0 constructs, as an example of how this was done. However, for some constructs, up to 8 colonies had to be screened to find a successful assembly. A final, definitive verification of correct assemblies into level 0 plasmids was done by sequencing the relevant part of the construct and aligning this with a reference. An example of such an alignment can be studied in Appendix C.2. At the end of this project, 4 of the 19 pro-

motor constructs were not yet successfully verified: pMC_0.48 (containing *peEF-2*), pMC_0.49 (containing *phxk*), pMC_0.53 (containing *pFKS*) and pMC_0.68 (containing *pTEF1*). Because there was still a wide choice of 15 other promoter constructs, these promoters were dropped without further investigation or effort.

3.1.2 Plasmids for Expression of Fluorescent Proteins

AMA plasmids were prepared to introduce extrachromosomal expression of differently tagged fluorescent proteins in *A. niger*. First, five versions of fluorescent protein constructs (DsRed-SKL, DsRed-NLS, DsRed-GlaA(LS), DsRed-GlaA(HS) and eGFP-GlaA(LS)) were cloned into expression cassettes in level 1 plasmids, all under the control of the strong promoter *phttA* and terminated by *tcgrA*. The relevant genetic modules, i.e. promoter, tagged fluorescent protein and terminator, were already present in MoClo level 0 plasmids (not shown), and could conveniently be assembled into the next hierarchical level. The resulting level 1 constructs are listed as pMC_1.27, pMC_1.28, pMC_1.29, pMC_1.35 and pMC_1.36 in Table A.4.

After verification of correct level 1 assemblies by BpiI restriction analysis, these plasmids were used to build the final multigene vectors in level 2. In level 2, the *AMA1* gene was introduced to allow for continued expression of the reporters from a non-integrative plasmid. Further, *hisB* was included as a selection marker for the *A. niger* transformation. The appended Figure B.3 shows the plasmid maps of one representative level 2 assembly, while a summary of all five can be found in Table A.5, as pMC_2.14, pMC_2.15, pMC_2.17, pMC_2.18 and pMC_2.19.

3.1.3 Reporter Constructs for Promoter Assay

In preparation for a promoter assay, expression cassettes with luciferase as a reporter were assembled in MoClo level 1 plasmids. Six promoters were chosen for the assay: *pANC1*, *prpl15*, *pL34.B*, *pNDK1*, *pleu2A* and *prad24*. All promoters were assembled into constructs with the firefly luciferase gene (*luc*) and *tcgrA* as the terminator. The assemblies were attempted following the standard protocol for restriction-ligation, however the assembly proved inefficient. Only three of the six constructs could be successfully assembled

on the first try, and after multiple failed attempts, the restriction-ligation reaction parameters were changed in order to assemble the remaining three constructs. Instead of combining 20 fmol destination vector and 40 fmol of each insert’s plasmid, the amount of the promoter plasmid was doubled relative to the other inserts. Thereby, the reaction composed 10 fmol destination vector, 40 fmol promoter plasmid and 20 fmol each of the *luc* plasmid and the *tcgrA* plasmid. Eventually, all six plasmids could be confirmed by restriction analysis. The agarose gel readout after digestion of the last three constructs to be verified is appended in Figure C.4 as an example of how restriction analysis was done. The resulting plasmids are presented in Table A.5 as pMC_1.39 to pMC_1.44, and Figure B.2 shows an *in silico* representation of one example assembly.

3.2 Localization Targeting of Fluorescent Proteins

3.2.1 Experimental Design

To investigate the use of fluorescent proteins as reporters in *A. niger*, fluorescent proteins tagged with different cellular localization signals were expressed in *A. niger* from non-integrative AMA plasmids. Signals targeting DsRed to peroxisomes, to the nucleus and for secretion were tested. For the first, the peroxisomal targeting signal was the motif -SKL, simply serine-lysine-leucine, fused to the carboxyl end of DsRed. The nuclear localization signal (NLS) fused to DsRed is derived from the SV40 Large T-antigen, proven effective in many organisms for most proteins [69]. The secretion signal was derived from the *A. niger* native gene *glaA*, encoding the most abundantly secreted protein in the fungus. Two versions of this signal were tested, one with the full putative signal sequence (low stringency, LS) and one with a shorter sequence (high stringency, HS) believed to be sufficient. The LS tag is 30 amino acids long, while the HS tag is only 22. Whereas both the SKL and the NLS tags were fused to DsRed’s C-terminus, the GlaA tags were fused to the N-terminus because the synthesis of the secreted protein is immediately directed to the rough ER. Finally, one parallel introduced eGFP as a comparative fluorescent protein to DsRed.

The tagged gene fusions were expressed on extra-chromosomally replicating plasmids, constructed in MoClo level 2 as described in section 3.1.2. Positive selection was done by including *hisB* markers in the plasmids. By transforming the histidine auxotroph *A. niger* MF41.3, only cells hav-

ing taken up this marker could grow on the minimal TM. Since the employed strain was also a pyrimidine auxotroph and this marker was not introduced in the experiment, any minimal medium used to grow the transformants was supplemented with uridine.

3.2.2 *A. niger* Transformation

A summary of how the parallels in this transformation experiment were prepared is shown in Table 3.1, while details of the donor DNA samples used and the pipetting scheme used for combining them can be found in the appended Table A.8.

Table 3.1: Outline of transformation experiment testing expression of differently tagged fluorescent proteins in *A. niger*. Here, SKL stands for serine-lysine-leucine, a peroxisomal targeting signal, NLS stands for nuclear localization tag, GlaA is a naturally secreted protein, and LS/HS stands for low and high stringency of the protein’s secretion signal. All added DNA are in the form of AMA plasmids also carrying the *hisB* gene.

Description	Added DNA
Peroxisomal DsRed	3 µg <i>dsRed</i> -SKL
Nuclear DsRed	3 µg <i>dsRed</i> -NLS
Secreted DsRed	3 µg <i>dsRed</i> -GlaA(LS)
Secreted DsRed	3 µg <i>dsRed</i> -GlaA(HS)
Secreted eGFP	3 µg <i>egfp</i> -GlaA(LS)
Positive control	5 µg <i>dsRed</i>
Negative control	(TE-Buffer)

In this transformation experiment, no growth could be seen for the negative control, whereas all parallels with added AMA plasmids yielded plates overgrown with transformants after incubation for 4 days. Colonies had grown into each other, forming a blanket of dark spores on all plates, and could therefore not be quantified. When these plates were illuminated by a UV lamp, faint fluorescence could be detected from the spores, indicating expression of DsRed.

3.2.3 Fluorescence Microscopy

Single colonies of the fluorescent strains were initially studied microscopically directly from MM plates. Hyphal regions were easy to find using DIC, and when switching to fluorescence microscopy, some strains showed clear signals. Fluorescence could be detected in the hyphae of transformants expressing DsRed tagged for peroxisomes (DsRed-SKL) and nucleus (DsRed-NLS),

but no fluorescence could be detected in transformants expressing a fluorescent protein tagged for secretion (DsRed-GlaA(LS), DsRed-GlaA(HS) or eGFP-GlaA(LS)). Figure 3.1a shows that a trail of fluorescence could be seen along a central filament transformed with the DsRed-SKL plasmid. For the NLS-tagged DsRed shown in Figure 3.1b, the fluorescent signal is much weaker, and an image had to be captured from a very densely packed region of mycelium to register the brightness at all. Further, Figure 3.1c shows how no fluorescence could be detected from transformants expressing secretion-tagged fluorescent proteins, exemplified by the low-stringency GlaA-tagged DsRed transformant.

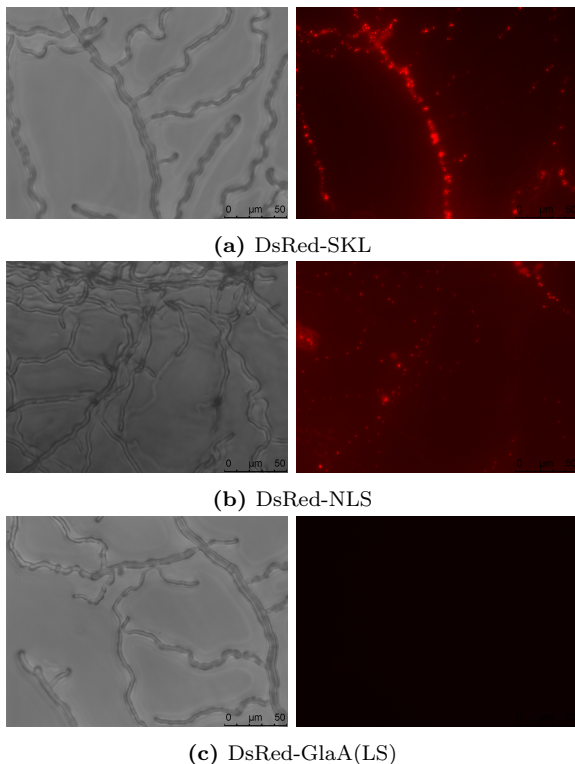


Figure 3.1: Microscopy images of *A. niger* transformants expressing differently tagged fluorescent protein (DsRed). On the left are DIC images. On the right, the cells are captured by fluorescence imaging using a Cy3 filter set.

An attempt to detect fluorescence in transformants with secretion-tagged fluorescent protein was done following the same approach as previously published by Fiedler *et al.* (2018) [12]. As a positive control, a strain created in this study (*A. niger* FH1.1) expressing the fluorescent protein dTomato fused to a GlaA tag, was used. Inoculations of spore suspensions with cover glasses were made, but the procedure proved troublesome. Even after several days' incubation, very few of the transformants' spores viewed with DIC microscopy had germinated, and no fluorescence could be detected

on the cover glasses that had been inoculated. On the contrary, fluorescence could be detected for the positive control FH1.1. This experiment has not yet been completed successfully.

3.3 CRISPR-Cas9 System Functionality

3.3.1 Experimental Design

A CRISPR-Cas9 system for genome editing of *A. niger* had been designed based on results from studies with similar objectives, and needed to be tested for functionality. The CRISPR machinery composed Cas9, two sgRNAs designed to target two sites (termed T3 and T14) within the first 1000 bp of the *fwnA* locus, and donor DNA introducing the desired genome edit with 100 bp homology flanks. Cas9 was expressed from an AMA plasmid constructed by MoClo. This can be viewed as pMC_2.6 in Table A.5, and also carries DsRed and a resistance marker (*ergA*) against the antifungal drug terbinafine in addition to the *cas9* gene. In this experiment, the plasmid was not selected for, and was therefore likely lost quickly. The two sgRNAs were similarly expressed from separate plasmids that were not selected for. Instead, selection was again facilitated by histidine auxotrophy, and introducing the HisB marker with the donor DNA. The *fwnA* locus was chosen as a target because disruption of this spore pigmentation gene would facilitate phenotypic screening of transformants, and to avoid position effects of the integrated HisB marker.

Two promoters were tested in front of the sgRNAs, tRNA^{Pro1} and tRNA^{Arg21}, both shown to yield high gene disruption rates previously [20]. This created a total of four sgRNA plasmids (psgRNA_1 to psgRNA_4 in Table A.6), since two promoters and two sgRNAs were tested. Also, two different donor DNAs were transformed. Both were linear fragments of the *DsRed* gene and the selection marker *hisB* with 100 bp homology arms targeting the *fwnA* locus in the *A. niger* genome, but the two introduced different inducible systems: TetON and MekON. These linear fragments were created by oligonucleotide extension PCRs, where the genetic components were amplified from MoClo level 2 constructs using primers that added the 100 bp homology flanks. The donor DNAs are shown as PCR_1 and PCR_2 in Table A.7. The design of this test of CRISPR-Cas9 functionality in *A. niger* is summarized in Figure 3.2.

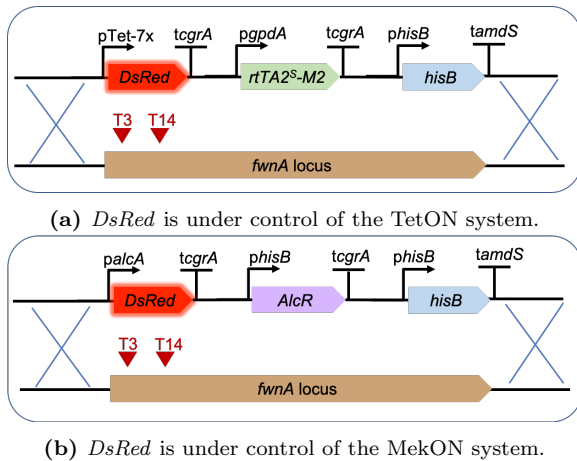


Figure 3.2: Visual representation of genomic integrations being made with CRISPR-Cas9 technology. A cassette carrying *DsRed* under the control of an inducible promoter and the *hisB* marker is flanked by homologous regions targeting the *fwnA* locus in the *A. niger* genome. Two DSBs are induced by Cas9 within *fwnA*; T3 and T14.

The two different donor DNAs that were used in this experiment were included to provide new strains for a different project. TetON is, as mentioned in section 1.1.3, an inducible system with proven functionality in *A. niger*, based on a tetracycline-induced promoter [33]. Similarly, the MekON system uses a promoter from *alcA*, which can be induced by adding methylethylketone, a cheaper inducer molecule than tetracycline. Adding an alternative inducible system to TetON would expand *A. niger*'s genetic toolbox, and so the transformants from this experiment were further studied to see the potential of MekON. However, for the purposes of this project, the aim of this experiment was to verify the functionality of the CRISPR-Cas9 system that was designed, including tRNA-derived promoters for sgRNA, donor DNA with homology flanks of 100 bp and *fwnA* as a disruption target.

3.3.2 *A. niger* Transformation and Editing Efficiency

In total seven parallels were set up to transform *A. niger* MF41.3 in this experiment, as shown in Table 3.2. Four parallels introduced all elements necessary for a functional CRISPR-Cas9 system, one parallel introduced an inactive Cas9 by not supplying sgRNA, one parallel introduced an AMA plasmid expressing *DsRed* and *hisB* genes as a positive control, and the final parallel was the negative control where no DNA was added. For the detailed pipetting scheme followed in this transformation experiment, see the appended Table A.9.

The functionality of the CRISPR-Cas9 system to be used for genome editing in this project was verified in this experiment, first indicated by phenotypic screening. All four parallels of the experiment that had the CRISPR-Cas9 machinery introduced yielded plates with growth of colonies exhibiting both light and the characteristically dark-colored WT spores, where the light phenotype pointed towards the *fwnA* gene being disrupted. This mixed population is shown in example images in Figure 3.3. The efficiency of the system was estimated by counting the number of colonies with white spores and comparing that to the total number of colonies. These results are also given in Table 3.2. The ratio of white colonies gives an indication of the likelihood of a successful genome edit relative to the overall regeneration frequency. Both the positive control and the control introducing inactive Cas9 had overgrown plates with dark colonies. In these parallels, growth was restored because *hisB* was introduced, but the pigment-giving locus *fwnA* was not disrupted, and the spores remained characteristically dark.

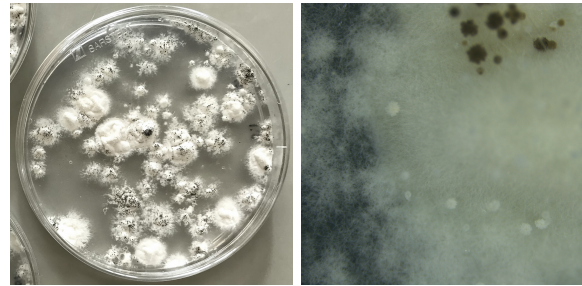


Figure 3.3: Transformed *A. niger* showing both white and black phenotype on spores, viewed on a plate and microscopically.

For further verification that the desired edit had occurred, colony PCR was completed on white mutants. A forward primer binding upstream of the *fwnA* locus and a reverse primer within *DsRed* (numbers 1445 and 2563 in Table A.1) were used to prove that the insertion had taken place in the intended site. This was proven for multiple colonies taken from each of the four parallels with complete CRISPR-Cas9 machineries introduced, whereas a control from a black sporulating colony did not have positive results. An agarose gel readout of this is presented as supplementary results in Figure C.2.

Table 3.2: Outline and results of transformation experiment testing CRISPR-Cas9 system functionality in *A. niger*. Two different promoters were tested for sgRNA transcription (tRNA^{Pro1} and tRNA^{Arg21}), and two different inducible systems were tested in donor DNA (TetON and MekON). “White colonies” refers to mutants with lightened spore colors compared to characteristically dark WT spores.

Description	Added DNA	Tot. no. colonies	No. white colonies	Ratio white colonies [%]
CRISPR-Cas9 (1)	850 ng Cas9 plasmid 1.5 µg per sgRNA-tRNA ^{Pro1} plasmid 3 µg donor DNA (TetON- <i>dsRed-hisB</i>)	82	9	11
CRISPR-Cas9 (2)	850 ng Cas9 plasmid 1.5 µg per sgRNA-tRNA ^{Pro1} plasmid 3 µg donor DNA (MekON- <i>dsRed-hisB</i>)	132	28	21
CRISPR-Cas9 (3)	850 ng Cas9 plasmid 1.5 µg per sgRNA-tRNA ^{Arg21} plasmid 3 µg donor DNA (TetON- <i>dsRed-hisB</i>)	75	17	23
CRISPR-Cas9 (4)	850 ng Cas9 plasmid 1.5 µg per sgRNA-tRNA ^{Arg21} plasmid 3 µg donor DNA (MekON- <i>dsRed-hisB</i>)	91	48	53
Cas9 expressed without sgRNA	850 ng Cas9 plasmid 3 µg donor DNA (TetON- <i>dsRed-hisB</i>)	122	0	0
Positive control	5 µg AMA- <i>dsRed-hisB</i> plasmid	TMTC	0	0
Negative control	None (TE-Buffer)	0	0	0

3.4 Promoter Assay

3.4.1 Experimental Design

A third and final transformation experiment was set up to create *A. niger* strains that could be used for a promoter assay. Using the CRISPR-Cas9 system described in the previous subchapter, expression cassettes carrying a promoter, a reporter gene (*luc*) and a terminator were to be integrated in the *fwnA* locus. However, in this experiment, donor DNA consisted of two individual fragments amplified by oligonucleotide extension PCR from MoClo level 1 plasmids instead of the single fragment used previously, which was amplified from MoClo level 2. Figure 3.4 illustrates this two-fragment donor DNA, where one fragment carries the reporter expression cassette intended to assay the promoters, while the other introduces the *hisB* gene as selection marker. In Table A.7, the donor DNAs are listed as PCR_3-8 for reporter cassettes and PCR_9 for selection cassette. Based on the results from the previous transformation experiment, it was decided that the promoter in control of sgRNA transcriptions should be tRNA^{Arg21}.

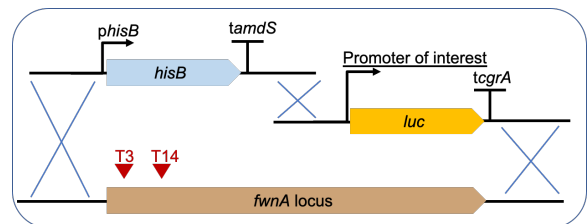


Figure 3.4: Visual representation of genomic integrations being made with CRISPR-Cas9 technology. Two cassettes are introduced, targeting the *fwnA* locus in the *A. niger* genome by homologous regions as shown. One cassette carries the *hisB* marker, and the other carries the luciferase reporter gene under control of a promoter of interest. Within *fwnA*, two DSBs are made by Cas9; T3 and T14.

Once transformants expressing the reporter cassettes had been grown, they were screened in a luciferase assay. By supplying luciferin to the growing fungi, a luminometer could be used to measure the light-producing reaction catalyzed by luciferase. These measurements should correlate with expression levels of luciferase, and thereby be linked to promoter strengths.

3.4.2 *A. niger* Transformation and Editing Efficiency

The transformation experiment is outlined in Table 3.3, with a more detailed scheme given in the appended Table A.10. In comparison to the first CRISPR-Cas9 experiment in this project, the efficiency of this transformation proved very low. As was done previously, transformants could be screened by spore phenotypes due to the chosen *fwnA* integration locus, and the results of counting white mutant colonies versus total number of colonies is shown in Table 3.3. In total, there were 11 colonies that showed the desired phenotype, coming from 4 of the 6 transformation parallels. Hereafter, these transformant strains are referred to as AA1-AA11, where the promoter in control of luciferase is *prpl15* for AA1-AA3, *pL34.B* for AA4-AA5, *pleu2A* for AA6-AA7 and *prad24* for AA8-AA11. All of these strains, as well as one of the black sporulating transformants, were streaked out on CM to grow spores for spore suspensions. Before the spores were harvested, images were taken of the plates to show the clear phenotypic difference between white mutants and strains with no disrupted *fwnA*. A comparison can be viewed in the supplemented Figure C.5.

For verification that the desired edit had occurred, colony PCR was completed on the white mutants, picked directly from the transformation plates. A forward primer binding within the *luc* gene and a reverse primer binding to the region downstream of the *fwnA* locus (numbers 446 and 2092 in Table A.1) were used to confirm that the insertion had taken place in the intended site. This was proven for all 11 colonies exhibiting the lightened spore phenotype. As positive controls, each colony was also screened for the housekeeping gene actin (using primers 2275 and 2278 in Table A.1), which also appeared for all screened mutants. As a negative control, one colony showing WT spore coloring was also included. This negative control tested positive for actin, but negative for *luc*, as expected. These supporting results of diagnostic PCR are appended in Figure C.3.

Further, to control whether single- or multi-copy integration had occurred, qPCR was done on the white mutants. Genomic DNA was successfully extracted from all transformed strains (AA1-AA11) as well as from two negative control strains (TS41.6 and TS41.13) and a positive control strain (MA169.4). 40 amplification cycles were completed, targeting *tamdS*. This terminator is part of the HisB cassette that had been co-integrated with the promoter-luciferase cassette and could therefore be used as an indication of a successful edit. Neither TS41.6 or TS41.13 contain this

sequence, whereas the MA169.4 genome has the AmdS selectable marker integrated once, thereby providing a control with known single-copy integration of *tamdS*. Further, as is shown in Table 2.1, the *A. niger* MF41.3 strain that was used as the genetic background for the CRISPR-Cas edit in question already expresses one AmdS cassette. Therefore, two copies of *tamdS* should be found in the transformant strains if the integration had occurred in single-copy. qPCR primers targeting *tamdS* had not yet been tested, so two reactions were set up in parallel for each strain with two different primer pairs, also adding statistical significance to the data. One parallel used the primer set 2734 and 2735, and the other used 2736 and 2737 (see Table A.1). Actin was selected as the reference gene, so separate qPCRs targeting this single-copy gene (using primers 2275 and 2276 in Table A.1) were set up in parallel.

Two copies of *tamdS* were found to be integrated in the genomes of transformed strains AA1-AA11. This conclusion was derived from a basic comparison of ΔC_T for the control strain MA169.4 and ΔC_T for the studied strains. Here, ΔC_T is the change in average threshold cycle between a sample with *tamdS* primers and the actin reference sample of the same strain. Figure 3.5 shows ΔC_T plotted for the mutant strains AA1-AA11, additional samples of AA1-AA3 tested in a repeat experiment, three parallel samples of MA169.4, and the two negative controls TS41.6 and TS41.13. By studying this column graph, it could be seen that twice as many copies of *tamdS* were present in the mutant strains constructed in this project compared to the MA169.4 control, which is known to express *tamdS* in single-copy. These double-copy qPCR results confirm that the HisB cassette has been integrated once in the strains of interest, indicating that the same is also true for insertion of the promoter-luciferase construct.

Table 3.3: Outline and results of transformation experiment introducing six different promoters in luciferase reporter constructs to the *A. niger* genome by CRISPR-Cas9 technology. “White colonies” refers to mutants with lightened spore coloring in comparison to characteristically dark wild-type spores.

Description	Added DNA	Tot. no. colonies	No. white colonies	Ratio white colonies [%]
<i>pANC1-luc</i>	1.5 µg Cas9 plasmid 1.5 µg per sgRNA-tRNA ^{Arg21} 1.5 µg reporter donor DNA 1.5 µg <i>hisB</i> donor DNA	1	0	0
<i>prpl15-luc</i>	1.5 µg Cas9 plasmid 1.5 µg per sgRNA-tRNA ^{Arg21} 1.5 µg reporter donor DNA 1.5 µg <i>hisB</i> donor DNA	6	3	50
<i>pL34.B-luc</i>	1.5 µg Cas9 plasmid 1.5 µg per sgRNA-tRNA ^{Arg21} 1.5 µg reporter donor DNA 1.5 µg <i>hisB</i> donor DNA	8	2	25
<i>pNDK1-luc</i>	1.5 µg Cas9 plasmid 1.5 µg per sgRNA-tRNA ^{Arg21} 1.5 µg reporter donor DNA 1.5 µg <i>hisB</i> donor DNA	1	0	0
<i>pleu2A-luc</i>	1.5 µg Cas9 plasmid 1.5 µg per sgRNA-tRNA ^{Arg21} 1.5 µg reporter donor DNA 1.5 µg <i>hisB</i> donor DNA	2	2	100
<i>prad24-luc</i>	1.5 µg Cas9 plasmid 1.5 µg per sgRNA-tRNA ^{Arg21} 1.5 µg reporter donor DNA 1.5 µg <i>hisB</i> donor DNA	5	4	80
Positive control	5 µg AMA- <i>dsRed-hisB</i>	TMTC	0	0
Negative control	(TE-Buffer)	0	0	0

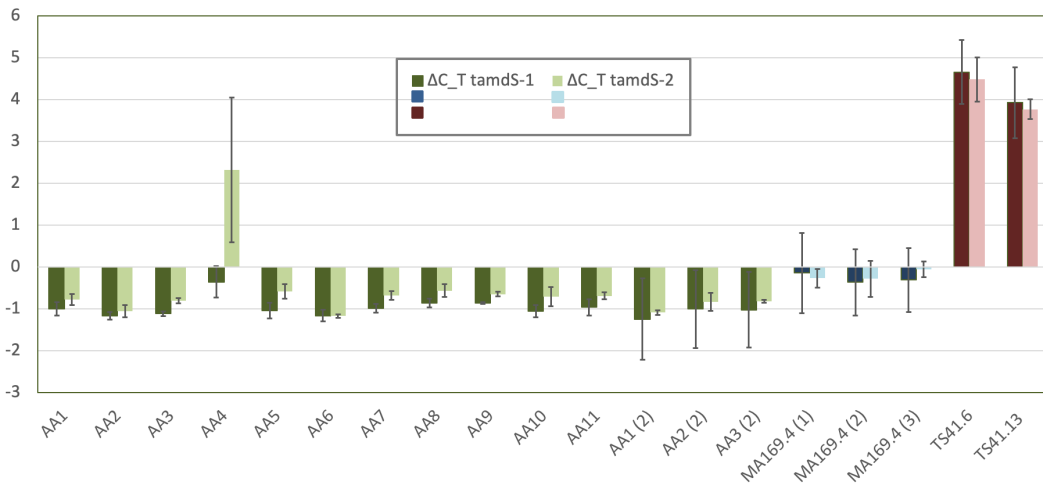


Figure 3.5: Graphical representation of ΔC_T results (C_T target - C_T actin) from a qPCR experiment done to control integration copy number. Two sets of primers, both targeting *tamdS* were used, where one is presented in dark colors and the other in lighter colors. Green columns correspond to strains constructed in this project (AA1-AA11), blue columns show three positive control samples (all of MA169.4) and red columns show strains used as negative controls (TS41.6 and TS41.13). Error bars are added from calculations of standard deviation.

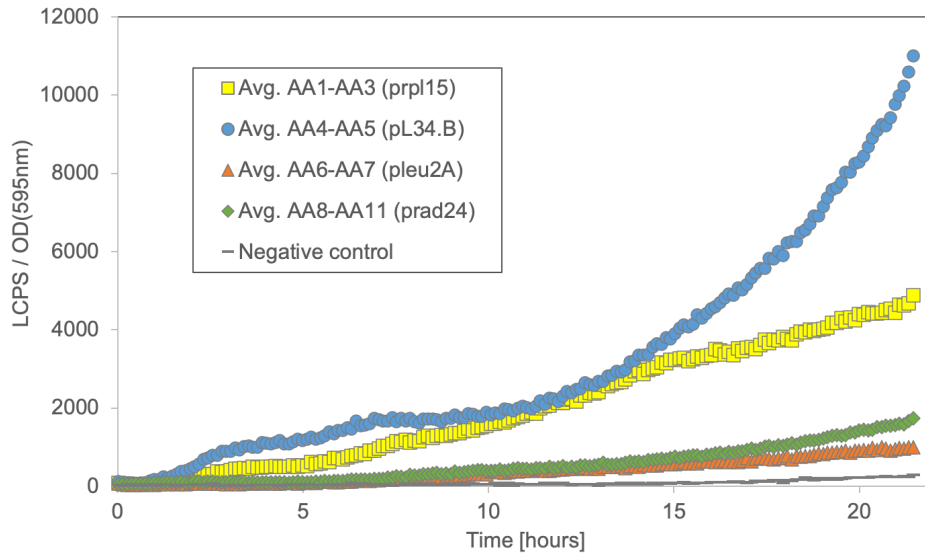
3.4.3 Luciferase Reporter Assay

Only four promoter-luciferase constructs were successfully integrated in the *A. niger* genome and could be assayed. The available promoters were *prpl15*, *pL34.B*, *pleu2A* and *prad24*. As positive controls, two previously made strains TS41.6 and TS41.13 were used. These are known to express luciferase under control of a TetON system, and were therefore induced by doxycycline. A negative control included a black sporulating colony from the transformation experiment described in section 3.4.2, which was also screened in the diagnostic colony PCR. This mutant does not express the *luc* gene and no luminescence could be detected.

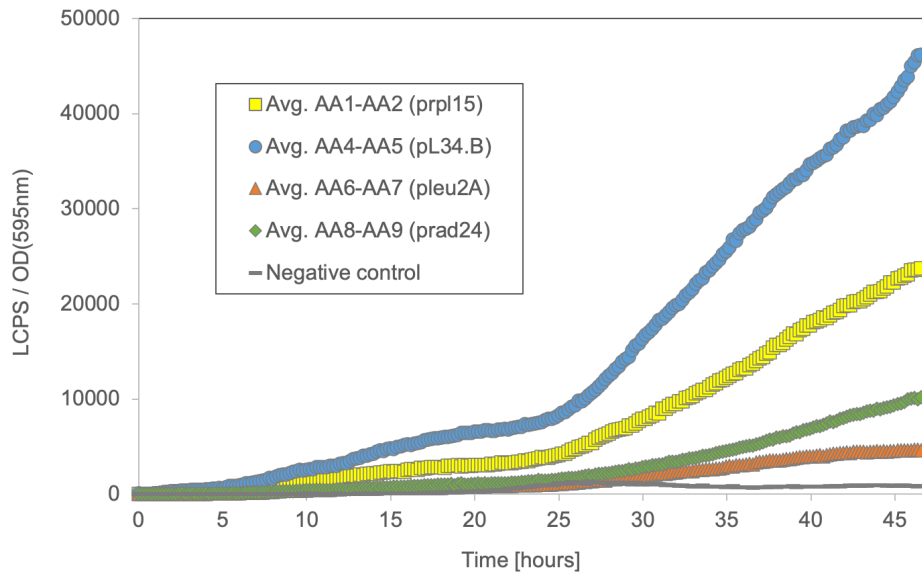
In an initial assay, growth and luciferase activities were monitored for all 11 available white colonies overnight, with measurements taken every 5 minutes. This was completed in duplicates, i.e. two inoculated wells per transformant strain and per control strain. After over 21 hours, both OD and LCPS were still rising sharply. Therefore, a decision was made to repeat the experiment a second time, but measuring activity for a longer period of two days. This second luciferase assay lasted over 46 hours with OD and LCPS measurements taken in 10 minute intervals, and included only two white mutants for each promoter being screened (AA1-AA2, AA4-AA5, AA6-AA7 and AA8-AA9). Again, well inoculations were done in duplicates. No heating was applied to the

systems in either of the two assays. Instead, room temperature was used, which was high and relatively stable at 30 °C.

Raw data from the bioluminescence and absorbance measurements of all wells was exported and presented graphically, as can be seen in Appendix C.6. OD₅₉₅ measurements clearly showed that the positive controls grew much more rapidly than the transformant strains. Moreover, the LCPS results were also higher for the positive controls. For the negative control, growth was more limited than for the transformation strains, and negligible amounts of luminescence could be detected. With an aim of presenting the assay results for each promoter, averages were calculated for all wells containing strains with the same promoter-luciferase construct, e.g. an average of the four wells inoculated with cells expressing the *pL34.B-luc* construct (strains AA4 and AA5, both in duplicates). As can be seen from the graphically presented raw data in Appendix C.6, one measured well containing the *prpl15-luc* integration showed some disturbance that caused big deviations/outliers from the rest of the data. This parallel was omitted when *prpl15*'s mean values were calculated. Additional data processing for better visualization of the results was done by normalizing the luminescence measurements (LCPS) against growth (OD). The resulting graphical data are presented in Figure 3.6. In this figure, results of the positive controls are not included.



(a) Initial luciferase assay conducted overnight.



(b) Luciferase assay conducted over two days.

Figure 3.6: Graphs showing results of luciferase assays. 11 transformed *A. niger* strains expressing luciferase under the control of 4 different promoters, as well as one negative control not expressing luciferase, were inoculated in wells with the substrate luciferin, and bioluminescence measurements were taken using a microplate reader. Luminescence data (LCPS) was normalized against optical density (OD) at 595 nm. The samples were labeled as strains AA1-AA11, and an average was found for each promoter in control of luciferase as indicated by graph labels. The negative control constitutes a transformation mutant with negative phenotype screen (black spores).

4 Discussion

4.1 How the MoClo System Allowed for Expedited Research

In the Weber *et al.* (2011) MoClo system, multiple DNA fragments can be assembled in a defined linear order and building of multigene constructs is facilitated by hierarchical plasmid levels. In addition, the method allows for establishment of a library of genetic parts. The MoClo library that was employed and expanded in this project was first established less than a year ago, but already comprises a vast array of modules in level 0, expression cassettes in level 1 and multigene constructs in level 2. As more and more researchers contribute, the library will keep growing, improving cloning efficiencies. Also, since this is a standardized approach, there is the possibility for exchange of validated MoClo modules or module libraries between scientific groups, leading to even higher efficiencies when multigene constructs are being cloned. This resembles BioBrick's module collection, but since type IIS restriction enzymes are used in MoClo, the resulting plasmids are scarless and multiple DNA parts can be assembled in one single reaction [57, 60]. Further, Weber *et al.* predict that this method has all the elements required for a completely automated cloning system. All the experimental steps described in subchapter 2.2 could be adapted to be performed by computer programs and lab automation robots, from the planning of cloning strategy to the experimental operations of preparing plasmid DNA, liquid handling to prepare reactions for restriction-ligation cycles, transforming hosts and plating, picking correctly colored colonies and subsequently digesting and analyzing the resulting plasmid. In principle, MoClo is an ideal standardized system for any basic plasmid cloning, including all the necessary cloning to prepare for the research described in this thesis.

However, despite the principles and the experimental methods being relatively simple, using the MoClo system was not always trouble-free in this project. For some constructs, there were repeated problems getting positive results from colony PCR of *E. coli* transformants, as well as several instances where the verification process had negative results. For instance, four of the intended promoter constructs have not yet been verified by sequencing, as described in section 3.1.1. When cloning these modules, white colonies (disrupted LacZ cassette) did appear on transformation plates and the colony PCR analysis also indicated successful assembly, but the sequencing analysis of the plasmids revealed major errors. The

problem had likely started already during the genomic amplification of the relevant part. Because alignments of the sequencing results to a reference indicated very few matching base-pairs, it was evident that the original primers used for PCR amplification of the part (promoter) must have experienced unspecific binding to the target. Therefore, it is recommended to design and order new primers if these promoters should ever be added to the MoClo library. However, in the interest of saving time and staying focused on the objectives of this project, the failed promoter modules have currently been dropped without further investigation or cloning effort.

Typically, restriction analysis of level 1 and level 2 plasmids was completed only using the MoClo-linked enzymes BpiI and BsaI. When either of these were used to digest the plasmid product, it could be verified that the correct cutsites were still present for this plasmid, clearing it to be employed as a module in the assembly of the next hierarchical level. The enzymes would cut on the sides of the inserted part(s), giving two bands on gel electrophoresis, where one corresponded to the plasmid backbone and one to the insert(s). In this way, it could also be controlled that the total size of the insert(s) was as expected. However, when using only BpiI or BsaI for this analysis, no cuts would be made within the actual insert, meaning that the direction and order of the assembled parts were not strictly verified. Normally, this was assumed to be correct because of the high efficiencies of MoClo, but in some cases restriction analysis was completed using other enzymes in addition to BpiI or BsaI, to increase the confidence that the conducted assembly had been successful. For example, because there had been problems assembling some of the promoter-luciferase constructs, they were in the end digested with supplementary enzymes to validate that the product was indeed what was desired. As shown from the example result in Appendix C.3, XbaI and/or XhoI were used for this, because they made cuts within the promoter of interest.

Weber *et al.* (2011) describe using 40 fmol of each DNA component in a 20 μ L reaction, something that was altered here. Prior to the start of this project, it had been found that optimized cloning efficiency could be reached when insert(s) were supplied in double amount compared to the destination vector, and therefore this approach was followed here. The current standard method describes addition of 40 fmol per insert, but only 20 fmol receiver plasmid. In addition, as

described in section 3.1.3, the protocol was further altered when there were problems assembling some of the promoter-luciferase constructs. There was no clear reason why three of the six plasmids did not assemble correctly straight away, particularly since all six consisted of the same modules except for the promoters, which were all the same length and with the same overhangs. However, when pMC_1.39, pMC_1.43 and pMC_1.44 had not been verified after three successive assemblies, certain parameters were changed. Therefore, the amount of added promoter plasmid was doubled relative to the other components. In the end, and for unknown reasons, this proved effective. Whether this was chance, that repeating the reaction again simply increased the odds of successful assemblies, or if this had to do with the altered DNA ratios, is not known.

Because of an already initiated MoClo library of standardized modules, this project was less limited by time requirements for cloning. Close to 50 MoClo plasmids are presented in Appendix A.3, some of which were constructed during the course of this project and some of which were already present in the library. The total number of MoClo plasmids that were used in this project, *or* combined to create those that were used, is likely over 100. This is surpassing what would have been possible to build in the time frame of this project, despite MoClo being relatively time-efficient. Without the existing MoClo modules in the growing library, more time would have been needed for cloning, which would have hampered the progress of the remaining research. Especially with the added time limitations due to COVID-19, it is likely that very few, if any, of the promoters could have been assayed within the time frames of this project without the MoClo library as a basis. Thus, this work clearly exemplifies how collaborative cloning by MoClo can speed up scientific research.

4.2 Suitable Reporters for Promoter Assays in *A. niger*

Choosing which reporter to use in a given assay is significant for the results that are yielded. In this project, a DsRed reporter system was originally selected for the screening of promoter strengths in *A. niger*. The fluorescent protein has been used for promoter assays in different organisms before [70], and was easily cloned into MoClo plasmids, making it readily available for use. As described in the background section 1.1.3, use of fluorescent proteins as reporters allows for more direct measurements of expression levels than alternative enzymatic reporters. Enzyme reporters are meas-

ured by their catalytic output, which means that any external factors impacting their activity could influence the measurements independently of the gene's expression strength, for example if the enzyme is inhibited. In contrast, fluorescent proteins are themselves the source of the signal that is measured. Therefore, it can be argued that DsRed as a reporter gives a more accurate indication of how much protein can actually be yielded when the gene is placed under control of a promoter of interest. For industrial enzyme production purposes, this is relevant because as long as a functional product can be harvested, it does not matter how active the enzyme is inside the cellular biofactory, only the product yield. An alternative exists, where reporter protein content is quantified by binding to antibodies. Here, detection also occurs whether the reporter protein is enzymatically active or not, but the antibody-based assays generally have reduced sensitivity [35].

A further reason for choosing DsRed as the general reporter in this project was to test the function of different localization signals in *A. niger*. This type of intracellular localization investigation would not be possible with an enzyme reporter, but when using a fluorescent protein, individual cellular compartments and coupled machinery can be highlighted by fluorescence. Therefore, an experiment was set up where differently tagged DsRed-Express constructs were transformed into *A. niger*. Four different tags were tested in fusion with the fluorescent protein; a peroxisomal targeting signal in the form of the SKL motif, a nuclear localization signal (NLS) derived from the SV40 large T-antigen, and two alternative versions of secretion signals, both derived from the *A. niger* native protein GlaA. No studies have ever reported the use of DsRed as a reporter in *A. niger*. However, the *dsRed* gene had been added to the MoClo library, and it was therefore interesting to study whether it could be used in future localization studies in this fungus. To add a comparison, an eGFP fusion was also made with one of the GlaA tags, since various GFPs have been expressed in *A. niger* previously [21, 71].

Product secretion is a highly desirable trait of filamentous fungi as cellular biofactories, and something that requires further optimization. Because our understanding of the secretory machinery in filamentous fungi still is incomplete [8, 12], a certain amount of trial and error is needed to discover the best suited genetic conditions for cellular production processes, for example which genetic modifications might create hyperproducing strains or which signal sequence will be most efficient. In this project, the signal sequence of GlaA was selected as a fusion tag to secrete the reporter DsRed.

GlaA is the most abundantly secreted protein in *A. niger*, and tags derived from this protein has been employed to secrete recombinant proteins before. Secretory fusions with the *A. niger glaA* gene have successfully been used for heterologous proteins in various *A. niger* at least since 1993 [72], and the first GlaA protein fusion with a fluorescent protein (GFP) in *A. niger* was already reported in 2000, by Gordon *et al.* [21, 73]. Truncated versions of the *glaA* gene were then used, yielding smaller-size fusions with only the first ~500 amino acids expressed. Similarly, Fiedler *et al.* (2018) secreted dTomato by creating a fusion with a GlaA₅₁₄ tag, in order to study the secretion machinery at *A. niger* septal junctions [12]. In this project, a much shorter signal sequence was fused to DsRed. In the signal peptide database (SPdb), it can be found that GlaA’s core secretion signal is only 18 amino acids long (*MSFRSLLALSGLVCT-GLA*) [23], and since similarly short sequences have been used with success to secrete recombinant proteins in other fungi [74], it was decided to attempt a similar approach here. The relevant sequence is the part of a newly synthesized peptide that is cleaved off during post-transcriptional modifications in order to release the main protein inside the ER before it is secreted [11, 22]. However, exactly how much scaffolding is required to support these 18 amino acids is uncertain, which is why two different signal sequences are tested here. These are here termed high-stringency (HS) and low-stringency (LS) GlaA-tags, where the HS tag encodes 22 amino acids and the LS tag encodes 30 amino acids.

In an initial analysis of transformant colonies on plates, clear fluorescent trails could be seen in the hyphae of strains expressing SKL-tagged DsRed, faint fluorescence was detected for NLS-tagged DsRed strains, and none could be seen for GlaA-tagged DsRed (or eGFP). This can be studied in Figure 3.1. Here, the DsRed-SKL-expressing transformants consisted of many highlighted cellular compartments along the extended filaments, presumed to be the peroxisomes. It is not clear why the peroxisomal tag yielded so much more fluorescent signal than the NLS. The DsRed-NLS-expressing transformants did show some fluorescence (which was more visible by eye than after capturing by camera), but generally fewer fluorescent spots could be seen and with reduced brightness. A simple explanation for this could be linked to the nature of the two cellular compartments. There are, of course, fewer nuclei than peroxisomes in the cells, so if the protein has been targeted here, fewer bright spots will be seen. Further, a possible reason for the reduced brightness could be that the combined shielding by both the cell membrane and the nuclear membrane blocks

much of the signal from NLS-tagged DsRed. This is, however, just speculation.

Following this initial screening of transformants, an attempt was made to study the secretion of DsRed by reproducing a microscopy technique conducted by Fiedler *et al.* (2018). However, the inoculations of cover glasses with spore suspensions did not succeed in showing secretion patterns either. The positive control strain FH1.1 did yield visible fluorescence on the cover glasses, as described in the 2018 study, proving that the method was functional. Nevertheless, the transformants from this experiment did not give positive results. The inoculated cover glasses revealed no cells when viewed microscopically, and upon further analysis of the medium, it became evident that the spores had not germinated. As mentioned in the results chapter (section 3.2.3), this experiment was abandoned at this point. This was due to unexpected and sudden closing of laboratory facilities in March 2020 because of COVID-19, and subsequent time limitations forcing more focused research on the core objectives of this project. However, the study of DsRed’s functionality in *A. niger* has already been restarted by other researchers, and is expected to reveal more conclusive results than presented here. In this thesis, one can only speculate concerning the problematic results of this experiment. Possible explanations could involve a destabilization of DsRed’s tetrameric form with the added GlaA tag, a disruption of the fluorophore’s function when the tag was added, or something related to environmental conditions of the expression.

DsRed’s proven acid sensitivity has further been postulated as a hindrance to visualizing secretion mechanisms with this reporter. *A. niger* famously produces and secretes high levels of organic acids [17], effectively acidifying their environment, which can reach pH levels below 2.0 shortly after inoculation if the growth medium is unbuffered [75]. As described in section 1.1.3, DsRed’s function fails in acid conditions. Its ability to emit, excite and absorb photons drops drastically at pH levels below 4.5 [41], which is shown in Figure by experimental data from a study published in 2000 4.1. It then follows that if the GlaA-DsRed fusion has been functional in marking the fluorescent protein for secretion, it could be possible that the fluorescent signal is extinguished by the acidic conditions in which *A. niger* grows. Further, intracellular DsRed might not be detectable, as secretory vesicles also tend to have low pH. Indeed, most fluorescent proteins’ signals, including from both reporters expressed in this experiment, are known to be quenched by acid [42]. More acid resistant fluorescent proteins exist, for example

dTomato or mCherry [42]. When using these as reporters in secretion studies, clear trails of fluorescence can show the protein’s journey through the cell, culminating in Spitzenkörper structures at the hyphal tips [71, 76], such as what was seen for the positive control strain FH1.1, which expressed GlaA-tagged dTomato [12]. In this current experiment, however, very little or no fluorescence could be seen inside transformants with secretion-tagged DsRed or GFP.

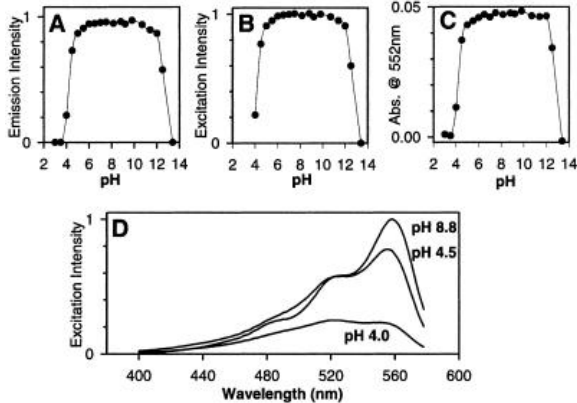


Figure 4.1: pH dependence of DsRed fluorescence and absorbance. (A) 583-nm emission monitored with 558-nm excitation. (B) 558-nm excitation monitored with emission at 583 nm. (C) Absorbance at 552 nm. (D) Excitation spectra of DsRed (emission monitored at 583 nm) at pH 8.8, 4.5, and 4 showing spectral shape change. Reprinted without modifications from “Biochemistry, mutagenesis, and oligomerization of DsRed, a red fluorescent protein from coral” by Baird, Zacharias and Tsien, 2000, *Proc. Natl. Acad. Sci. USA* 97(22): 11984–11989 [41]. Copyright (2000), The National Academy of Sciences.

The DsRed-derivative used in this study was the improved protein with reduced maturation and folding time, DsRed-Express, which lowers the likelihood that acid sensitivity is the main reason behind the lacking fluorescent signal. DsRed-Express is described as a more acid resistant alternative to the native DsRed [40], so the pH dependency shown in Figure 4.1 will be different. It will, however, probably exhibit some acid sensitivity despite the optimizations, and since no pH measurement was done for the transformants that were viewed microscopically, we cannot tell how acidic the conditions actually were in this experiment. When Gordon *et al.* (2000) secreted GFP by a GlaA fusion, no GFP could be detected in the medium afterwards, but the hyphae were visibly lit up by functional GFP [21]. The lack of fluorescence found in the medium was discussed to be due to extracellular proteolytic degradations, and corresponds to the results that were yielded in this current experiment. On the con-

trary, hyphae, particularly hyphal tips and septal junctions, were not highlighted in this project’s experiments in the same way as by Gordon *et al.* The 2000 research proves that *A. niger*’s secretory vesicles generally are not too acidic for the relatively acid-sensitive GFP, and should therefore not prevent DsRed-Express from displaying fluorescence in similar conditions.

Generally, it cannot be drawn any conclusions about DsRed-Express’s functionality in *A. niger* based on the incomplete experiments presented here. It could be possible that the protein is unsuited to be a reporter for secretion in this fungal strain. This is, as mentioned, being further investigated currently, for example by inoculations in differently buffered media. However, DsRed-Express would likely have been functional in a reporter assay to investigate promoter strengths, because this does not require any secretion and DsRed *was* shown to be functional intracellularly. Despite this, when the time frame for conducting experiments in this project became so significantly diminished, it was easily decided to base the promoter assay on luciferase reporters instead of a fluorescent protein. Luciferase assays are well-characterized in *A. niger*, for example after use by Meyer *et al.* in development and testing of the TetON system [33]. Using a luciferase reporter was therefore seen as a safer alternative to using DsRed, whose use has never been reported in *A. niger* studies. In addition to being more dependable because of previous reports, luciferase also has other advantages. Table 4.1 summarizes some key features of both reporters that were considered for this project’s promoter assay.

The most important documented advantage of luciferase over fluorescent proteins, is its precision at low concentrations. For a promoter assay, precision is important in order to be able to detect minute differences in expression levels caused by the promoters of interest. Bioluminescence from a luciferase-catalyzed reaction might therefore be the most exact available indicator of promoter strengths. This increased assay sensitivity stems from reduced background interference when measuring signals. Both DsRed and luciferase are reporters whose outputs are light, i.e. photons released as a consequence of energy transitions from high-energy to lower-energy orbitals. What differentiates bioluminescence from fluorescence is how excitation appears in the first place [45]. DsRed and other fluorophores get their energy from absorbing incoming photons, e.g. from a UV lamp or a fluorescence microscope. Therefore, the light used for excitation of the protein could disturb the measurements. Particularly for detection of low concentration signals, a high influx of photons for

Table 4.1: Comparison between the types of reporters considered for this project; a fluorescent protein (DsRed) and a bioluminescence-producing enzyme (luciferase).

	DsRed	Luciferase
Detection	Fluorometric	Luminometric
Source of signal	Protein itself	Enzyme activity
Accuracy	Poor for low-strength signals, better for high-signal	High precision for low-signal, but can easily get saturated
Stability	Long half-lives, but signal is subject to photobleaching	Different options available commercially
Acid tolerance	Sudden drop of fluorescence below pH 4.5	Reduced catalytic activity in low-pH conditions
Intracellular targeting	Allows visualization of individual compartments	Not possible
Cost	Low	Higher due to substrate expense

excitation of the fluorophore compared with the limited efflux of photons caused by this causes interference, limiting the measurements' accuracy. Furthermore, the separation of wavelengths from incoming light and outgoing signal is complicated by scattering of the wavelengths by the cell wall and membrane [35]. On the contrary, bioluminescence in a luciferase assay requires no external light, emitted photons are simply the by-products of an exothermic chemical reaction, and can be accurately quantified using the metric LCPS (luminescent counts per second). This means that there is no disturbance of signal during measurements, allowing for more precise detection at lower concentrations [45].

On the other end of the scale, for high-concentration measurements, it must be taken into account that signals can get saturated. If a promoter is too strong, so that an excess of reporter is expressed, or if the reporter protein is overly stable, causing accumulation, an output level could be reached where changes in expression no longer can be detected. Hence, reporters with lower stability are often desired because the rate and magnitude of response to transcriptional events increases [45]. For luciferase, if the stability is too high and the enzyme accumulates, insufficient cellular fluxes of substrate (luciferin) and product (oxy-luciferin) might prevent all the expressed reporters from catalyzing the light-producing reaction. Thereby, the assay cannot accurately indicate promoter strength. In contrast, DsRed and other fluorescent proteins do not rely on fluxes of substrates inside the cells, and are therefore not so easily prevented from displaying high levels of expression. However, low-expression scenarios are dependent on a semi-stable to stable reporter. Low stability of luciferase translates to reduction of the enzyme's catalytic ability over time, which might mean that the luminescent signal does not reach detectable levels. There there-

fore exists a range of commercially available luciferase genes with different inherent stabilities. The firefly luciferase used in this project is among the less stable, reported as having a shorter half-life than other available luciferases such as NanoLuc or Renilla luciferase [35]. For fluorescent proteins, stability is generally high. However, the signals are not able to be measured for long periods of time, because photobleaching causes gradual fading of fluorescence. Further, some fluorescent proteins, including monomer versions of DsRed, tend to have limited brightnesses [42]. Similarly to low-stability luciferases, this can lead to so low signals that detection fails because of shielding of the photon wavelengths by the cell.

Also the environmental conditions of an experiment are important for the functionalities of different reporters. As described, low pH could affect fluorescent proteins negatively. Acidic conditions delay or prevent correct peptide maturation and folding, so that the secondary structures responsible for excitation of photons are not formed. The same can occur at more extreme temperatures, but, generally, this is not an issue in biological systems [42]. Likewise, the maturation and catalytic activity of luciferase will be affected by extreme pH levels and temperatures. For the luciferase-luciferin reaction, peak wavelength emission is found when pH is 7.8 [44], with a gradual shift to longer emission wavelengths in more acidic conditions. Further, the luciferase-luciferin reaction has an optimal temperature at 28 °C [44]. Because these reporters are typically used in comparative assays, any small changes in functionality caused by experimental conditions should be the same for all parallels. In the promoter assay conducted in this project, the direct signals from the luciferase reporter will only be compared to internal results, i.e. between the different tested promoters, not to external studies. If more generalized results are desired, more extensive assays are required, typ-

ically necessitating the use of dual-reporter systems. By using two different reporters, such as the Dual-Glo luciferase assay system [35], normalization methods giving higher statistical significance and confidence in the results can be used. However, as will be discussed in the coming subchapter 4.4, luciferase was a reasonably reliable reporter of promoter strengths in the assay conducted in this project. Further, since the signals that were detected from the promoters were quite low, it was likely beneficial that luciferase was used rather than DsRed, even though DsRed also likely could have been functional for the purposes described here.

4.3 Precise Genome Editing Using CRISPR-Cas9 Technology

The genome editing system in this project was designed based on reviews and published studies of different approaches to CRISPR-based modification of filamentous fungi's genomes [1, 4, 13, 16, 20, 29]. This involved decisions to be made regarding a long list of considerations, including how to deliver the editing machinery, alternative Cas proteins, choice of sgRNAs, promoters for relevant genes, homology flanks in donor DNA, selectable markers, and more. Nødvig *et al.* were the first to publish CRISPR-Cas9 editing in filamentous fungi in 2015 [4]. The research edited the genomes of six *Aspergillus* species that had never before been edited, providing the scientific community with several relevant vectors for introduction of the efficient editing tool in other fungi. In 2016, Pohl *et al.* reported the development of a highly flexible CRISPR-Cas9 toolbox for *Penicillium chrysogenum*, which could also be applied to other filamentous fungi [13]. In this current project, MoClo-based strategies for cloning of the CRISPR machinery and subsequent delivery by *in vivo* expression, as well as deliberations regarding homology flank length, were all based on the previous work by Pohl *et al.* This 2016 study thoroughly describes both marker-based and marker-free CRISPR-Cas9 editing, as well as both *in vivo* and *in vitro* (RNP) expression of the editing machinery. Furthermore, the decisions to express sgRNA under the control of tRNA genes and some features of the employed Cas9 expression vector were based on results published by Song *et al.* (2018) [20]. This current subchapter explains in more detail the reasoning behind why the CRISPR system used in this project was designed as it was, and describes how the system twice proved effective in editing *A. niger*'s genome very precisely, but with different efficiencies.

Both Cas9 and sgRNA were expressed *in vivo* from non-integrative plasmids. The alternative of using RNPs, i.e. assembling sgRNA oligos into the Cas protein prior to transforming the cells, can in some cases be a more efficient method because Cas9 activity is immediate, not delayed by the need for protein translation and maturation [13]. Further, off-targeting by Cas9 is limited when using RNPs because the nuclease's presence in the nucleus is transient. RNPs will naturally deteriorate quite quickly, preventing repercussions of unstable transformants and eliminating the necessity to remove the CRISPR machinery after a gene edit is completed [50]. In contrast to this, plasmids are much less prone to intracellular degradation and could therefore impact the cells long-term by incorporating components into the genome. Despite this, the stability of DNA is very useful in most cases, which is why gene-based delivery of CRISPR machinery is most common, and also used in this project. The *in vivo* expression makes it possible to maintain effective concentrations of Cas9 and sgRNA in the nucleus over time, whereas RNP has to be supplied in excess initially, only for the concentrations to fall rapidly [16]. An additional drawback to *in vivo* expression is, however, increased cloning efforts [13]. When using RNPs, Cas9 proteins can be purchased commercially (although this is expensive) or harvested from e.g. *E. coli* expressing the gene, and sgRNA oligos can be designed, ordered and annealed without any additional cloning. On the contrary, both the *cas9* gene and the sgRNAs need to be cloned into plasmids if they are to be expressed *in vivo*. However, with efficient cloning methods such as MoClo and the ability to deliver Cas9 and sgRNA(s) on separate plasmids, as was done in this project, the cloning efforts are reasonably sustainable even with *in vivo* CRISPR machinery expression.

Alternative nucleases to Cas9 have also been investigated in filamentous fungi, notably Cas12a, also known as Cpf1 [16]. Contrary to Cas9, which makes blunt-end cuts in the protospacer region proximal to the 5'-NGG-3' PAM site, Cpf1's nuclease activity leaves sticky ends with 4-5 nt overhangs distal to the protospacer and PAM site, which is 5'-(T)TTN-3' for Cpf1 [16, 53]. This makes Cpf1 more suited for cutting in AT-rich regions and when sticky ends are necessary to make NHEJ-mediated ligations. It also has the characteristic of not needing tracrRNA as a scaffold in the assembly of guide RNA into the Cas nuclease, but rather maintaining its functionality with only crRNA. Research in human cells further indicates that Cpf1 is more sensitive to mismatches between guide and chromosomal target than Cas9. Despite these postulated advantages over Cas9, and the proven usefulness in filamentous fungi by Kwon *et al.* (2019) [16], Cpf1 is currently employed mostly when no 5'-NGG-3' PAM site can be found

close to the desired target. In this project, there was no issue finding Cas9-appropriate protospacers targeting cuts within the *funA* locus, and so there was no need to investigate alternative Cas nucleases too extensively.

Selections of the two *funA* cut sites, as well as the assembly of corresponding sgRNA oligos into a plasmid, were done prior to the start of the project. Targeting the *funA* gene allowed for phenotypic screening of transformants because spore pigmentation was disrupted [77]. In addition, the genomic locus was known to be expressed stably, eliminating the adverse risks of position effects when integrating the *hisB* marker, making *funA* a highly convenient target in CRISPR-Cas editing. However, choice of protospacer sequence has been shown to have great influence on the success of genome engineering events with CRISPR [13], and because neither of the two selected sgRNAs had been tested for functionality previously, both were included in CRISPR-Cas editing in this project. It was hypothesized that if the sgRNAs had limited targeting ability, chances of at least one successful DSB being induced was simply higher when both options were included. As shown in Figures 3.2 and 3.4, both of the cutsites T3 and T14, which are named after the online protospacer selection tool ccTop's suggestions, cut near the 5' end of the *funA* locus. By cutting closer to where transcription starts, it is more likely that the gene's function is successfully disrupted. The T3 and T14 sgRNAs were ordered as oligos (shown in Table A.1) and added to plasmids (pMC_0_26 or pMC_0_27) which had previously been installed with tRNA genes in a vector backbone using MoClo. The entire plasmids were then amplified by oligonucleotide extension PCR, where the ordered sgRNA oligos were used as primers. In the end, the PCR amplicon was religated, forming a plasmid expressing the tRNA-sgRNA fusion that is pictured in Figure 1.2.

The method of using tRNA promoters for sgRNA transcription was first reported by Mefferd *et al.* in a human cell line in 2015 [78], and for the first time in *A. niger* by Song *et al.* in 2018. The *A. niger* native genes tRNA^{Pro1} and tRNA^{Arg21} were the two promoters with highest average editing efficiencies in Song *et al.*'s sgRNA expression study [20], and were therefore selected for use this project. As described in section 1.1.4, use of tRNA genes as promoters for sgRNA is ideal. This is both because the genes are transcribed by Pol III, which facilitates nuclear retention of the guide sequence, and because tRNA is naturally cleaved from its surrounding transcripts by RNases, which effectively matures the sgRNA to be loaded into Cas9. The tRNA^{Pro1} gene that was used consists of a 91 bp long coding sequence and a 625 bp long promoter that gave gene disruption rates between 92 and 97 % in the 2018 research article, whereas tRNA^{Arg21} has a 72 bp long coding sequence with a 405 bp long promoter and disruption rates of 88-93 %. In the initial CRISPR-Cas9 functionality experiment outlined in subchapter 3.3, both sgRNAs were tested for function. They were encoded in sgRNA plasmids of just under 4 kb, assembled as described in the pre-

vious paragraph. The results from the experiment showed that both tRNA^{Pro1} and tRNA^{Arg21} had been functional promoters for the sgRNAs. Editing efficiencies, estimated by ratio white colonies (Table 3.2), were between 11 and 53 %, with the tRNA^{Arg21} gene having yielded slightly higher ratios. Although this single experiment is not enough to definitively state that tRNA^{Arg21} is the better candidate of the two that were investigated here, it was selected for use in the next CRISPR-Cas9 editing experiment.

In addition to the tRNA promoters that were used for sgRNA expression, also the nuclease *cas9* gene that was used in this project was taken from Song *et al.* (2018) [20]. The gene is fused to an NLS signal to target it to the nucleus, and has been codon-optimized for *A. niger*. In this project, *cas9* is placed under control of the *phttA* promoter and is terminated by *tamdS*. The *httA* gene encodes one of the monomers in *A. niger*'s histone octamers, Histone H2A, a constitutively and strongly expressed housekeeping gene. Expression of Cas9 from the plasmid should be high as long as the plasmid is retained in the cells, and so a strong promoter such as *phttA* was beneficial. Similarly, Song *et al.* employ the strong *ppkiA* promoter, but this was altered to *phttA* here because of availability in the MoClo library. The plasmid carrying NLS-tagged *cas9* (called pMC_2.6 in this project, see Table A.5) also harbors the *AMA1* gene, allowing extrachromosomal replication, and the *ergA* selectable marker. *ergA* confers resistance against the antifungal drug terbinafine, which means that the Cas9 plasmid could have been continuously expressed in cells if this selection pressure was applied in the medium. However, prolonged expression of Cas9 was not necessary in this project, and no terbinafine was therefore used. In the end, this Cas9 plasmid was expressed quite similarly to the sgRNA plasmids, which lacked replication abilities whatsoever.

This project's CRISPR system included selection of transformants only by the integrated marker introduced with donor DNA. Both *amdS* and *pyrG* are examples of well-established selectable markers in *A. niger*, but here *hisB* was used. This marker has previously been used with success in *A. niger* [12], and both the histidine auxotroph strain MF41.3 as well as MoClo plasmids containing the HisB cassette were readily available in frozen stocks. As described, the MF41.3 strain was also a pyrimidine auxotroph, but this was not used for selection in this project. However, if the strains developed here are to be further genetically modified, it is highly advantageous to have this *pyrG* marker ready to be used.

Donor DNA was, in both the CRISPR editing experiments described here, made by amplifying relevant genes from MoClo plasmids using primers that created homology flanks targeting upstream and downstream of the *funA* locus. The final consideration when designing the CRISPR-Cas system used in this project was lengths of these donor DNA homology flanks. Typically, the homologous regions that are used for HR, also when DSBs are introduced within the tar-

geted region, are close to 1 kb (e.g. 800-1000 bp by van Leeuwe *et al.* (2019) [1], 600 bp by Song *et al.* (2018) [20]). However, Pohl *et al.* (2016) showed that donor DNA with much shorter homologous flanks could be functional in CRISPR-Cas editing. When editing the genome of the filamentous fungal species *Penicillium chrysogenum*, flanks as short as 60 bp were used with success, as long as the editing was marker-based, i.e. including the marker as part of the donor DNA to be integrated [13]. Such short flanks are very beneficial in limiting the cloning efforts. The flanks can simply be added via oligonucleotide extension PCR, something that was taken advantage of in this project, where it was decided to use 100 bp flanks. When determining the necessary flank length for an experiment, also the length of the donor DNA itself should be taken into consideration. If over 10 kb are being integrated, it is natural to assume that one would benefit from having homology flanks of increased lengths, but when the inserts are shorter, such as the ones applied in this project (2.5 - 8.3 kb), these short flanks should suffice. In addition, HDR efficiency is generally higher when the repair template is linear instead of circular [4]. Therefore, it was strategic to use PCR products as donor DNA instead of assembling the donor DNA with flanks into a MoClo plasmid and using this circular vector directly.

It was further observed by Pohl *et al.* (2016) that when the flanks were long (more than 500 bp), colonies grew also when no sgRNA was introduced, i.e. despite the targeted region being intact [13]. This proves that HR is effective without CRISPR-Cas cuts, as long as there is strong similarity between genome and donor DNA. In the initial CRISPR-Cas experiment performed in this project, a parallel was set up where Cas9 and donor DNA were delivered as normally, but no sgRNA was supplied. This “DSB-free” edit did result in growth of colonies, indicating that the HisB marker had integrated. However, these transformants exhibited wild-type spore coloring, so the integration had likely not been targeted by the homology flanks, which was the case when the T3 and T14 DSBs were included. Exactly where in the genome the marker had integrated was not investigated, but it is probable that it re-integrated where the native *hisB* locus is. This locus was disrupted when the auxotroph strain was made, but retains most of its sequence, which would match the HisB cassette that was part of the donor DNA.

The initial CRISPR-Cas experiment done here proved that the designed system, including *in vivo* expression of Cas9 and sgRNAs, 100 bp homology flanks and using the *fwnA* locus as target, was functional. Each transformation plate where MF41.3 had been supplied with all the components necessary for the editing machinery, grew mixed populations of both white and black-colored spores (Table 3.2). Further, it was verified by diagnostic colony PCR that the inserts had been successfully incorporated in the region of interest. This analysis was done on transformants with positive phenotypes (white spores), and all of these indicated correct integration. As mentioned, the strains that

were constructed, expressing DsRed under control of two different inducible systems, were not relevant to be studied here. However, these will be relevant to future research aiming to establish the MekON system as a cheaper alternative to the TetON system, and the CRISPR editing functionality testing that was conducted here therefore served an additional, valuable purpose. The editing efficiency of this experiment, determined by count of colonies with positive phenotypes versus colonies with negative phenotypes, was found to be between 11 and 53 % for the four parallels. In an attempt to improve this ratio, the masses of added DNA were altered in the next experiment.

When promoter-luciferase constructs were to be integrated genomically, the transformation efficiency was drastically decreased (Table 3.3). Two experimental modifications had been made to the initial CRISPR-Cas experiment. Firstly, more of the Cas9 plasmid was added in comparison to what was done previously. The hypothesis was that by increasing the nuclease concentration, the ratio of successful edits would correspondingly increase. Second, since donor DNA consisted of two individual expression cassettes (*luc* and *hisB*) with homology to each other and the target, instead of the single multigene cassette used previously (TetON/MekON-*dsRed-hisB*), the mass of added donor DNA PCR products (3 µg) was divided by two, so that each PCR product had a mass of 1.5 µg. Because the respective lengths of the donor DNA cassettes (2.5 and 3.3 kb) were shorter than in the previous experiment (7.5-8.3 kb), this change of mass should not affect the molecular amounts of available repair templates. However, the fact that the donor DNA is delivered in two separate molecules has been postulated as a possible explanation for the reduced transformation efficiency. No literature could be found to support this claim, but the conjecture seems logically sound from a statistical point of view. The statistical likelihood of a split repair template finding and sealing the DSB would probably be lower than a single repair template, simply because two molecules need to find the *fwnA* locus instead of just one.

However, the results show that despite very limited growth on the transformation plates, the ratio of positive phenotype versus negative was not very different from the initial experiment with single donor DNA molecules, in some cases even higher. This, combined with positive results on the colony PCR, which verified luciferase insertion in the *fwnA* locus for all white mutants (AA1-AA11), proves that the CRISPR-Cas system has again been an effective editing tool. The lowered transformation efficiency could indeed be because of unforeseen difficulties during transformation, such as experimental errors or inaccuracies, and not a reflection on the effectiveness of the the CRISPR-Cas experimental setup. In order to control this, repeat experiments would have been necessary. However, time restriction on the project lead to acceptance of the results as they were, despite positive transformants growing only for four of the intended six strains. This meant that two of the promoters that were supposed to be assayed were not available in *A. niger*, i.e.

p*ANC1* and p*NDK1*. It is believed that a repeated transformation experiment might have integrated also these missing cassettes genomically, but the project proceeded without these efforts being made. This project did not aim to optimize the efficiency of CRISPR-Cas9 editing in *A. niger*. The goal was rather to construct strains that could be used for a reporter assay, meaning that the system did not need to be particularly efficient, as long as it was effective. It should, of course, be emphasized that two intended strains were not successfully prepared, and certain alterations to the system should therefore be made to increase the efficiency. However, this was not extensively focused on in this project.

The edited strains expressing luciferase under control of different promoters (AA1-AA11) were further studied by qPCR to confirm that the integration that had occurred was single-copy. This experiment is based on quantification of double-stranded DNA present in a sample during PCR amplifications, by use of a fluorescent dye. In this case, the PCR targeted *tamdS*. This terminator was part of the HisB cassette that had been co-integrated with the promoter-luciferase constructs, and was chosen as the qPCR target because of availability of primers. The genomic background of strains AA1-AA11, *A. niger* MF41.3, was already expressing one *tamdS* because *AmdS* had previously been used as a selectable marker in the disruption of *kusA*, involved in the NHEJ repair response. Therefore, the qPCR results were in this case positive when two copies of the *tamdS* target were indicated.

For the purposes of the luciferase assay, it is important that the reporter construct has been stably integrated in the genome in single-copy. As two separate donor DNA cassettes had been co-introduced, a positive verification that *tamdS* had been integrated in single-copy did not strictly verify that only one copy of the promoter-luciferase cassette had been integrated. However, this is strongly believed to be true. The HisB marker that was used directly derives from the *A. niger* genome, and although the MF41.3 strain is *hisB*⁻, it still shares much homology with the marker that was used. This is also reflected, as described previously, in the survival of transformants where no sgRNA was added in the initial CRISPR-Cas experiment, likely due to re-integration of *hisB* in its native locus. On the contrary, very little homology can be found between the MF41.3 genome and the promoter-luciferase cassette. Therefore, it is much more likely that the HisB cassette would have integrated in double-copy by some HR-mediated fashion near the native *hisB* locus, than it is likely that the promoter-luciferase cassette similarly found a site to integrate in. In summary, this means that the verification of single-copy integration of *tamdS* by extension confirms a very probable single-copy integration of the promoter and reporter.

The qPCR verification method was, as is summarized in section 3.4.2, based on evaluating the difference between target (*tamdS*) amplification and control (actin) amplification, giving ΔC_T , which could then be compared to the control strain MA169.4's ΔC_T .

Here, C_T is defined as the threshold cycle. In a qPCR experiment, this translates to the cycle number when the fluorescent signal from double-stranded DNA molecules reaches a certain threshold level. This will occur faster for PCR targets that are in high abundance from the start, thereby allowing comparisons of copy number. A negative correlation will be found between C_T and copy number, i.e. a high-copy target has a low C_T . In the qPCR of this project, the three MA169.4 parallels all have ΔC_T signals close to 0, as can be seen in Figure 3.5. This means that the respective threshold cycles for *tamdS* were the same as actin's, because the amplification rate of *tamdS* was the same as actin. Since we know that actin has a copy number of one, it follows that the same is true for *tamdS* in this strain. In contrast to this, all but one of the AA1-AA11 strains have ΔC_T signals near -1, indicating that their fluorescent signals appear an average of one cycle before actin's signal, and thereby have double copy numbers of *tamdS*. From the raw data (not shown), it can be observed that the tested parallels had average threshold cycles (C_T) in the range of 24-33, making 40 cycles a well-chosen parameter for the experimental procedure.

Because PCRs are exponential, any misbinding of primers in the qPCR experiment will create a product that is also quickly amplified and can reach the threshold signal. This type of false positive is likely the reason that the negative controls (TS41.6 and TS41.13) also have C_T scores at all, despite not harboring *tamdS*. It is clear from their high ΔC_T s of 4-5 that there is much less amplified signal from these strains than from actin, i.e. less than one integration of the gene, which is not possible. Such false signals can also cause disturbances in strains with one or more copies of the target. Therefore, the standard deviation error bars are quite large in some of the columns presented in Figure 3.5, especially observed for the three strains AA1-AA3 on the second repeat of the qPCR experiment. Despite this, the repeated run had very similar ΔC_T s as the initial qPCR, confirming the results as reliable. Also the experiment's duality due to the two employed primer sets (*tamdS*-1 and *tamdS*-2) adds some statistical significance to the results. It is clear that the second set (*tamdS*-2) has slightly lower binding affinities than the first set (*tamdS*-1), because the lighter colored columns are slightly smaller than the dark ones in Figure 3.5 (although still comparable). However, for strain AA4, containing the p*L34.B* promoter, the two primer sets have yielded very different ΔC_T results, and none of the two resemble any of the other strains' ΔC_T s. Whether this strain has integrated *tamdS* at all or not, remains unclear. The strain did have positive results on the diagnostic colony PCR (Figure C.3), but this was only proving insertion of luciferase in the *funA* locus, not the HisB marker. Since this strain's genotype is brought into question by these qPCR results, it would be recommended to instead use the other p*L34.B*-expressing strain (AA5) for future research.

There are more precise methods that could have been used to absolutely confirm the intended CRISPR edit

more precisely than those that are presented here. Firstly, the colony PCR could have been done with a primer binding to the promoter of interest. Although the 1 kb promoter sequences are relatively dependable due to the performed sequencing of level 0 MoClo plasmids containing the promoter modules, there is still a chance that unforeseeable mutations or mix-ups have occurred before the genomic integration. Amplifying each promoter and the *fwmA* genomic locus as a diagnostic colony PCR could therefore have been done to prove correct integrations of the promoters. Similarly, as discussed, it cannot be absolutely verified that the promoter-luciferase cassettes are only integrated in single-copy due to the choice of *tamdS* as qPCR target. Furthermore, the integration of this target was double-copy, something which is not ideal (and was overlooked in the design of the experiment). If the target had been the promoter or luciferase instead, there would only have been one copy, which could have created a clearer presentation of results. For example, log2-fold change of mutant strains AA1-AA11 relative to a positive control with the target in single-copy was near could have been presented, also known as the $2^{(-\Delta\Delta C_T)}$ method. Both of the two chosen PCR-based verification methods could in this way have been improved by using different sets of primers for a more stringent verification of the AA1-AA11 strains. However, in the interest of saving time, a common set of primers was used in the colony PCR (targeting the *luc* gene which was the same for all mutants), and qPCR primers that were already available were similarly chosen (without a need to order new primers targeting the reporter cassette). Despite these simplifications in the verification process, the results of both colony PCR and qPCR strongly indicate that the CRISPR edit has been successful. Both the the integration site and integration copy number appear precisely as intended, once again reflecting the major scientific value of CRISPR-Cas9 technology.

4.4 An Expansion of *A. niger*'s Promoter Library

Prior to the start of this project, a set of putative promoter sequences had been selected to study based on an *A. niger* RNA microarray dataset. The dataset comes from publicly available *omics* data of *A. niger* strain CBS 513.88, published as part of a transcriptome meta-analysis by Paegle *et al.* (2016) [62]. It comprises more than 14,000 putative genes whose microarray signals were measured under 155 distinct cultivation conditions, developmental stages and environmental stress conditions. The signals are given relative to actin's signal, and therefore indicates the gene in question's expression levels in comparison to this housekeeping gene. A statistical analysis was completed on the dataset to reveal the steadiness of the genes' expression levels across the meas-

ured conditions, in order to select stable genes as candidates for constitutive promoters. As will be further explained in the next paragraph, this was done using the metric cumulative interpercentile ranges (Σ IPR). In the graph in Figure 4.2, the Σ IPRs of all genes that were analyzed in the RNA microarray analysis are plotted against their respective average microarray signals, and the genes that were selected as candidates for promoters are highlighted in red. These genes, 19 in total, all score relatively low on Σ IPR, meaning they should have stable expression in varying conditions, and span a wide range of average microarray signals, constituting their typical expression levels relative to actin. For looking up some of the raw data in this microarray analysis and information about the selected genes, see the attached Table A.2.

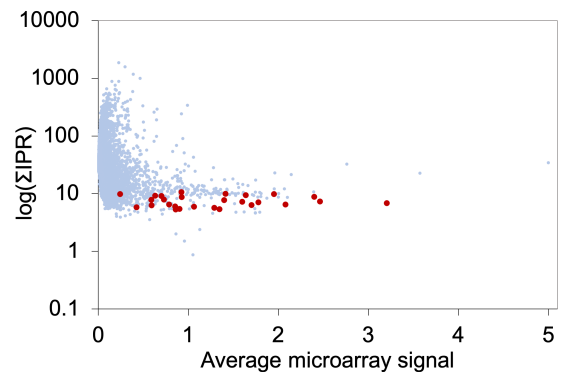


Figure 4.2: All genes screened in the RNA microarray analysis plotted logarithmically with cumulative IPR versus average signal (relative to actin). The 19 genes selected as candidates for constitutive promoters are highlighted in red.

Genes with stable expression levels were selected because they are likely to be under control of constitutive promoters. Therefore, the RNA microarray dataset was analyzed statistically in order to find and evaluate data points (genes) with minimal fluctuation in their measured microarray signals. This analysis was conducted by calculating the genes' Σ IPR, a metric that can be used as an indication of steadiness. Similarly, the data points could have been evaluated by standard deviation or variance, but here Σ IPR was used. A percentile is defined as the score or value (here: microarray signal) below which a given percentage of observations (here: the 155 measured conditions) can be found for a statistical population (here: more than 14,000 genes) [79]. This for example means that for a given gene in the dataset, the 30th percentile is the microarray signal below which 30 % of the measurements were. Then, IPR can be calculated as the difference between an upper and a lower percentile, for example is IPR 70-30 the difference between the 70th percentile and the 30th

percentile. For the current dataset, five IPRs were calculated for each gene (99-1, 95-5, 90-10, 80-20 and 70-30), meaning a perfectly steady gene would have Σ IPR of 5. If any one of the measured IPR values was high, the Σ IPR would correspondingly increase, indicating a less steady gene. As can be seen in Table A.2, all 19 selected genes had Σ IPR values between 5 and 10, thus clearly exhibiting steadiness.

Putative promoter sequences were amplified from the *A. niger* N402 genome and assembled into MoClo modules as described in section 3.1.1. The promoters were assumed to be expressed within 1 kb upstream of the coding sequences of the 19 selected genes, so all amplifications were done with primers targeting exactly this region. Cloning into the MoClo library makes the promoters readily available for rapid assembly into expression cassettes of interest, and is the first step to augmenting the *A. niger* promoter library. However, for the added promoters to be useful, they require characterization. In this project, because of limited time, only 6 of the 19 initially chosen and cloned promoters were selected for further characterization. In the microarray analysis it could be seen that two of these come from genes with considerably higher expression levels than actin, two are closer to actin, and two have lower average signals, as presented in Table 4.2. It was hypothesized that the promoters' strengths would be similarly ranked as these genes' average microarray signals, after they had been assayed.

Table 4.2: The promoters selected to be assayed in this project. Their names are derived from the genes they are amplified from, and "avg. signal" refers to the measured expression levels of these genes, relative to actin, in an *A. niger* RNA microarray analysis.

Name	Avg. signal
p <i>ANC1</i>	2.46
p <i>rp115</i>	1.95
p <i>L34.B</i>	1.41
p <i>NDK1</i>	0.93
p <i>leu2A</i>	0.63
p <i>rad24</i>	0.42

Each of the six promoters presented in Table 4.2 were put in control of luciferase in level 1 MoClo plasmids, but only four of these cassettes were successfully integrated in *A. niger*'s genome for the assay. As discussed in subchapter 4.1, there were significant delays in the construction of three of the promoter-luciferase constructs, but eventually the repeated efforts paid off and all six constructs were available. It is believed, as discussed in subchapter 4.3, that also the two failed

genomic integrations of reporter cassettes could have been rectified if the transformation experiment had been repeated. However, time limitations hindered this possibility. Therefore, two promoters were not available to be assayed, i.e. both the putatively strongest promoter (p*ANC1* with average microarray signal 2.46) as well as the one with putatively closest expression levels to actin (p*NDK1* with average microarray signal 0.93). Despite this reduction of the assay, the remaining four promoters do have a reasonably broad range of signals (0.42 to 1.95), which did lead to assay results that were similarly spread out.

Before discussing these results, some potential sources of experimental variability in the luciferase assay should be clarified. Firstly, the cultivation conditions in the wells were suboptimal. Insufficient aeration can be an effect when cultivating in these microtiter plates, and temperatures as high as 30 °C, which was the average temperature during plate monitoring, can cause condensation on the plate cover glass, which would disturb measurements. Also the growth morphology in these wells is not ideal for luminescence measurements. This is because the fungi tend to grow along the walls of the wells and start to sporulate. An image of the microtiter plate after the second luciferase assay had been conducted has been appended in Figure C.6. Although not strictly easy to see from this photograph, all wells had sporulated quite heavily when the two-day experiment was stopped. Finally, signal disturbances between the wells is a factor that should be taken into consideration. This was attempted to be accounted for by spacing the different strains apart on the microtiter plate, but might still cause interference with results from low-concentration measurements. Ideally, reporter assays should rather be completed in shake-flasks than microtiter plates. This is less stressful for the cells due to improved cultivation conditions, as well as removing some of the experimental inaccuracies caused by the well plate, giving more reliable measurements of the reporter's expression levels in non-stressed conditions.

Furthermore, an experimental factor that could be affecting the results includes variabilities in cell densities between the measured wells. The spore suspensions that were used to inoculate the cells were made from each strain (AA1-AA11) and counted microscopically in triplicates using a Thoma chamber, before being diluted to 10⁶ spores/mL which was then added to the microtiter plate. In this process, there are several steps with uncertainties leading to likely variances in the final added spore concentration. Any inaccuracy in

starting cell number would lead to different densities in the wells throughout the experiment, giving luminescence reads that are unrelated to the promoter strengths. However, based on the growth curves seen in the presentation of raw data in Appendix C.6, all 11 mutant strains had quite similar growth (apart from one measured well with significant outlier tendencies that caused it to be omitted; AA1.2 in the second experiment). Therefore it is assumed that the growth disturbances due to variabilities in starting cell number are negligible.

In the data presentation chosen for display in Figure 3.6, LCPS measurements are normalized against OD measurements. The idea is that luminescence is measured per cell instead of for the entire sample, and because OD corresponds to growth, this is used as an indicator of cell density. As all mutant strains had similar OD graphs (Figures C.7a and C.8a), this normalization did not alter the perception of the LCPS results significantly. In most bioluminescent reporter assays such as this one, other types of normalization are recommended, with the purpose of correcting for variations caused by experimental factors other than what is directly being tested [80], such as those discussed above. The choice of normalization depends, of course, on the purpose of the assay. In this assay, a normalization method that could have increased the statistical significance and confidence in the data is to compare the mutant strains' LCPS data to a strain expressing luciferase under the control of a well-characterized constitutive promoter. Here, the positive control strains express luciferase under control of the TetON system, the inducible and tunable system with expression-independent strength developed by Meyer *et al.* (2011) [33]. Although this promoter is well-characterized, its inducibility makes it less suited for normalization of data. Instead, as will be discussed in the coming paragraphs, the positive controls were here mostly used for visual comparisons of plots.

The positive control strains *A. niger* TS41.6 and TS41.13, known to be expressing functional luciferase under control of the TetON system, both grew faster and exhibited stronger luminescence signals than any of the strains constructed in this project. The decreased growth rates of AA1-AA11 in comparison is assumed to be due to their auxotrophy. Although *hisB* was restored in the genome editing that was done, the transformants are still *pyrG*⁻ due to their MF41.3 genetic background, which can be hampering their efficient growth, even in the complete medium that was supplied. The growth medium has all components required for auxotrophic strains to grow, but it is still likely that they will struggle more to

do so than non-auxotrophs. In optical density raw data from the initial luciferase assay (Figure C.7a), only one of the two positive controls' graphs clearly demonstrated increased growth. This was seen for TS41.6, whereas TS41.13 seemed closer to the the studied strains. However, in the two-day monitoring of samples, both positive controls exhibited much stronger growth than any other strains (Figure C.8a). Firstly, their growth curves appear to start rising earlier, pointing to shorter lag phases than the non-control strains. Then, in the time span between 5 and 35 hours, growth rate is similar for all strains, but the curves are higher for the positive controls because they had a more rapid initial growth spurt. Eventually, after over 35 hours, the wells inoculated with positive controls experience a drastic increase in optical density that is not matched in the other samples' wells. The reason for this sudden shift is likely linked to sporulation.

The increased luminescent signals from the positive controls, displayed in Figures C.7b and C.8b, is likely due to how the *luc* gene is expressed in these strains. Also when the LCPS measurements of positive controls were normalized against their increased growths, their signals remained much higher than for non-control strains (not shown). In TS41.6 and TS41.13, *luc* is placed under control of the inducible TetON promoter. It appears that with addition of 10 $\mu\text{g mL}^{-1}$ doxycycline, the expression of luciferase in these strains was very high, leading to very strong LCPS measurements. Further, it can be seen that in the first ~ 30 hours of both assays, TS41.6 is more luminescent than TS41.13. This is due to TS41.6 having the *luc* gene integrated in multiple copies in the genome, causing stronger expression of the reporter initially. However, in Figure C.8b, this imbalance appears to even out near 35 hours, before TS41.13 is the strain exhibiting highest LCPS signals. This could be a consequence of too high expression of luciferase over time, leading to accumulation in the cells or saturation of the enzyme's catalytic capabilities. The comparison between single- and multi-copy integration allowed by the two positive controls proves how important it was that the promoter-reporter cassette was integrated only once by the CRISPR-Cas edit. As discussed in subchapter 4.3, the qPCR analysis indicates that this is the case.

Evidenced by the optical density raw data (Figures C.7a and C.8a), the chosen negative control had limited growth in comparison to the other strains. This control strain was picked from transformation plates from the same experiment that yielded strains AA1-AA11, but from a colony with WT spore phenotype. This transformant had

previously been used as the negative control in diagnostic colony PCR of the successfully edited transformants, and was confirmed not to express luciferase. Therefore, it was considered convenient to keep using this mutant as a control. However, this should not have been done because of the uncertainties tied to using a transformant whose genotypes are not precisely known. Since this strain grew on the transformation plates, it must have incorporated the HisB marker that was used for selection, but it is not known where in the genome this has occurred. The limited growth curve indicates that this is a mutant with reduced viability. Instead of this control choice, an established strain without the *luc* gene should have been selected, with the most obvious choice being MF41.3, which was the genomic background before *luc* was integrated. In future repetitions of this assay, this should be taken into account.

Based on the LCPS graphs plotted for each well separately, it was decided that calculating a mean for each studied promoter was a reasonable and acceptable simplification of the data. It can be seen in Figure C.7c, where the colors correspond to the integrated promoter, that the measured wells' graphs in the first luciferase assay tend to cluster according to promoter. Blue (*pL34.B*) is highest, then yellow (*prpl15*), then green (*prad24*), and finally orange (*pleu2A*). A similar tendency is seen in Figure C.8c from the second, longer assay, but here the graphs are slightly less ordered. Despite this, based on the visual confirmation of a trend separating the promoters' strengths in all studied wells, averages were calculated and presented in this thesis (Figure 3.6). For a more scientific approach, standard deviation or a similar statistical measurement for uncertainty should have been analyzed for each calculated average, so that the choice of presenting averages could have been defended with more merit.

Repeating the assay twice was a good way to gain some confidence in the results that were yielded. Both the general trends of the OD and LCPS graphs, as well as the putative expression level rankings of different strains were the same for both assays, showing a reproducibility of results. When comparing the OD or LCPS measurements at the end of the initial assay (around 21 hours) to the same time in the second, two-day assay, it was generally found that they were very similar to each other. For monitoring of OD, the most important take-away was that all studied strains (AA1-AA11) had similar growth curves in both assays. Further, when plotting the normalized luminescence, the strains were ranked in the same order in both assays. This ranking from highest to lowest recorded luminescence was: TS41.6 (PC),

TS41.13 (PC), AA4-AA5, AA1-AA3, AA8-AA11, AA6-AA7 and NC. Assuming that luminescence corresponds to expression level of the reporter luciferase, this means that the four studied promoters can be ranked from high to low strength as: *pL34.B*, *prpl15*, *prad24* and *pleu2A*.

A comparison of this strength-based ranking of promoters to the average microarray signals of the genes they are derived from shows some similarities, but not entirely the same order. The hypothesis for this research, presented in the Objectives (subchapter 1.2), stated that there would be a link between the genes' microarray signals and the promoters' relative strengths. What the results of the two assays show, is that the two promoters that derive from genes with stronger expression than actin (*prpl15* and *pL34.B*) also produced the strongest luminescence signals, however flipped, i.e. *pL34.B* scoring higher than *prpl15* despite *prpl15* having higher average microarray signal. Likewise, the order of strengths from the two remaining promoters has been switched. Whereas *pleu2A* came from the gene with highest average microarray signal, *prad24* was found to be the stronger promoter of the two in both assays conducted here. These results are summarized in Table 4.3, to facilitate conceptualization and comparison of the different rankings.

Table 4.3: Promoters that were assayed in this project, ranked from strongest to weakest based on two different analytical methods; an RNA microarray analysis (Rank 1) and a luciferase reporter assay (Rank 2).

Name	Rank 1	Rank 2
<i>prpl15</i>	1	2
<i>pL34.B</i>	2	1
<i>pleu2A</i>	3	4
<i>prad24</i>	4	3

To discuss the possible reasons for these minor discrepancies between the hypothesized strengths of the promoters and what the assay results show, differences in how the two were obtained should be clarified. The microarray results used to predict promoters come from Paegle *et al.*'s meta-analysis of several independent expression profiling microarrays [62]. In each of these, oligo probes on a biochip have been used to bind to mRNA transcripts and indicate transcription levels of a vast array of genes simultaneously, indicating patterns of cellular expression in different conditions (155 distinct cultivation conditions). Based on this, genes with minor fluctuations in expression levels despite changes in growth conditions were selected as candidates for constitutive promoters. There-

fore, these 19 selected promoters should be robust, able to constitutively express the genes they precede even in suboptimal growth conditions. The cultivation methods during luciferase assays in this project are, as described, among these suboptimal conditions. Cells are likely stressed to a certain extent in the microtiter wells, but according to the meta-analysis of microarrays, this should not change the promoters' strengths.

On the other hand, there are facets of what the fungal cells are subjected to in this project that are not "covered" in the 155 different conditions that were used to determine average microarray signals. First, the effects of expressing a reporter gene can be mentioned. Although not toxic to the cells, the expression of luciferase could be a metabolic load that affects the operation of the promoters that were assayed. Because the microarray analysis was conducted on the transcriptome of *A. niger* CBS 513.88, no luciferase is expressed here. Further, the studied strains in this project (AA1-AA11) remain pyrimidine auxotrophs, which, as mentioned, could be a growth-limiting factor. However, even though there exists genomic differences between the strain studied in the microarray analysis and the transformants assayed here, it is unlikely that these differences are the true cause of the discrepancies in postulated promoter strengths. Typically, when a promoter has been proven to be robust in such a vast array of conditions as those covered by the meta-analysis, its strength can be considered an intrinsic property, and not something that varies due to extrinsic factors.

This supposition poses the question of whether the natural promoters' intrinsic properties are actually maintained during this research. The promoter sequences used here were amplified from regions 1 kb upstream of the genes they derive from. These putative sequences have never been analyzed when separated from their native genomic loci, and it is therefore not strictly known that the strength-determining sequences are within the 1 kb. However, the choice of length was not entirely arbitrary. During promoter characterizations, serial 5' deletion constructs are often tested in order to identify which segment of the upstream

region of a gene is responsible for promoting transcription [36]. Most promoters that are characterized this extensively typically have lengths between 100 bp and 1000 bp. Aspergilli promoters specifically tend to lie around 800 bp in length [32], but there are also articles describing longer promoters. The *pgpdA* promoter, often used for strong gene expression in different Aspergilli, has historically been 2.3 kb long. However, a recent study published results showing that a truncated form of *pgpdA* of only 836 bp was similarly strong as the traditional 2.3 kb version in *A. nidulans* [32]. Most likely, the 1 kb amplifications that were used in this project were sufficient, and including a longer segment of the promoters would not have changed the results of the assay.

The next consideration when evaluating the measured promoter strengths in comparison to the RNA microarray analysis concerns differences in an organism's transcriptome versus proteome. The RNA microarray dataset has measured the expression levels of each gene based on the amount of mRNA present in a sample at a specific time. Therefore, it can be seen as a direct measurement of how strong a promoter is, by how much mRNA it can produce when placed in front of a gene. This transcriptomic analysis method does, however, not account for the fact that mRNA degradations occur unequally for different transcripts. Some genes' mRNA molecules will be more stable than others, and can thereby give indications that the promoter is stronger than it actually is. Contrarily, unstable transcripts are degraded quicker, giving microarray signals that are lower, even for strong promoters. On the other hand, luciferase assays are analyzing a part of the cells' proteome. The proteome is naturally subject to even more changes from the actual promoter strength because further regulatory mechanisms and mRNA degradation has occurred, and is therefore a less direct approach to studying promoter strength. However, reporter assays such as this allow *in vivo* modeling, revealing facts about actual products that can be yielded from a given promoter. As was discussed in section 1.1.3, a complete characterization of a promoter necessitates that both of these characterization methods are analyzed for a full picture of how the promoter operates.

5 Conclusions

This research aimed to contribute to the expansion of *A. niger*'s genetic engineering toolbox by augmenting the promoter library. The MoClo method provided rapid and efficient cloning of recombinant plasmids, and allowed for use of standardized genetic modules constructed by other researchers. In total, this minimized the time required for cloning, thereby opening up for more comprehensive research to be completed within the time frames of this project. Because of this, the three large experiments described here, i.e. investigating DsRed expression in *A. niger*, testing a CRISPR-Cas system and assaying a set of promoters, have laid the groundwork for future projects with similar aims as this one. Although the evaluation of DsRed's functionality as a reporter in *A. niger* remains incomplete, the transformants expressing fluorescent proteins that were made in the course of this project are already being researched further, something that was expedited by the strain construction described here. Moreover, it has here been shown that the combination of *in vivo* expressed Cas9 and sgRNA, integration of a HisB marker for selection and only 100 bp long homology flanks is an efficient approach for stable, single-copy integrations in the genome of *A. niger*. In later promoter assays to be completed in this fungus, the same system can be employed to integrate reporter constructs reliably. Finally, the use of luciferase for this type of assay was proven to be dependable, having given identical internal results for the same four promoters in two separate experiments.

Despite slight differences between how the two analytical methods that were used to predict promoter strengths ranked the promoters, the main results are the same. In the microarray analysis, it was shown that the *rpl15* and *L34.B* genes had higher expression levels than actin, while the *leu2A* and *rad24* genes had around half of actin's expression. Correspondingly, the two promoters *prpl15* and *pL34.B* caused stronger ex-

pressions in the reporter assay than *pleu2A* and *prad24*. Therefore, it can be said that the introduced hypothesis is confirmed - there is a link between the genes' expression levels and the promoters' strengths. However, this general statement is far from a full characterization of the four promoters, and further analysis is therefore recommended. If the goal is that these promoters should be employed for industrial purposes, they need to be so precisely characterized that they can be used to compose a fine-tuned metabolic network with stable and defined expression levels of all genes. Then, it is not enough that the promoters' strengths are compared to each other in a single reporter assay, they also need to be evaluated by standardized methods, improving statistical significance and confidence in the data by analyzing differently normalized signals in more detail that was done here. To start with, the current reporter assay should be scaled up and conducted in shake-flasks, using an improved selection of control strains including a control promoter that is well-characterized, e.g. *pgpdA*. The effects of different media should also be tested, hopefully demonstrating some robustness in promoter strengths that translates to stable, constitutive expression of genes.

Available promoters are currently limited for *A. niger*, making any addition of constitutive promoters to the library very attractive. The cloning that was done here, preparing all 19 putative promoter sequences in MoClo modules for further study, is the first step to a library expansion. Thereafter, the promoters need characterization, something which was also initiated in this project. A comparison between a direct transcriptome analysis and an indirect proteome analysis was done, thereby contributing valuable knowledge about the behavior of the four selected 1 kb promoter regions. This paves the way for successful completion of the remaining promoter constructs in the near future.

References

- [1] T. M. van Leeuwe et al. 'Efficient marker free CRISPR/Cas9 genome editing for functional analysis of gene families in filamentous fungi'. In: *Fungal Biology and Biotechnology* 6 (2019), p. 13. ISSN: 2054-3085. DOI: 10.1186/s40694-019-0076-7.
- [2] V. Meyer et al. 'Growing a circular economy with fungal biotechnology: a white paper'. In: *Fungal Biology and Biotechnology* 7.1 (2nd Apr. 2020), p. 5. ISSN: 2054-3085. DOI: 10.1186/s40694-020-00095-z.
- [3] R. Fischer. *Mycology: unravelling the riddle of the filamentous fungi*. 1st June 2017. URL: <https://researchfeatures.com/2017/06/01/mycology-unravelling-riddle-filamentous-fungi-2/?cn-reloaded=1> (visited on 08/04/2020).
- [4] C. S. Nødvig et al. 'A CRISPR-Cas9 System for Genetic Engineering of Filamentous Fungi'. In: *PLoS ONE* 10.7 (15th July 2015). ISSN: 1932-6203. DOI: 10.1371/journal.pone.0133085.
- [5] V. Meyer et al. 'Current challenges of research on filamentous fungi in relation to human welfare and a sustainable bio-economy: a white paper'. In: *Fungal Biology and Biotechnology* 3 (31st Aug. 2016). ISSN: 2054-3085. DOI: 10.1186/s40694-016-0024-8.
- [6] H. A. El-Enshasy. 'Chapter 9 - Filamentous Fungal Cultures – Process Characteristics, Products, and Applications'. In: *Bioprocessing for Value-Added Products from Renewable Resources*. Ed. by S.-T. Yang. Amsterdam: Elsevier, 1st Jan. 2007, pp. 225–261. ISBN: 978-0-444-52114-9. DOI: 10.1016/B978-044452114-9/50010-4. URL: <http://www.sciencedirect.com/science/article/pii/B9780444521149500104> (visited on 30/03/2020).
- [7] S. C. Watkinson. 'Chapter 5 - Physiology and Adaptation'. In: *The Fungi (Third Edition)*. Ed. by S. C. Watkinson, L. Boddy and N. P. Money. Boston: Academic Press, 1st Jan. 2016, pp. 141–187. ISBN: 978-0-12-382034-1. DOI: 10.1016/B978-0-12-382034-1.00005-0. URL: <http://www.sciencedirect.com/science/article/pii/B9780123820341000050> (visited on 27/03/2020).
- [8] S.-Y. Zhu, Y. Xu and X.-W. Yu. 'Improved Homologous Expression of the Acidic Lipase from *Aspergillus niger*'. In: *Journal of Microbiology and Biotechnology* 30.2 (28th Feb. 2020), pp. 196–205. ISSN: 1738-8872. DOI: 10.4014/jmb.1906.06028.
- [9] P. F. Stanbury, A. Whitaker and S. J. Hall. 'Chapter 12 - The production of heterologous proteins'. In: *Principles of Fermentation Technology (Third Edition)*. Ed. by P. F. Stanbury, A. Whitaker and S. J. Hall. Oxford: Butterworth-Heinemann, 1st Jan. 2017, pp. 725–775. ISBN: 978-0-08-099953-1. DOI: 10.1016/B978-0-08-099953-1.00012-0.
- [10] S. Kilaru et al. 'Optimised red- and green-fluorescent proteins for live cell imaging in the industrial enzyme-producing fungus *Trichoderma reesei*'. In: *Fungal Genetics and Biology* 138 (1st May 2020), p. 103366. ISSN: 1087-1845. DOI: 10.1016/j.fgb.2020.103366.
- [11] *Signal Peptide Database*. URL: <http://www.signalpeptide.de/> (visited on 07/04/2020).
- [12] M. R. M. Fiedler et al. 'Conditional Expression of the Small GTPase ArfA Impacts Secretion, Morphology, Growth, and Actin Ring Position in *Aspergillus niger*'. In: *Frontiers in Microbiology* 9 (8th May 2018). ISSN: 1664-302X. DOI: 10.3389/fmicb.2018.00878.
- [13] C. Pohl et al. 'CRISPR/Cas9 Based Genome Editing of *Penicillium chrysogenum*'. In: *ACS Synthetic Biology* 5.7 (15th July 2016). Publisher: American Chemical Society, pp. 754–764. DOI: 10.1021/acssynbio.6b00082.
- [14] M. Ward et al. 'Characterization of humanized antibodies secreted by *Aspergillus niger*'. In: *Applied and Environmental Microbiology* 70.5 (May 2004), pp. 2567–2576. ISSN: 0099-2240. DOI: 10.1128/aem.70.5.2567-2576.2004.
- [15] H. H. Huynh et al. 'Functional production of human antibody by the filamentous fungus *Aspergillus oryzae*'. In: *Fungal Biology and Biotechnology* 7.1 (28th May 2020), p. 7. ISSN: 2054-3085. DOI: 10.1186/s40694-020-00098-w.
- [16] M. J. Kwon et al. 'Practical guidance for the implementation of the CRISPR genome editing tool in filamentous fungi'. In: *Fungal Biology and Biotechnology* 6.1 (17th Oct. 2019), p. 15. ISSN: 2054-3085. DOI: 10.1186/s40694-019-0079-4.
- [17] T. C. Cairns, C. Nai and V. Meyer. 'How a fungus shapes biotechnology: 100 years of *Aspergillus niger* research'. In: *Fungal Biology and Biotechnology* 5.1 (24th May 2018), p. 13. ISSN: 2054-3085. DOI: 10.1186/s40694-018-0054-5.
- [18] β -Galactosidase (*Aspergillus niger*). Megazyme. URL: <https://www.megazyme.com/beta-galactosidase-aspergillus-niger> (visited on 09/04/2020).

- [19] H. J. Pel et al. ‘Genome sequencing and analysis of the versatile cell factory *Aspergillus niger* CBS 513.88’. In: *Nature Biotechnology* 25.2 (Feb. 2007). Number: 2 Publisher: Nature Publishing Group, pp. 221–231. ISSN: 1546-1696. DOI: 10.1038/nbt1282.
- [20] L. Song et al. ‘Efficient genome editing using tRNA promoter-driven CRISPR/Cas9 gRNA in *Aspergillus niger*’. In: *PloS One* 13.8 (2018), e0202868. ISSN: 1932-6203. DOI: 10.1371/journal.pone.0202868.
- [21] C. L. Gordon et al. ‘A glucoamylase::GFP gene fusion to study protein secretion by individual hyphae of *Aspergillus niger*’. In: *Journal of Microbiological Methods*. Microbial Analysis at the Single Cell Level. 42.1 (1st Sept. 2000), pp. 39–48. ISSN: 0167-7012. DOI: 10.1016/S0167-7012(00)00170-6.
- [22] K. H. Choo, T. W. Tan and S. Ranganathan. ‘SPdb – a signal peptide database’. In: *BMC Bioinformatics* 6.1 (13th Oct. 2005), p. 249. ISSN: 1471-2105. DOI: 10.1186/1471-2105-6-249.
- [23] *SPdb : A Signal Peptide Database*. URL: <https://proline.bic.nus.edu.sg/spdb/> (visited on 20/04/2020).
- [24] K. R. Boppidi et al. ‘Altered secretion patterns and cell wall organization caused by loss of PodB function in the filamentous fungus *Aspergillus nidulans*’. In: *Scientific Reports* 8 (30th July 2018). ISSN: 2045-2322. DOI: 10.1038/s41598-018-29615-z.
- [25] T. R. Jørgensen et al. ‘Transcriptomic comparison of *Aspergillus niger* growing on two different sugars reveals coordinated regulation of the secretory pathway’. In: *BMC Genomics* 10.1 (23rd Jan. 2009), p. 44. ISSN: 1471-2164. DOI: 10.1186/1471-2164-10-44.
- [26] M. Fiedler et al. ‘Construction of an improved *Aspergillus niger* platform for enhanced glucoamylase secretion’. In: *Microbial Cell Factories* 17 (1st Dec. 2018). DOI: 10.1186/s12934-018-0941-8.
- [27] N. Taheri-Talesh et al. ‘The Tip Growth Apparatus of *Aspergillus nidulans*’. In: *Molecular Biology of the Cell* 19.4 (Apr. 2008), pp. 1439–1449. ISSN: 1059-1524. DOI: 10.1091/mbc.E07-05-0464.
- [28] D. Li et al. ‘Methods for genetic transformation of filamentous fungi’. In: *Microbial Cell Factories* 16.1 (3rd Oct. 2017), p. 168. ISSN: 1475-2859. DOI: 10.1186/s12934-017-0785-7.
- [29] M. Schuster and R. Kahmann. ‘CRISPR-Cas9 genome editing approaches in filamentous fungi and oomycetes’. In: *Fungal Genetics and Biology* 130 (1st Sept. 2019), pp. 43–53. ISSN: 1087-1845. DOI: 10.1016/j.fgb.2019.04.016.
- [30] M. Blumhoff et al. ‘Six novel constitutive promoters for metabolic engineering of *Aspergillus niger*’. In: *Applied Microbiology and Biotechnology* 97.1 (Jan. 2013), pp. 259–267. ISSN: 1432-0614. DOI: 10.1007/s00253-012-4207-9.
- [31] Y. Honda et al. ‘Stable and transient transformation, and a promoter assay in the selective lignin-degrading fungus, *Ceriporiopsis subvermispora*’. In: *AMB Express* 9.1 (24th June 2019), p. 92. ISSN: 2191-0855. DOI: 10.1186/s13568-019-0818-1.
- [32] J. K. H. Rendsvig, C. T. Workman and J. B. Hoof. ‘Bidirectional histone-gene promoters in *Aspergillus*: characterization and application for multi-gene expression’. In: *Fungal Biology and Biotechnology* 6.1 (9th Dec. 2019), p. 24. ISSN: 2054-3085. DOI: 10.1186/s40694-019-0088-3.
- [33] V. Meyer et al. ‘Fungal Gene Expression on Demand: an Inducible, Tunable, and Metabolism-Independent Expression System for *Aspergillus niger*’. In: *Applied and Environmental Microbiology* 77.9 (May 2011), pp. 2975–2983. ISSN: 0099-2240. DOI: 10.1128/AEM.02740-10.
- [34] T. J. Rudge et al. ‘Characterization of Intrinsic Properties of Promoters’. In: *ACS Synthetic Biology* 5.1 (15th Jan. 2016), pp. 89–98. ISSN: 2161-5063. DOI: 10.1021/acssynbio.5b00116.
- [35] *Bioluminescent Reporters, Reporter Gene Applications, An Introduction to Reporter Genes*. Promega Germany. URL: <https://www.promega.de/resources/guides/cell-biology/bioluminescent-reporters/> (visited on 11/07/2020).
- [36] H.-Y. Song et al. ‘A Novel Rapid Fungal Promoter Analysis System Using the Phosphopantetheinyl Transferase Gene, *npgA*, in *Aspergillus nidulans*’. In: *Mycobiology* 46.4 (17th Dec. 2018), pp. 429–439. ISSN: 1229-8093. DOI: 10.1080/12298093.2018.1548806.
- [37] K. D. Piatkevich and V. V. Verkhusha. ‘Guide to Red Fluorescent Proteins and Biosensors for Flow Cytometry’. In: *Methods in cell biology* 102 (2011), pp. 431–461. ISSN: 0091-679X. DOI: 10.1016/B978-0-12-374912-3.00017-1.
- [38] S. J. Remington. ‘Negotiating the speed bumps to fluorescence’. In: *Nat Biotech* 20.1 (Jan. 2002). Publisher: Nature Publishing Group, pp. 28–29. ISSN: 1087-0156. DOI: 10.1038/nbt0102-28.
- [39] T. Lambert. *EGFP at FPbase*. FPbase. URL: <https://www.fpbase.org/protein/egfp/> (visited on 11/07/2020).
- [40] T. Lambert. *DsRed-Express at FPbase*. FPbase. URL: <https://www.fpbase.org/protein/dsred-express/> (visited on 02/05/2020).

- [41] G. S. Baird, D. A. Zacharias and R. Y. Tsien. ‘Biochemistry, mutagenesis, and oligomerization of DsRed, a red fluorescent protein from coral’. In: *Proceedings of the National Academy of Sciences of the United States of America* 97.22 (24th Oct. 2000), pp. 11984–11989. ISSN: 0027-8424.
- [42] N. C. Shaner, P. A. Steinbach and R. Y. Tsien. ‘A guide to choosing fluorescent proteins’. In: *Nature Methods* 2.12 (8th Nov. 2005). DOI: 10.1038/NMETH819.
- [43] J. M. Hurley et al. ‘Analysis of clock-regulated genes in *Neurospora* reveals widespread posttranscriptional control of metabolic potential’. In: *Proceedings of the National Academy of Sciences* 111.48 (2nd Dec. 2014), p. 16995. DOI: 10.1073/pnas.1418963111.
- [44] S. C. Company. *Bioluminescent Determination of ATP with Luciferase-Luciferin*. Nov. 1991. URL: <https://www.sigmaaldrich.com/content/dam/sigma-aldrich/docs/Sigma/Bulletin/10633bul.pdf> (visited on 03/07/2020).
- [45] S. T. Allard. *Bioluminescent Reporter Genes*. Promega Corporation Web site. Oct. 2008. URL: <https://www.promega.de/resources/pubhub/enotes/bioluminescent-reporter-genes/> (visited on 02/06/2020).
- [46] I. Mougiakos et al. ‘Next Generation Prokaryotic Engineering: The CRISPR-Cas Toolkit’. In: *Trends in Biotechnology* 34.7 (1st July 2016), pp. 575–587. ISSN: 0167-7799. DOI: 10.1016/j.tibtech.2016.02.004.
- [47] D. L. Nelson and M. M. Cox. *Lehninger Principles of Biochemistry*. 7th. New York, NY 10004-1562: W.H. Freeman & Co. Ltd, 2017. 1271 pp. ISBN: 978-1-4641-2611-6.
- [48] L. Cong et al. ‘Multiplex genome engineering using CRISPR/Cas systems’. In: *Science (New York, N.Y.)* 339.6121 (15th Feb. 2013), pp. 819–823. ISSN: 1095-9203. DOI: 10.1126/science.1231143.
- [49] M. C. Bassalo et al. ‘Rapid and Efficient One-Step Metabolic Pathway Integration in *E. coli*’. In: *ACS Synthetic Biology* 5.7 (15th July 2016), pp. 561–568. DOI: 10.1021/acssynbio.5b00187. (Visited on 15/12/2019).
- [50] A. Idnurm and V. Meyer. ‘The CRISPR revolution in fungal biology and biotechnology, and beyond’. In: *Fungal Biology and Biotechnology* 5.1 (20th Dec. 2018), p. 19. ISSN: 2054-3085. DOI: 10.1186/s40694-018-0064-3.
- [51] H. Nevalainen. *Grand Challenges in Fungal Biotechnology*. Google-Books-ID: I9jIDwAAQBAJ. Springer Nature, 2019. 534 pp. ISBN: 9783030295417.
- [52] K. S. Makarova et al. ‘An updated evolutionary classification of CRISPR–Cas systems’. In: *Nature Reviews Microbiology* 13.11 (Nov. 2015), pp. 722–736. ISSN: 1740-1534. DOI: 10.1038/nrmicro3569.
- [53] F. Safari et al. ‘CRISPR Cpf1 proteins: structure, function and implications for genome editing’. In: *Cell & Bioscience* 9 (9th May 2019). ISSN: 2045-3701. DOI: 10.1186/s13578-019-0298-7.
- [54] J. McDade. *The PAM Requirement and Expanding CRISPR Beyond SpCas9*. URL: <https://blog.addgene.org/the-pam-requirement-and-expanding-crispr-beyond-spcas9> (visited on 24/11/2019).
- [55] N. D. S. P. Carvalho et al. ‘Expanding the ku70 toolbox for filamentous fungi: establishment of complementation vectors and recipient strains for advanced gene analyses’. In: *Applied Microbiology and Biotechnology* 87.4 (July 2010), pp. 1463–1473. ISSN: 0175-7598. DOI: 10.1007/s00253-010-2588-1.
- [56] V. Meyer et al. ‘Highly efficient gene targeting in the *Aspergillus niger kusA* mutant’. In: *Journal of Biotechnology* 128.4 (10th Mar. 2007), pp. 770–775. ISSN: 0168-1656. DOI: 10.1016/j.jbiotec.2006.12.021.
- [57] E. Weber et al. ‘A modular cloning system for standardized assembly of multigene constructs’. In: *PLoS One* 6.2 (18th Feb. 2011), e16765. ISSN: 1932-6203. DOI: 10.1371/journal.pone.0016765.
- [58] Addgene: *MoClo Modular Cloning System Plasmid Kits*. URL: <https://www.addgene.org/cloning/moclo/> (visited on 21/04/2020).
- [59] iGEM Boston University. *Modular Cloning DNA Assembly*. igem.org, 2013. URL: <http://2013.igem.org/Team:BostonU/MoCloChara>.
- [60] NEB. *BioBrick Assembly - NEB*. URL: <https://international.neb.com/applications/cloning-and-synthetic-biology/dna-assembly-and-cloning/biobrick-assembly> (visited on 15/05/2020).
- [61] *Type IIS Restriction Enzymes - NEB*. URL: <https://international.neb.com/tools-and-resources/selection-charts/type-iis-restriction-enzymes> (visited on 21/04/2020).
- [62] N. Paegle et al. ‘A Transcriptome Meta-Analysis Proposes Novel Biological Roles for the Antifungal Protein AnAFP in *Aspergillus niger*’. In: *PLOS ONE* 11.11 (11th Nov. 2016). Publisher: Public Library of Science, e0165755. ISSN: 1932-6203. DOI: 10.1371/journal.pone.0165755.
- [63] C. J. Bos et al. ‘Genetic analysis and the construction of master strains for assignment of genes to six linkage groups in *Aspergillus niger*’. In: *Current Genetics* 14.5 (Nov. 1988), pp. 437–443. ISSN: 0172-8083. DOI: 10.1007/BF00521266.
- [64] M. R. M. Fiedler et al. ‘HisB as novel selection marker for gene targeting approaches in *Aspergillus niger*’. In: *BMC Microbiology* 17 (8th Mar. 2017). ISSN: 1471-2180. DOI: 10.1186/s12866-017-0960-3.

- [65] T. Schuetze and V. Meyer. ‘Polycistronic gene expression in *Aspergillus niger*’. In: *Microbial Cell Factories* 16 (1st Dec. 2017), p. 162. DOI: 10.1186/s12934-017-0780-z.
- [66] S. Werner et al. ‘Fast track assembly of multigene constructs using Golden Gate cloning and the MoClo system’. In: *Bioengineered* 3.1 (Jan. 2012), pp. 38–43. ISSN: 2165-5979, 2165-5987. DOI: 10.4161/bbug.3.1.18223.
- [67] NEB. *Nucleic Acid Data*. New England Biolabs Inc. URL: <https://international.neb.com/tools-and-resources/usage-guidelines/nucleic-acid-data> (visited on 01/07/2020).
- [68] F. Wanka et al. ‘Tet-on, or Tet-off, that is the question: Advanced conditional gene expression in *Aspergillus*’. In: *Fungal Genetics and Biology*. The Era of Synthetic Biology in Yeast and Filamentous Fungi 89 (1st Apr. 2016), pp. 72–83. ISSN: 1087-1845. DOI: 10.1016/j.fgb.2015.11.003.
- [69] D. Kalderon et al. ‘A short amino acid sequence able to specify nuclear location’. In: *Cell* 39.3 (Dec. 1984), pp. 499–509. ISSN: 0092-8674. DOI: 10.1016/0092-8674(84)90457-4.
- [70] M. Maeda, T. Shimada and A. Ishihama. ‘Strength and Regulation of Seven rRNA Promoters in *Escherichia coli*’. In: *PLOS ONE* 10.12 (2015), e0144697. ISSN: 1932-6203. DOI: 10.1371/journal.pone.0144697.
- [71] A. Vinck et al. ‘Heterogenic expression of genes encoding secreted proteins at the periphery of *Aspergillus niger* colonies’. In: *Environmental Microbiology* 13.1 (2011), pp. 216–225. ISSN: 1462-2920. DOI: 10.1111/j.1462-2920.2010.02322.x.
- [72] D. J. Jeenes et al. ‘A truncated glucoamylase gene fusion for heterologous protein secretion from *Aspergillus niger*’. In: *FEMS microbiology letters* 107.2 (1st Mar. 1993), pp. 267–271. ISSN: 0378-1097. DOI: 10.1111/j.1574-6968.1993.tb06041.x.
- [73] C. L. Gordon et al. ‘Glucoamylase::green fluorescent protein fusions to monitor protein secretion in *Aspergillus niger*’. In: *Microbiology (Reading, England)* 146 (Pt 2) (Feb. 2000), pp. 415–426. ISSN: 1350-0872. DOI: 10.1099/00221287-146-2-415.
- [74] L. Wang et al. ‘Secretory overproduction of a raw starch-degrading glucoamylase in *Penicillium oxalicum* using strong promoter and signal peptide’. In: *Applied Microbiology and Biotechnology* 102.21 (Nov. 2018), pp. 9291–9301. ISSN: 1432-0614. DOI: 10.1007/s00253-018-9307-8.
- [75] M. R. Andersen, L. Lehmann and J. Nielsen. ‘Systemic analysis of the response of *Aspergillus niger* to ambient pH’. In: *Genome Biology* 10.5 (2009), R47. ISSN: 1465-6906. DOI: 10.1186/gb-2009-10-5-r47.
- [76] E. B. J. T. Buren et al. ‘Toolkit for visualization of the cellular structure and organelles in *Aspergillus niger*’. In: *ACS synthetic biology* 3.12 (19th Dec. 2014), pp. 995–998. ISSN: 2161-5063. DOI: 10.1021/sb500304m.
- [77] T. R. Jørgensen et al. ‘The molecular and genetic basis of conidial pigmentation in *Aspergillus niger*’. In: *Fungal Genetics and Biology* 48.5 (1st May 2011), pp. 544–553. ISSN: 1087-1845. DOI: 10.1016/j.fgb.2011.01.005.
- [78] A. L. Mefferd et al. ‘Expression of CRISPR/Cas single guide RNAs using small tRNA promoters’. In: *RNA* 21.9 (Sept. 2015), pp. 1683–1689. ISSN: 1355-8382. DOI: 10.1261/rna.051631.115.
- [79] *percentile*. Merriam-Webster.com Dictionary. URL: <https://www.merriam-webster.com/dictionary/percentile> (visited on 08/07/2020).
- [80] C. Eggers et al. ‘Designing a Bioluminescent Reporter Assay: Normalization’. In: *Promega Corporation* (Sept. 2016). URL: <https://www.promega.de/resources/pubhub/designing-a-bioluminescent-reporter-assay-normalization/> (visited on 10/07/2020).

Appendices

A Supplementary Tables

A.1 Primers

Table A.1 can be used to find primer (and other oligonucleotide) sequences. Their appearance in the table is sorted by purpose, as indicated by a short description above each list. Numbers were given to the primers in the order of them being designed and their names briefly describe functions. All of these primers were at some point used in this project, while primers used to construct plasmids that were already made at the start of this project are not shown.

Table A.1: Primers used directly in this project. Uppercase lettering indicates nucleotides binding to the target, and lowercase indicates overhangs. FW stands for forward and R for reverse direction of the primers, where forward means 5'-3'. Underlined sequences identify relevant restriction enzyme recognition sites.

Number	Name	Sequence (5'-3')
PCR amplifications of promoters (p-) and terminators (t-) for MoClo level 0:		
2442	prpl15_FW	<u>cggaagacaaggag</u> ATTCACATTTCCCTACTGTTCTTCTCGTTGAC
2443	prpl15_R	<u>cggaagacaacat</u> TCTGGACGAAAATCGGAATATCAGTCTCTGG
2444	pleu2A_FW	<u>cggaagacaaggag</u> TCATTGGACTGTACCTGCTCTCTTTCTCTTC
2445	pleu2A_R	<u>cggaagacaacat</u> TGATGAGGACAAGCAGGGAAGATAGTTTGG
2446	peEF-2_FW	<u>cggaagacaaggag</u> GATGTTATCTTCAATGAAAAGAAGCTGACCAAG
2447	peEF-2_R	<u>cggaagacaacat</u> FCTTGACTGATTTTTTCTCGTCAACTGCCG
2448	phxk_FW-1	<u>cggaagacaaggag</u> GAAGTGGACCGGCTCACGGAG
2449	phxk_R-1	<u>cggaagacaagaacacat</u> GAGCCAATCCCCAATCC
2450	phxk_FW-2	<u>cggaagacaa</u> GTTCCCGCATCTGGCGCGAATG
2451	phxk_R-2	<u>cggaagacaa</u> CATTGATGACGGTGAATAGATATTAGATGGAGAAAG- AGG
2452	thxK_FW	<u>cggaagacaagctt</u> TGACCTGGCGCACATAAATATGAATTCTTTGG
2453	thxK_R	<u>cggaagacaagcg</u> CATCCATGATGGTTCCCTACATGATACATGC
2454	ppyc_FW	<u>cggaagacaaggag</u> ATTGACCGAGCGTCCATGGCG
2455	ppyc_R	<u>cggaagacaacat</u> TGGCGGGCGGGGTGTGTTTGTGATAAGG
2456	tpyc_FW	<u>cggaagacaagctt</u> AAGAGTAACACCGTTATAACGGCAAGG
2457	tpyc_R	<u>cggaagacaagcg</u> CATCGGAGATGAGGACCCCTG
2458	pFKS_FW	<u>cggaagacaaggag</u> GGGGAGGGTGAAGCGGGCTTG
2459	pFKS_R	<u>cggaagacaacat</u> TGTTGAATAGCCACAATCACCGAACC
2460	ptal1_FW	<u>cggaagacaaggag</u> TCCCATTTTAAAAGGCGAAATGAACGCG
2461	ptal1_R	<u>cggaagacaacat</u> TGGTGGAGGTAGAGAATGAGATGAAGAAAG
2462	pL34.B_FW	<u>cggaagacaaggag</u> TAGCCCATTGGGCGTGGAAC
2463	pL34.B_R	<u>cggaagacaacat</u> TTTTGTCTGTCTTGAACCTCTAGGTCGGTGT- CTCAAGAGATTGGCGGCG
2464	prad24_FW-1	<u>cggaagacaaggag</u> ACTTCCCTTCCCCCTCCC
2465	prad24_R-1	<u>cggaagacaaca</u> GTTCTCCAGCATCATGAGGG
2466	prad24_FW-2	<u>cggaagacaa</u> ACTGATACGTATGACGGGATTTCCC
2467	prad24_R-2	<u>cggaagacaa</u> CATTTGTGAAAGATTATCTGAACGAGAGAAGAGATG- TTAG
2468	pcypA_FW	<u>cggaagacaaggag</u> GTGGGACTGGATTTCTTTCTTGTTTTCTTC
2469	pcypA_R	<u>cggaagacaacat</u> TGGCTGCGGATGATGATGGAAAGG
2470	tcypA_FW	<u>cggaagacaagctt</u> GCGGTTTTCAAGGATAACAGATGGC
2471	tcypA_R	<u>cggaagacaagcg</u> CAGCAAGCAAGGAAAGCAAAGTGGAAATG
2472	pH3_FW	<u>cggaagacaaggag</u> TGTGAAGGTTGTCTAAAAAGTAAACGGAAATA- GAG
2473	pH3_R	<u>cggaagacaacat</u> FCTTAGTGGATTAAGTTTGTGATGGATTTAGTTGTT- TTAG
2474	pH4_FW	<u>cggaagacaaggag</u> CTTAGTGGATTAAGTTTGTGATGGATTTAGTTGTT- TTAG
2475	pH4_R	<u>cggaagacaacat</u> TTGTGAAGGTTGTCTAAAAAGTAAACGGAAATAG- AG
2476	pcpY_FW	<u>cggaagacaaggag</u> GCCGAAGGCCTTTGTTAACTCGG

2477	pcpY_R	cggaagacaacatTTGTTGCTGAAACCCTACGGGG
2478	tcpY_FW	cggaagacaagcttAGACGTGCTACCACCGCATATAGAC
2479	tcpY_R	cggaagacaaaGCGCCTGGGACCGGGAACAATATTAGAAAATG
2480	pNDK-1_FW	cggaagacaaggagTATCGTGTGCGAAGCTGGATGTCACC
2481	pNDK-1_R	cggaagacaacatTTTTGATGGATTTGAGAGTATAACAATGAAGTC- ACTG
2482	pcitA_FW	cggaagacaaggagGCCATGAGAACTGTGTTCTTACAGGC
2483	pcitA_R	cggaagacaacatTGGCGAATGTGAACAACCTTGCAGTAAG
2484	pL10_FW	cggaagacaaggagCAAGACCTCCGCGTGAGTATACC
2485	pL10_R	cggaagacaacatTCTTGACTGCTGGAAATGGGGC
2486	ptpiA_FW	cggaagacaaggagGGGCCCGGAACGATATTCGGG
2487	ptpiA_R	cggaagacaacatTTTTGAAGATGTGTTGGTGTGATTGGAAAAGAC
2488	pANC1_FW	cggaagacaaggagATTTAAGTAACTGAGTTTTGTGAGTTGTCTCCAA- ACAATTTCTACACAGGAGG
2489	pANC1_R	cggaagacaacatTTTTGACGGCTGTGATGAACGAAAACCTAAGG
2490	pTEF-1_FW	cggaagacaaggagTTTTCCCTCACATGTTTTGCCCGC
2491	pTEF-1_R	cggaagacaacatTGATGACGGTTGTGAATGAACTCGAAG
MoClo plasmid screening:		
2173	Lvl-0-screening-FW	AATAGGCGTATCACGAGGC
2174	Lvl-0-screening-R	AGTCAGTGAGCGAGGAAGC
2175	Lvl-1-screening-FW	CACATTGCGGACGTTTTTAATGTAAGT
2176	Lvl-1-screening-R	CCGCCAATATATCCTGTCAAACACTG
2177	Lvl-2-screening-FW	GCCTGGTGTCTTACTACGTGAT
2178	Lvl-2-screening-R	GCATGTTCTTACAACAACATCCG
Oligos for annealing sgRNAs targeting <i>fwnA</i> locus:		
2287	sgRNA_fwnA-T3_F	CGTCTCAGGCCCATCTTGTGGCCTGTGCACGTTTTGAGACG
2288	sgRNA_fwnA-T3_R	CGTCTCAAACCGTGCACAGGCCAACAAAGATGGGCCTGAGACG
2289	sgRNA_fwnA-T14_F	CGTCTCAGGCCTCGCTTGGAGCAGACGGCGCGTTTTGAGACG
2290	sgRNA_fwnA-T14_R	CGTCTCAAACCGCGCCGTCTGCTCCAAGCGAGGCCTGAGACG
PCR amplifications for making CRISPR-Cas donor DNA targeting <i>fwnA</i> locus:		
2341	TU-X-fwnA-targ-fw	agcattagtggattattatgcgagttccatcaataggatggtaggtgtgtcagtcctagcgcgagtc- ttggaggaaggcgaatgatacaaatCCGCCAATATATCCTGTCAAACA- CTG
2342	TU-X-fwnA-targ-rev	aaagtgtgcgtctcatcgacacggatgtggaaggccagatggactttggtctgacaacggcgattga- ccgatcaatagacatcttcgcaaacCACATTGCGGACGTTTTTAATGTA- CTG
2334	TU-1-rev	gtagggaatggattctcggtgccctttatgggaattatgatacattggcttctactttgataca- gagattattacaccgacacctcattCACATTGCGGACGTTTTTAATGTA- CTG
2335	TU-2-fw	aatgaggtgtcgtgtaataatctctgtatcaaagtagcaagccaatgtatcataattccataaag- ggggcaccgagaatccattccccTACCCGCCAATATATCCTGTCAAACA- CTG
Colony PCR verifying insertion of <i>dsRed</i> in <i>fwnA</i> locus:		
1445	fwnA_fw	AGCCAGTCCCCTGTCAGT
2563	DsRed-CN_2_R	ACCTTGATGATGAAGGAGCCG
Colony PCR verifying insertion of <i>luc</i> in <i>fwnA</i> locus:		
446	mlucfw	GGATTACGTGCGCCAGTCAAG
2092	fwnA_term_rev	TTCCTATCGCCGATTGCG
qPCR verifying copy number of <i>tamdS</i>:		
2734	tamdS-qPCR_Fw-1	CCTGCCGTAGAACCGAAGAG
2735	tamdS-qPCR_Rev-1	GTGAGAGACACTTGTGCCGT
2736	tamdS-qPCR_Fw-2	GGCACAAGTGTCTCTCACCAA
2737	tamdS-qPCR_Rev-1	TCACCTGTGGCAGCATGAG
Positive control for colony PCR and qPCR, actin:		
2275	An15g00560_qPCR-1F	ACAATGAACTCCGTGTGCT
2276	An15g00560_qPCR-1R	GATGGAGACGTAGAAGGCGG
2278	An15g00560_qPCR-2R	CTCGTCTACTCCTGCTTGG

A.2 Promoters

Table A.2 presents the promoters originally chosen for this project. Their selection was based on a RNA microarray dataset, giving microarray signals for more than 14,000 *A. niger* genes in 155 different conditions. The genes' average signals and steadiness (metric used is cumulative IPR) are given here, and can be seen graphically in Figure 4.2.

Table A.2: The 19 promoters originally selected for research in this project. Average signals relative to actin (“Avg. signal”) and cumulative interpercentile range (\sum IPR, metric for steadiness) are listed, based on a 2016 meta-analysis of measured RNA microarray signals in 155 cultivation conditions [62]. Promoter names indicate the genes they derive from (also presented with ProbeID gene names), and are explained in the description column.

Name	Gene	Description	Avg. signal	\sum IPR
<i>phxk</i>	An02g14380	Hexokinase (hxx), <i>Aspergillus niger</i>	0.24	9.855
<i>prad24</i>	An07g07760	Strong similarity to DNA damage checkpoint protein rad24, <i>Schizosaccharomyces pombe</i>	0.42	5.798
<i>pcpY</i>	An08g08750	Carboxypeptidase Y (cpy) of patent WO9609397-A1, <i>Aspergillus niger</i>	0.59	7.815
<i>pleu2A</i>	An01g14130	β -isopropylmalate dehydrogenase A (leu2A), <i>Aspergillus niger</i>	0.63	9.178
<i>pcitA</i>	An09g06680	Citrate synthase citA, <i>Aspergillus niger</i>	0.73	7.875
<i>ptpiA</i>	An14g04920	Triose-phosphate-isomerase tpiA of patent WO8704464-A, <i>Aspergillus niger</i>	0.79	6.504
<i>pFKS</i>	An06g01550	Strong similarity to glucan synthase FKS, <i>Paracoccidioides brasiliensis</i>	0.85	6.015
<i>ptal1</i>	An07g03850	Strong similarity to transaldolase tal1, <i>Saccharomyces cerevisiae</i>	0.90	5.433
<i>ppycA</i>	An04g02090	Pyruvate carboxylase pyc, <i>Aspergillus niger</i>	0.92	10.595
<i>pNDK-1</i>	An09g05870	Strong similarity to nucleoside-diphosphate kinase NDK-1, <i>Neurospora crassa</i>	0.93	8.690
<i>pH4</i>	An08g06940	Strong similarity to histone H4.1, <i>Emericella nidulans</i>	1.29	5.666
<i>peEF-2</i>	An02g05700	Strong similarity to translation elongation factor eEF-2 <i>Cricetulus griseus</i>	1.40	7.703
<i>pL34.B</i>	An07g07430	Strong similarity to cytoplasmic ribosomal protein of the large subunit L34.B, <i>Saccharomyces cerevisiae</i>	1.41	9.942
<i>pL10</i>	An12g04870	Strong similarity to cytoplasmic ribosomal protein of the large subunit L10, <i>Saccharomyces cerevisiae</i>	1.60	7.235
<i>pcypA</i>	An07g08300	Cyclophilin-like peptidyl prolyl cis-trans isomerase cypA, <i>Aspergillus niger</i>	1.70	6.309
<i>prpl15</i>	An01g03460	Cytoplasmic ribosomal protein of the large subunit L15 rpl15, <i>Aspergillus niger</i>	1.95	9.862
<i>pH3</i>	An08g06960	Strong similarity to histone H3, <i>Emericella nidulans</i>	2.08	6.501
<i>pANC1</i>	An18g04220	Strong similarity to mitochondrial ADP/ATP carrier ANC1, <i>Schizosaccharomyces pombe</i>	2.46	7.286
<i>pTEF-1</i>	An18g04840	Strong similarity to translation elongation factor 1 α , <i>Podospora anserina</i>	3.21	6.857

A.3 Plasmids

The following sections present the MoClo plasmids that are relevant to this project. Some were made in the course of this project and some were constructed prior to the project starting, but were used in experiments directly. MoClo plasmids are named “pMC_<level>_<number>” in order of design. A short description listing relevant modules (promoters, coding sequences, terminators etc.) and the plasmid backbone that was used (pICH-/pAGM-) are also indicated.

A.3.1 MoClo Level 0

Table A.3 gives an overview of the MoClo level 0 plasmids that were made or used directly in the course of this project. Some plasmids were, at the end of the project, still not successfully constructed, as indicated by an asterisk and no given concentration.

Table A.3: Level 0 MoClo plasmids prepared in, or relevant for, this project. Plasmids marked by * are not yet verified and/or were dropped.

Name	Description	Size	Conc.
		[bp]	[ng μL^{-1}]
pMC_0_15	tcgrA pICH41295	2549	95
pMC_0_26	pANtRNA-Pro1-sgRNA-dummy pICH41331	3970	192
pMC_0_27	pANtRNA-Arg21-sgRNA-dummy pICH41331	3731	173
pMC_0_46	prpl15 pICH41295	3251	25
pMC_0_47	pleu2A pICH41295	3251	17
pMC_0_48*	peEF-2 pICH41295	3251	-
pMC_0_49*	phxk pICH41295	3251	-
pMC_0_50	thxK pICH41276	2751	18
pMC_0_51	ppyc pICH41295	3251	24
pMC_0_52	tpyc pICH41276	2751	16
pMC_0_53*	pFKS pICH41295	3251	-
pMC_0_54	ptal1 pICH41295	3251	16
pMC_0_55	pl34.B pICH41295	3251	25
pMC_0_56	prad24 pICH41295	3251	25
pMC_0_57	pcypA pICH41295	3251	24
pMC_0_58	tcypA pICH41276	2751	20
pMC_0_59	pH3 pICH41295	3079	24
pMC_0_60	pH4 pICH41295	3079	29
pMC_0_61	pcpY pICH41295	3251	30
pMC_0_62	tcpY pICH41276	2751	18
pMC_0_63	pNDK-1 pICH41295	3251	23
pMC_0_64	pcitA pICH41295	3251	25
pMC_0_65	pL10 pICH41295	3251	24
pMC_0_66	ptpiA pICH41295	3230	54
pMC_0_67	pANC1 pICH41295	3251	39
pMC_0_68*	pTEF1 pICH41295	3251	-
pMC_0_69	Firefly-Luc pICH41308	3907	62

A.3.2 MoClo Level 1

Table A.4 gives an overview of the MoClo level 1 plasmids that were used during this project.

Table A.4: Level 1 MoClo plasmids prepared in, or relevant for, this project.

Name	Description	Size [bp]	Conc. [ng μL^{-1}]
pMC_1.6	pHisB-HisB-tamdS pICH47761	6627	280
pMC_1.27	phttA-DsRed-glaA-tag-HS-tcgrA pICH47742	6173	23
pMC_1.28	phttA-DsRed-SKL-tcgrA pICH47742	6131	82
pMC_1.29	phttA-DsRed-NLS-tcgrA pICH47742	6188	62
pMC_1.35	phttA-DsRed-glaA-tag-LS-tcgrA pICH47742	6197	66
pMC_1.36	phttA-eGFP-glaA-tag-LS-tcgrA pICH47742	6175	62
pMC_1.39	pANC1-firefly-Luc-tcgrA pICH47742	7338	93
pMC_1.40	prpl15-firefly-Luc-tcgrA pICH47742	7338	200
pMC_1.41	pL34.B-firefly-Luc-tcgrA pICH47742	7338	245
pMC_1.42	pNDK1-firefly-Luc-tcgrA pICH47742	7338	171
pMC_1.43	pleu2A-firefly-Luc-tcgrA pICH47742	7338	107
pMC_1.44	prad24-firefly-Luc-tcgrA pICH47742	7338	86

A.3.3 MoClo Level 2

Table A.5 gives an overview of the MoClo level 2 plasmids that were used in this project.

Table A.5: Level 2 MoClo plasmids prepared in, or relevant for, this project.

Name	Description	Size [bp]	Conc. [ng μL^{-1}]
pMC_2.2	AMA-DsRed-hisB pAGM4723	11543	391
pMC_2.4	TetON-DsRed-hisB pAGM4723	12029	44
pMC_2.5	MekON-DsRed-hisB pAGM4723	12879	95
pMC_2.6	AMA-DsRed-phttA-Cas9-ergA pAGM4723	18049	76
pMC_2.14	AMA-DsRed SKL-hisB pAGM4723	11564	92
pMC_2.15	AMA-DsRed NLS-hisB pAGM4724	11621	99
pMC_2.17	AMA-DsRed-glaA-LS-hisB pAGM4723	11630	88
pMC_2.18	AMA-DsRed-glaA-HS-hisB pAGM4723	11606	163
pMC_2.19	AMA-eGFP-glaA-LS-hisB pAGM4723	11672	80

A.3.4 sgRNA Plasmids

Table A.6 presents the four plasmids used in this project to supply guide RNA in CRISPR-Cas9 genome editing. All were made by assembling tRNA genes (tRNA^{Pro1} or tRNA^{Arg21}) into a MoClo level 0 receiver plasmid, adding the sgRNA (T3 or T14) by oligonucleotide extension PCR, and religating the resulting fragment into a functional plasmid.

Table A.6: Plasmids for transcription of sgRNA. “Conc. 1” refers to sample concentration for the experiment detailed in Table A.9 and “Conc. 2” refers to sample concentration for the experiment detailed in Table A.10.

Name	Description	Size [bp]	Conc. 1 [ng μL^{-1}]	Conc. 2 [ng μL^{-1}]
psgRNA_1	<i>fwnA</i> -T3 tRNA ^{Pro1}	3403	108	-
psgRNA_2	<i>fwnA</i> -T14 tRNA ^{Pro1}	3403	105	-
psgRNA_3	<i>fwnA</i> -T3 tRNA ^{Arg21}	3164	71	454
psgRNA_4	<i>fwnA</i> -T14 tRNA ^{Arg21}	3164	108	123

A.4 PCR Products

In transformations of *A. niger* using the CRISPR-Cas system, donor DNA was supplied as PCR products. Table A.7 presents the PCR products numbered in the order that they were made, with a brief description of the genetic components, the amplification’s template DNA and primers, and the resulting amplicon size. All have 100 bp flanks designed to target the *funA* locus, added from primers by oligonucleotide extension PCR. The concentrations presented here correspond to the samples used during transformation experiments, i.e. after PCR clean-up was done.

Table A.7: PCR products used as donor DNA in *A. niger* transformation experiments.

Name	Description	Template	Primer fwd.	Primer rev.	Size [bp]	Conc. [ng μL^{-1}]
PCR_1	TetON-DsRed-hisB	pMC_2.4	2341	2342	7488	158
PCR_2	MekON-DsRed-hisB	pMC_2.5	2341	2342	8338	71
PCR_3	pANC1-firefly-Luc-tcgrA	pMC_1.39	2341	2334	3295	415
PCR_4	prpl15-firefly-Luc-tcgrA	pMC_1.40	2341	2334	3295	385
PCR_5	pL34.B-firefly-Luc-tcgrA	pMC_1.41	2341	2334	3295	270
PCR_6	pNDK1-firefly-Luc-tcgrA	pMC_1.42	2341	2334	3295	255
PCR_7	pleu2A-firefly-Luc-tcgrA	pMC_1.43	2341	2334	3295	400
PCR_8	prad24-firefly-Luc-tcgrA	pMC_1.44	2341	2334	3295	466
PCR_9	pHisB-HisB-tamdS	pMC_1.6	2335	2342	2583	320

A.5 Details of Transformation Experiments

Tables A.8, A.9 and A.10 show the volumes added to each *A. niger* transformation parallel completed in this project. Each DNA sample is named as in Tables A.3-A.7, and the samples’ concentrations and sizes/lengths were taken into consideration to determine volumes.

Table A.8: Volumes of DNA samples pipetted in each parallel of the *A. niger* transformation experiment using non-integrative plasmids to express fluorescent proteins (DsRed and eGFP) targeted to different cellular localizations. Here, V is volume, SKL stands for serine-lysine-leucine (a peroxisomal targeting signal), NLS is a nuclear localization signal, GlaA is the naturally secreted protein glucoamylase A, and LS/HS stands for low and high stringency of the secretion signal (30 amino acids/22 amino acids).

Description	Plasmid	V [μL]
DsRed-SKL	pMC_2.14	33
DsRed-NLS	pMC_2.15	30
DsRed-GlaA(LS)	pMC_2.17	33
DsRed-GlaA(HS)	pMC_2.18	18
eGFP-GlaA(LS)	pMC_2.19	38
Positive control	pMC_2.2	20
Negative control	(TE-Buffer)	33.5

Table A.9: Volumes of DNA samples pipetted in each parallel of an *A. niger* transformation experiment demonstrating CRISPR-Cas9 system functionality. Here, V is volume, pMC.2.6 is the Cas9-carrying plasmid, psgRNA.1-4 are the guide-carrying plasmids and PCR.1-2 are donor DNA cassettes.

Description	$V_{\text{pMC.2.6}}$ [μL]	$V_{\text{psgRNA.1}}$ [μL]	$V_{\text{psgRNA.2}}$ [μL]	$V_{\text{psgRNA.3}}$ [μL]	$V_{\text{psgRNA.4}}$ [μL]	$V_{\text{PCR.1}}$ [μL]	$V_{\text{PCR.2}}$ [μL]
CRISPR-Cas9 (1)	10	14	14	-	-	32	-
CRISPR-Cas9 (2)	10	14	14	-	-	-	42
CRISPR-Cas9 (3)	10	-	-	21	14	32	-
CRISPR-Cas9 (4)	10	-	-	21	14	-	42
Cas9, no sgRNA	10	-	-	-	-	32	-
Positive control	(20 μL pMC.2.2)						
Negative control	(33.5 μL TE-Buffer)						

Table A.10: Volumes of DNA samples pipetted in each parallel of an *A. niger* transformation to integrate promoter-luciferase constructs genomically by CRISPR-Cas technology. Here, V is volume, pMC.2.6 is the Cas9-carrying plasmid, psgRNA.3-4 are the guide-carrying plasmids and PCR.3-9 are donor DNA cassettes.

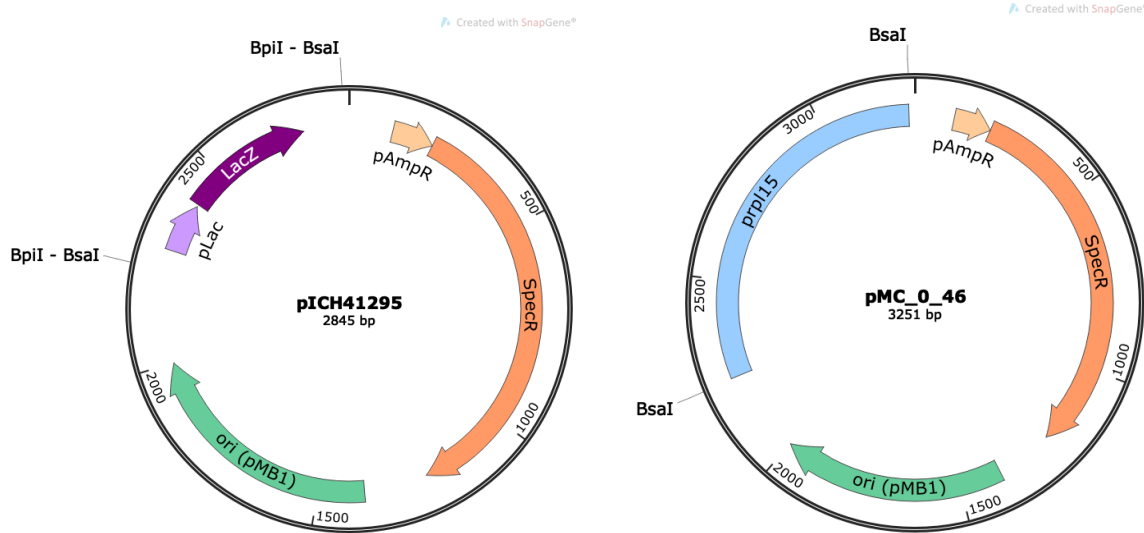
Description	$V_{\text{pMC.2.6}}$ [μL]	$V_{\text{psgRNA.3}}$ [μL]	$V_{\text{psgRNA.4}}$ [μL]	$V_{\text{PCR.3-8}}$ [μL]	$V_{\text{PCR.9}}$ [μL]
p <i>ANC1</i>	7	3.5	12	4 (PCR.3)	5
p <i>rpl15</i>	7	3.5	12	6 (PCR.4)	5
p <i>L34.B</i>	7	3.5	12	6 (PCR.5)	5
p <i>NDK1</i>	7	3.5	12	6 (PCR.6)	5
p <i>leu2A</i>	7	3.5	12	4 (PCR.7)	5
p <i>rad24</i>	7	3.5	12	4 (PCR.8)	5
Positive control	(42 μL pMC.2.2)				
Negative control	(42 μL TE-Buffer)				

B Supplementary Figures

B.1 Plasmid Maps

B.1.1 MoClo Level 0

Figure B.1 shows an example *in silico* assembly of a MoClo level 0 plasmid by first showing the plasmid map of a MoClo level 0 destination vector with relevant restriction sites, and then a promoter module assembled into the backbone by restriction-ligation.



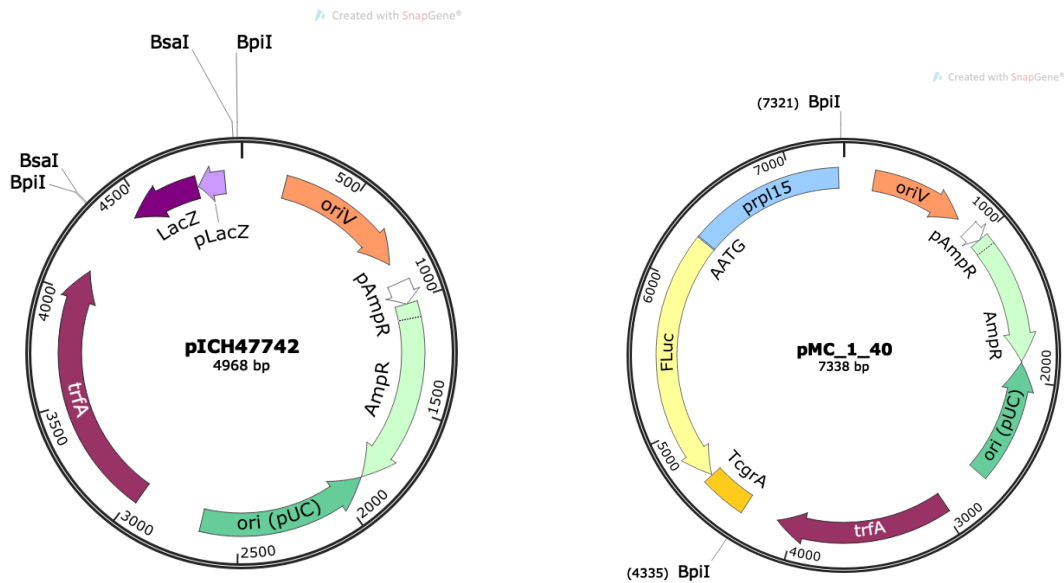
(a) Level 0 destination vector pICH41295.

(b) Level 0 plasmid pMC_0_46 carrying *prpl15*.

Figure B.1: MoClo level 0 assembly. By cutting the destination vector with BpiI, the promoter module could be ligated in place of the LacZ cassette. The resulting plasmid can again be restricted by BsaI for assembly of the promoter in a level 1 plasmid. Here, “ori” stands for origin of replication, “SpecR” is the spectinomycin resistance gene and “pAmpR” is the promoter for ampicillin resistance.

B.1.2 MoClo Level 1

Figure B.2 shows an example *in silico* assembly of a MoClo level 1 plasmid by first showing the plasmid map of a MoClo level 1 destination vector with relevant restriction sites, and then a promoter-luciferase-terminator expression cassette assembled into the backbone by restriction-ligation.



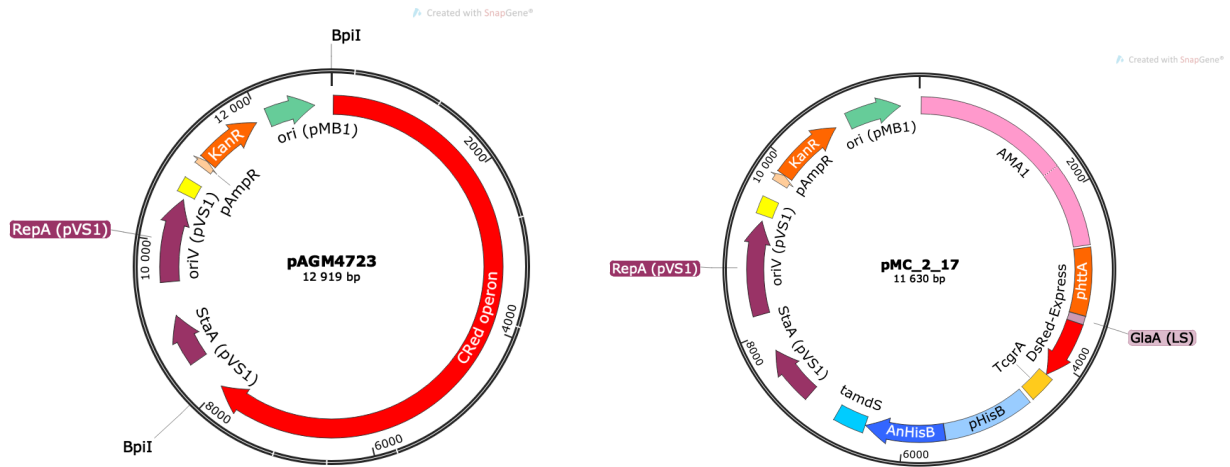
(a) Level 1 destination vector pICH47742.

(b) Level 1 plasmid pMC.1_40 carrying *FLuc* (firefly luciferase) under the control of *prpI5*.

Figure B.2: MoClo level 1 assembly. By cutting the destination vector with BsaI, inserts can be assembled in place of the LacZ cassette. The resulting plasmid can again be restricted by BpiI for assembly of the promoter in a level 2 plasmid. Here, “ori” stands for origin of replication, “trfA” is encoding a trans-acting replication protein that binds to and activates oriV, “AmpR” is the ampicillin resistance gene with “pAmpR” as the corresponding promoter.

B.1.3 MoClo Level 2

Figure B.3 shows an example *in silico* assembly of a MoClo level 0 plasmid by first showing the plasmid map of a MoClo destination vector with relevant restriction sites, and then a multigene assembly of *AMA1*, *dsRed* and *hisB* into the backbone.



(a) Level 2 destination vector pAGM4723.

(b) Level 2 AMA plasmid pMC.2.17 carrying *GlaA*-tagged *DsRed* under control of the *phttA* promoter, and the *HisB* marker (*A. niger hisB*).

Figure B.3: MoClo level 2 assembly. By cutting the destination vector with *BpiI*, inserts can be assembled in place of the *CRed* operon. Here, “ori” stands for origin of replication, “RepA” encodes a plasmid replication protein, “StaA” encodes a plasmid stability protein, “KanR” is the kanamycin resistance gene and “pAmpR” is the promoter for ampicillin resistance.

C Supporting Results

C.1 Diagnostic Colony PCR

C.1.1 MoClo Plasmid Integration

To illustrate how MoClo colony PCR results were interpreted, Figure C.1 shows the agarose gel readout when two colonies of each *E. coli* transformant with pMC_0.56-pMC_0.67 (twelve constructs) were screened. In these level 0 MoClo plasmids, either a terminator or a promoter has been inserted in the MoClo receiver plasmid. The primers are designed to amplify the region of interest where the insert is, giving amplicons of 652 bp for terminator constructs and 1152 bp for promoter constructs. In the case presented here, positive results were found for at least one colony of each of the twelve constructs.

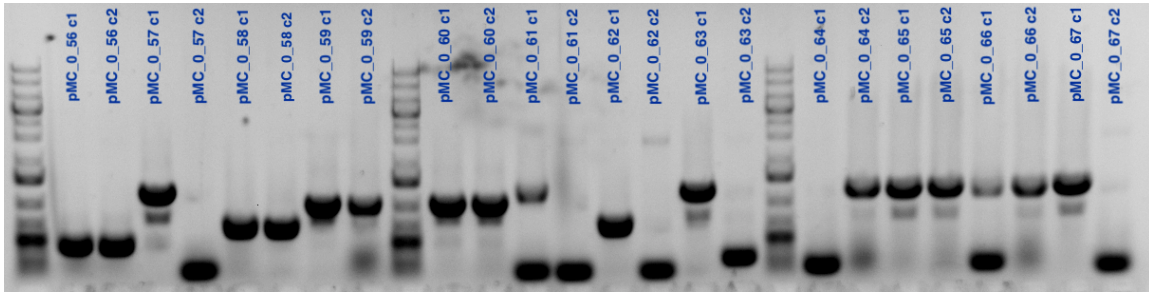


Figure C.1: Picture from an agarose gel where two colonies each from twelve MoClo level 0 plasmids have been screened.

C.1.2 *A. niger* Genomic Integration of DsRed Cassettes

Colony PCR of *A. niger* transformants was done to verify correct genomic integration of TetON-DsRed-hisB or MekON-DsRed-hisB cassettes in the *fwnA* locus, and the readout is shown in Figure C.2. Primers 1445 and 2563 (see Table A.1), which bind upstream of the *fwnA* locus and within the DsRed gene, were used. For the TetON-carrying inserts, the amplicon should be 1314 bp, and for the MekON, the amplicon should be 1754. The results indicate that a correct integration has occurred in all 8 colonies that were screened (4 different transformation experiment parallels). A black sporulating colony was picked as a negative control, and this did not yield any bands in the colony PCR.

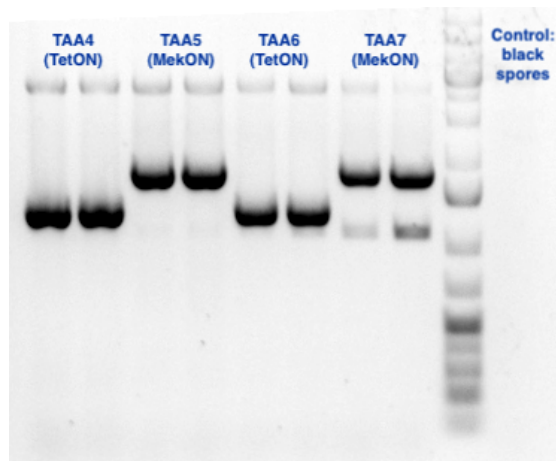


Figure C.2: Picture from an agarose gel where two colonies each of four different *A. niger* transformants (TAA4-TAA7) were analyzed by colony PCR. The transformants had inserted DsRed cassettes in the *fwnA* locus, and primers were designed to verify correct insertion.

C.1.3 *A. niger* Genomic Integration of Luciferase Cassettes

A diagnostic colony PCR was done to verify correct genomic integration of promoter-luciferase constructs in the *fwnA* locus of *A. niger*, and the readout is shown in Figure C.3. Primers 2093 and 446, which bind downstream of the *fwnA* locus and within the *luc* gene, were used. 11 colonies were screened (AA1-AA11), all giving positive results with amplicons of 1040 bp. As positive control for the PCR, actin was also amplified with primers 2275 and 2278, giving amplicons of 880 bp. Four negative controls were also included, which all were transformants that had negative phenotype screens (black spores).

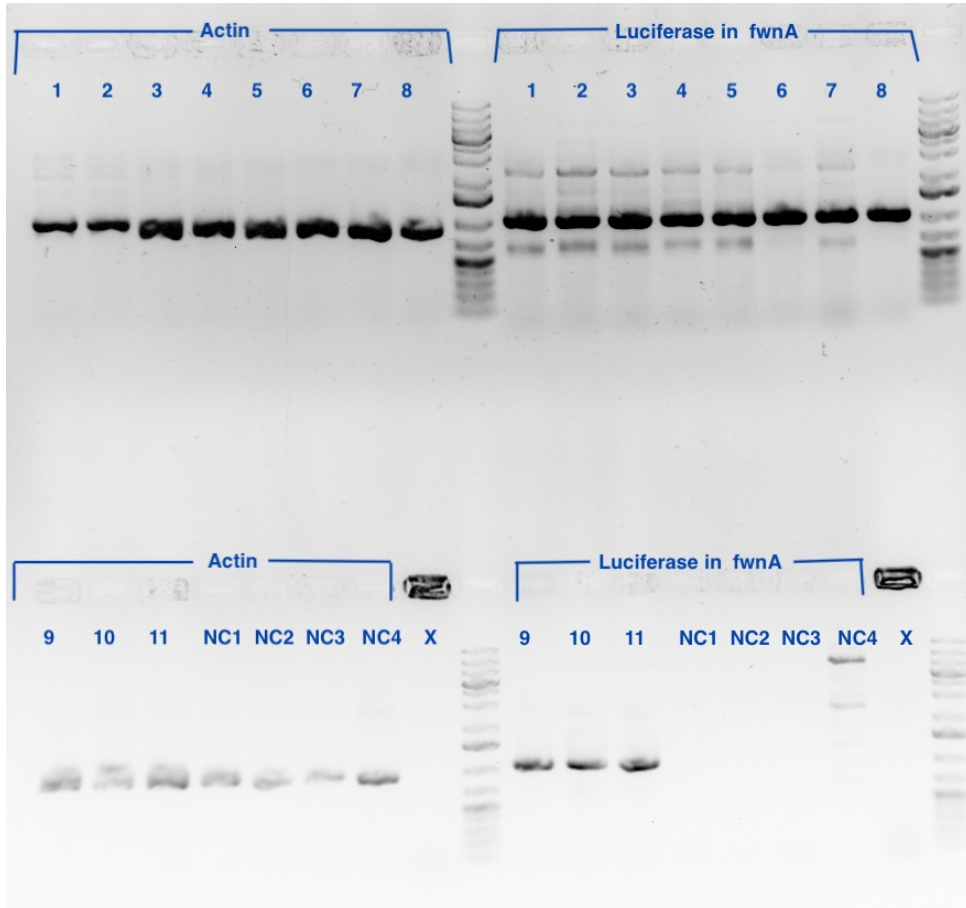


Figure C.3: Picture from an agarose gel where 11 CRISPR-Cas-edited *A. niger* transformants were analyzed by colony PCR. The transformants had inserted promoter-luciferase cassettes in the *fwnA* locus, and primers were designed to verify correct insertion. Actin served as a positive control. NC stands for negative control and were colonies with negative phenotype screens (black spores).

C.2 Sequencing of MoClo Level 0 Plasmid

An exemplary aligning of sequencing results from a level 0 plasmid can be seen attached on the next page. pMC_0.55, harboring *pL34.B*, was amplified with primers 2173 and 2174. The alignment was generated using the software ApE (Davis, M. Wayne. *ApE - A plasmid Editor*. <https://jorgensen.biology.utah.edu/wayned/apE/>). Within the region of interest, only single-nt mismatches are found, and never in both sequencing directions, indicating a successful assembly of promoter *pL34.B* into the destination vector pICH41295.

Wed Jun 03, 2020 11:50 CEST
0_55.fa from 1152 to 1

Alignment to
55F.ab1-- Matches:1112; Mismatches:14; Gaps:196; Unattempted:0
55R.ab1-- Matches:1117; Mismatches:6; Gaps:172; Unattempted:0

```
* * * * *
1152<AA-----T-A-----G-GC-G-----T-----A-T-C-----A-----C-G-A-G-G-----C--C-TTT-C--G-----T-C-C-----AC-T-<1121
1>-----G-C-----G-C-----G-A-A-A-A-A-T-T-T-G-A-T-T-T-T-T-T-T-A-A-A-A-A-T-A-A-A-C-A-A-A-T-G-G-G-T-C-G-G-C-A-C-----C--G-----C-----A----->12
1264<AAGGGGT-TT-TT-TT-C-TT-G-G-C-G-A-A-A-A-T-T-T-G-A-T-T-T-T-T-T-T-A-A-A-A-A-T-A-A-A-C-A-A-A-T-G-G-G-T-C-G-G-C-A-C-----C--G-----C-----A----->1160
```

```
* * * * *
1120<--G-A--A-----G-A-----G-C-----C-A-C-----T-TCG-----T--G-G-----T-C-T---C--ACATTTTGTCTGTCC<1084
13>--G--A-----G--A-----G-C-----C-A-C-----T-TCG-----T--G-G-----T-C-T---C--ACATTTTGTCTGTCC>45
1159<TAAAGAACCAATTATTATCAAGACATTACCCCTATAAAAAATAGCCGATACAGAGGCGCTTCGTTCCACTGAAGAGCCACTTCCTGGTCTCAATTTTGTCTGTCC>1055
```

```
* * * * *
1083<TTGAACCTCTAGGTCGGTGTCTCAAGAGATTGGCGGGCGGCTCGTGGTGTGTCGTCGTGACCTCGTAGAATTCGCGGTAATCTGGATTGTGTGGGTTTCG<979
46>TTGAACCTCTAGGTCGGTGTCTCAAGAGATTGGCGGGCGGCTCGTGGTGTGTCGTCGTGACCTCGTAGAATTCGCGGTAATCTGGATTGTGTGGGTTTCG>150
1054<TTGAACCTCTAGGTCGGTGTCTCAAGAGATTGGCGGGCGGCTCGTGGTGTGTCGTCGTGACCTCGTAGAATTCGCGGTAATCTGGATTGTGTGGGTTTCG<950
```

```
* * * * *
978<CTCGGAGCCCTGGGCGGGCCGCTAGCGCTAATTTGGCGAGAACCGCCTATCCCAAATGCGGACTAGTACCAGCCCGAGCAGAGCCGCCACCTCTTTTCAGACTT<874
151>CTCGGAGCCCTGGGCGGGCCGCTAGCGCTAATTTGGCGAGAACCGCCTATCCCAAATGCGGACTAGTACCAGCCCGAGCAGAGCCGCCACCTCTTTTCAGACTT>255
949<CTCGGAGCCCTGGGCGGGCCGCTAGCGCTAATTTGGCGAGAACCGCCTATCCCAAATGCGGACTAGTACCAGCCCGAGCAGAGCCGCCACCTCTTTTCAGACTT<845
```

```
* * * * *
873<GCTTCATCAAAACAAGGCAGGAGAAGCAAGAAGAGACTGGAGCAAGCTGTCTTATCACCCTCCCGTCGTGAGAAGGGATCGTCCAGGAGTGGTTTATCTTCTTCG<769
256>GCTTCATCAAAACAAGGCAGGAGAAGCAAGAAGAGACTGGAGCAAGCTGTCTTATCACCCTCCCGTCGTGAGAAGGGATCGTCCAGGAGTGGTTTATCTTCTTCG>360
844<GCTTCATCAAAACAAGGCAGGAGAAGCAAGAAGAGACTGGAGCAAGCTGTCTTATCACCCTCCCGTCGTGAGAAGGGATCGTCCAGGAGTGGTTTATCTTCTTCG<740
```

```
* * * * *
768<GGGCAAAGCTTTCATTTCTCCGACGCGATTTCTTTTATCCACGTGTTTAAATCCCCCTCCTCCATTCCGTTTTTTCGCGTCGCTGAGCTGCAGTCGATGAGCTC<664
361>GGGCAAAGCTTTCATTTCTCCGACGCGATTTCTTTTATCCACGTGTTTAAATCCCCCTCCTCCATTCCGTTTTTTCGCGTCGCTGAGCTGCAGTCGATGAGCTC>465
739<GGGCAAAGCTTTCATTTCTCCGACGCGATTTCTTTTATCCACGTGTTTAAATCCCCCTCCTCCATTCCGTTTTTTCGCGTCGCTGAGCTGCAGTCGATGAGCTC<635
```

```
* * * * *
663<GCGATAAGTCACGACCCGTGCATCTTTTGACGCGACTTAGTCACGAAACTTCCAGCCCGTCTATCAGAGCAGAGAGCGTCTTTCATATATACAACCATTACCAT<559
466>GCGATAAGTCACGACCCGTGCATCTTTTGACGCGACTTAGTCACGAAACTTCCAGCCCGTCTATCAGAGCAGAGAGCGTCTTTCATATATACAACCATTACCAT>570
634<GCGATAAGTCACGACCCGTGCATCTTTTGACGCGACTTAGTCACGAAACTTCCAGCCCGTCTATCAGAGCAGAGAGCGTCTTTCATATATACAACCATTACCAT<530
```

```
* * * * *
558<GGCATCATTTGCTCCCGCTCCGCTCCGCGTGGGGTGGCTCGGCGCCCGCTTCGATGCGCTTGCTCCTCCGCCACCGGGATATCAACCCTGCGGATCCGAC<454
571>GGCATCATTTGCTCCCGCTCCGCTCCGCGTGGGGTGGCTCGGCGCCCGCTTCGATGCGCTTGCTCCTCCGCCACCGGGATATCAACCCTGCGGATCCGAC>475
529<GGCATCATTTGCTCCCGCTCCGCTCCGCGTGGGGTGGCTCGGCGCCCGCTTCGATGCGCTTGCTCCTCCGCCACCGGGATATCAACCCTGCGGATCCGAC<425
```

```
* * * * *
453<GTTCGCAAAAGTTTGGCCAGAAGAAGATGAATGGCTGCGGACGCAACCGAACCCTTCGGCGAGAAGAGAAAGGGTGGATTGTTGAAACACAAAAGGCTGATAT<349
676>GTTCGCAAAAGTTTGGCCAGAAGAAGATGAATGGCTGCGGACGCAACCGAACCCTTCGGCGAGAAGAGAAAGGGTGGATTGTTGAAACACAAAAGGCTGATAT>780
424<GTTCGCAAAAGTTTGGCCAGAAGAAGATGAATGGCTGCGGACGCAACCGAACCCTTCGGCGAGAAGAGAAAGGGTGGATTGTTGAAACACAAAAGGCTGATAT<320
```

```
* * * * *
348<GCCCGCGGAGCATCTGCGAAAGATCGTTAGGGACATTGGCGATGTGTCGAAAAGAAAGTTAGCAACGAGAAGCGCAGCTACCTCGGCGCGTTGAAGTTTCATGCC<244
781>GCCCGCGGAGCATCTGCGAAAGATCGTTAGGGACATTGGCGATGTGTCGAAAAGAAAGTTAGCAACGAGAAGCGCAGCTACCTCGGCGCGTTGAAGTTTCATGCC>885
319<GCCCGCGGAGCATCTGCGAAAGATCGTTAGGGACATTGGCGATGTGTCGAAAAGAAAGTTAGCAACGAGAAGCGCAGCTACCTCGGCGCGTTGAAGTTTCATGCC<215
```

```
* * * * *
243<CCATGCTGTGTTGAAGCTGCTGGAGAACATGCCATGCTTGGGAATCGGCTAGGGAAGTTAAGGATTTGATATCATGTTAATGGTTGCCCTTACCTTGGTCAATGA<139
886>CCATGCTGTGTTGAAGCTGCTGGAGAACATGCCATGCTTGGGAATCGGCTAGGGAAGTTAAGGATTTGATATCATGTTAATGGTTGCCCTTACCTTGGTCAATGA>990
214<CCATGCTGTGTTGAAGCTGCTGGAGAACATGCCATGCTTGGGAATCGGCTAGGGAAGTTAAGGATTTGATATCATGTTAATGGTTGCCCTTACCTTGGTCAATGA<110
```

```
* * * * *
138<GACTCCCGTGTCAATTGAGCCCGTGTCCACGCCAATGGGCTACTCTGAGACCACAGAGTGATTAATGAATCGGCCAA-C---G-----C-G-----C---<54
991>GACTCCCGTGTCAATTGAGCCCGTGTCCACGCCAATGGGCTACTCTGAGACCACAGAGTGATTAATGAATCGGCCAA-C---G-----C-G-----C--->1094
109<GACTCCCGTGTCAATTGAGCCCGTGTCCACGCCAATGGGCTACTCTGAGACCACAGAGTGATTAATGAATCGGCCAA-C---G-----C-G-----C---<25
```

```
* * * * *
53<--G-G-----G-----G-A--G-A-G-G-----C--GG-T-T-T-G-----C-G-----T--A--T---T--G-G-G-CG-CT-C-T-T--C-CGC<18
1095>ATGGGCCCCCTTCCGCTCCCGGCAAGAGGCTGCTGGTTGTTGTTGGTGGCGGAAGGGGTTTCACTTACCTTAAAGGGGGGAAATAGGTTTTCCTCC>1199
24<--G-----G-----G-A--G-A-G-G-----C--GG-T-T-T-G-----C-G-----T--A--T---T--G-G-G-CG-CT-C-T-T--C-CGC<7
```

```
*
17<--TT-C-----C-----T--C--G-C-T-----C-A-CT--G-A-----C-T<1
1200>AATTTCCGGGAAAAACCGGGGAAAAATTCCTGCTGTGTAAGAAAGGCTAATAAGGGGAAAACTT>1267
6<--T--C-----C-----C-----C-----C-----G-----<1
```

C.3 Plasmid Restriction Analysis

To illustrate how restriction analysis results were interpreted, Figure C.4 shows the agarose gel readout from a trial digestion of three MoClo level 1 plasmids; pMC_1.39, pMC_1.43 and pMC_1.44. All these plasmids contain an expression cassette of promoter-luciferase-terminator, and have the same sizes. Digestion with BpiI verifies that these level 1 plasmids can be used to build level 2, and yields two bands of 4352 bp and 2986 bp. Digestion with XbaI and XhoI was also completed on one selected colony from each, because these enzymes are cutting within the MoClo insert, giving two bands of 5557 bp 1781 bp in the case of pMC_1.39 and three bands of 5025 bp, 1781 bp and 532 bp in the cases of pMC_1.43 and pMC_1.44. Thereby, this digestion can prove that the fragments assembled in the correct order. Apart from pMC_1.44 c3, all plasmids in this figure were verified.

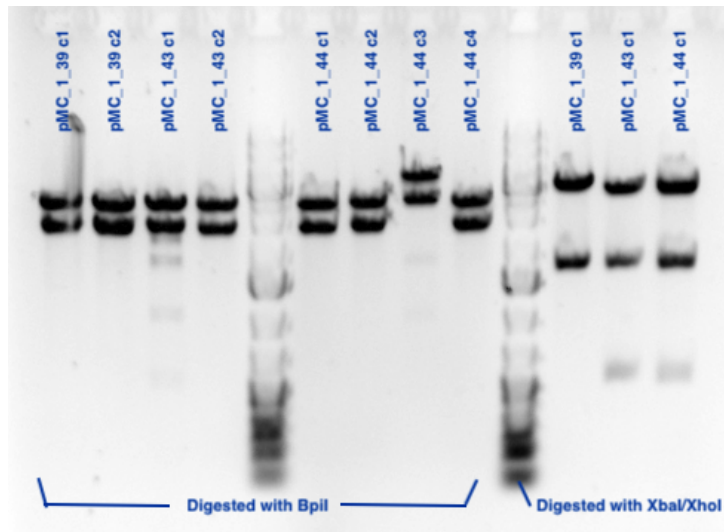
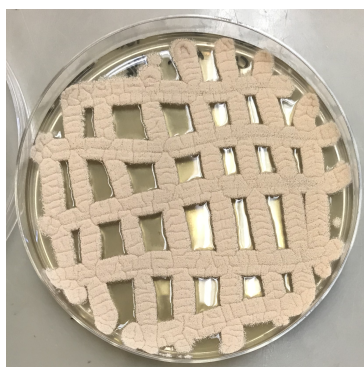


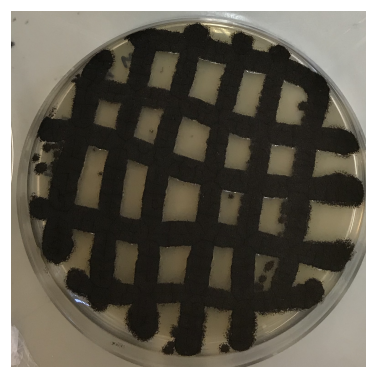
Figure C.4: Picture from an agarose gel where MoClo level 1 plasmids have been digested with restriction enzymes BpiI, XbaI and XhoI, as indicated.

C.4 Spore Phenotypes

Mutant strains carrying promoter-luciferase constructs integrated in the *fwnA* locus were grown on CM plates and spore phenotype was recorded by imaging before the spores were harvested. As a comparison, a transformant colony exhibiting WT phenotype on its spores was similarly prepared. The two images can be seen in Figure C.5.



(a) The mutant strain AA1.



(b) A strain exhibiting WT phenotype.

Figure C.5: A comparison between the spore phenotype resulting from disrupted *fwnA* and WT spore coloring. Spores are grown on CM agar.

C.5 Microtiter Cultivation During Luciferase Assay

After the two-day luciferase assay, the microtiter well inoculations of transformed *A. niger* strains had sporulated. This was recorded by imaging, and can be seen in Figure C.6.

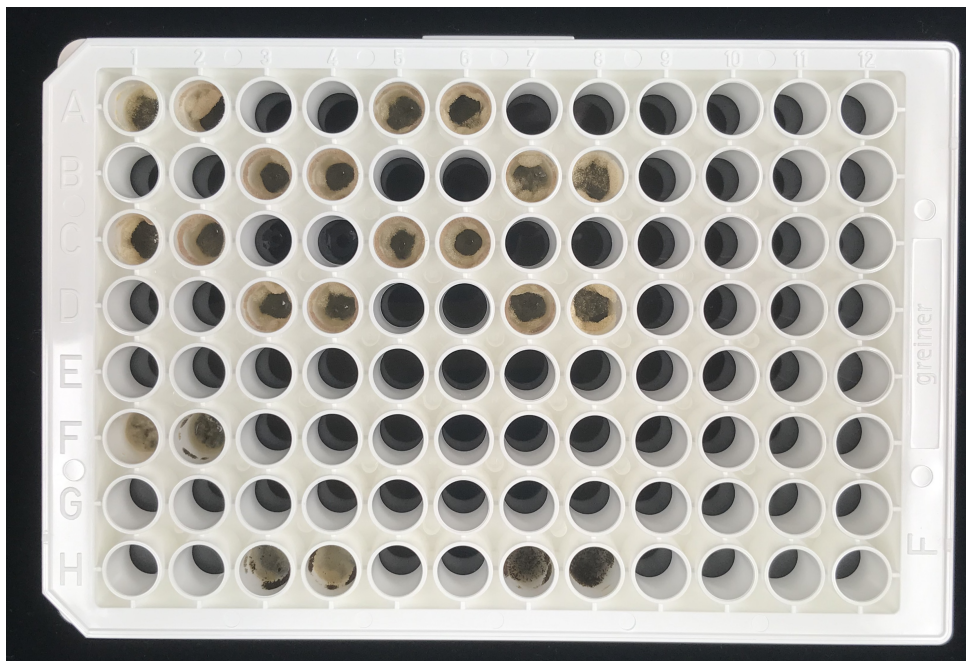
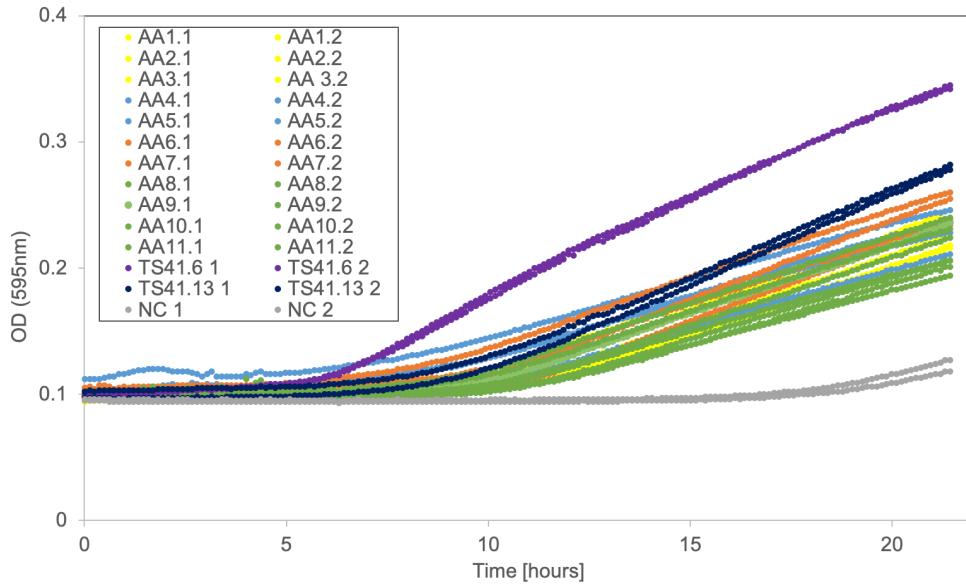


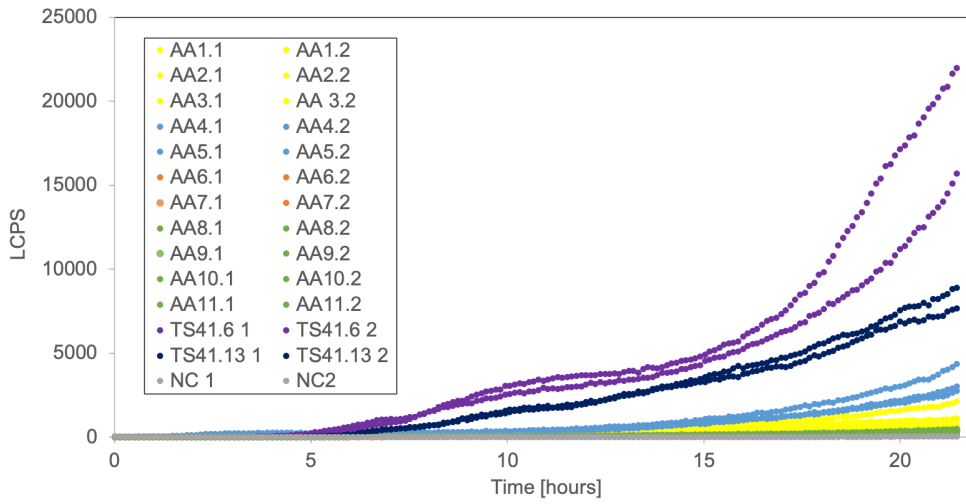
Figure C.6: Photograph of inoculated microtiter well plate after a two-day luciferase assay, showing evidence of fungal sporulation. All inoculated wells in rows A-D were inoculated with white sporulating *A. niger* mutants, whereas the wells in rows F and H contain control strains with WT dark spore coloring.

C.6 Luciferase Assay Raw Data

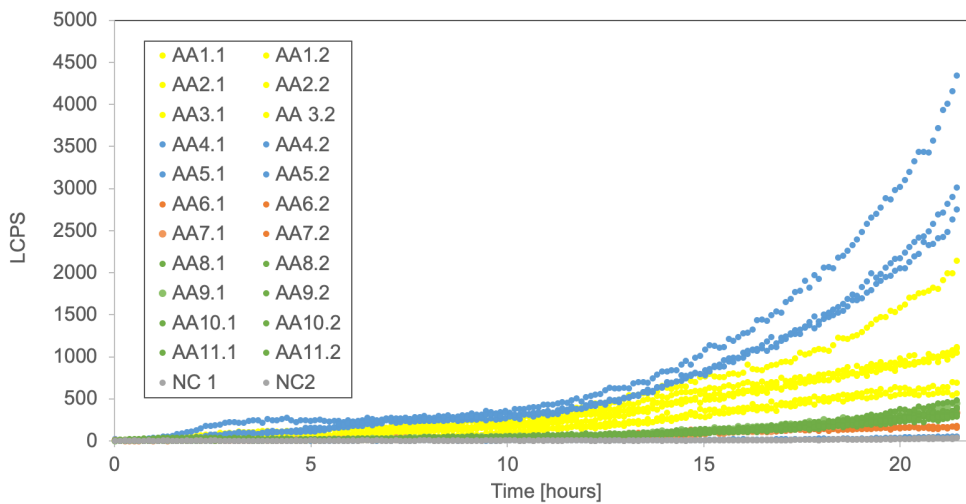
The two luciferase assays' raw data constitutes over 400 measurements of 11-14 duplicate samples, and is too vast to be presented here. Instead, the LCPS and OD graphs for each measured well is presented, before averages were calculated and normalization was done. The colors of the graphs correspond to the colors in Figure 3.6, where yellow is mutants AA1-AA3, blue is mutants AA4-AA5, orange is mutants AA6-AA7, green is mutants AA8-AA11, and the negative control is shown in gray. Figure C.7 shows the raw data of LCPS and OD measurements for the initial luciferase assay that was conducted, and Figure C.8 presents the same data for the second luciferase assay. Graphs of positive control strains are also included, illustrating why these were omitted from other LCPS graphs to better visualize strains of interest.



(a) Optical density measurements.

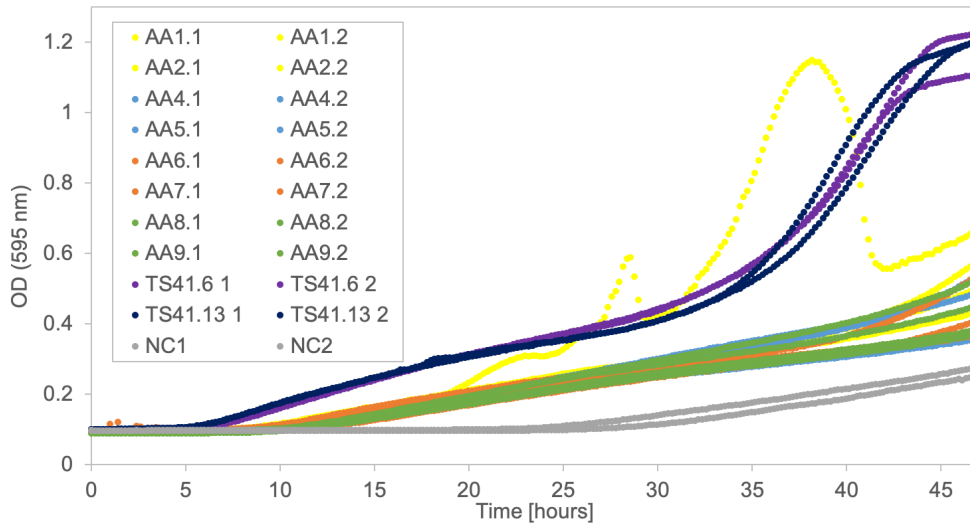


(b) Luminescence measurements including positive controls.

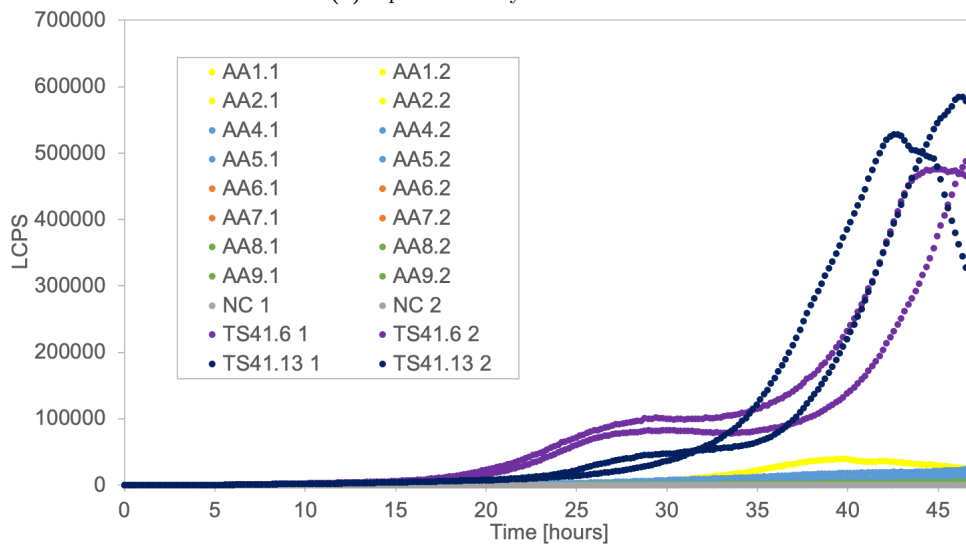


(c) Luminescence measurements excluding positive controls.

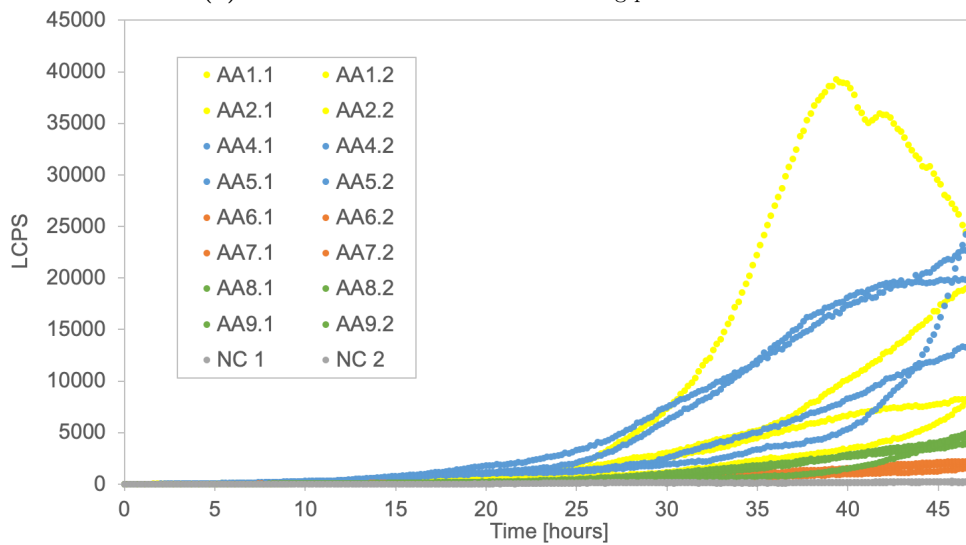
Figure C.7: Raw data of the initial luciferase assay conducted overnight.



(a) Optical density measurements.



(b) Luminescence measurements including positive controls.



(c) Luminescence measurements excluding positive controls.

Figure C.8: Raw data of the luciferase assay over 2 days. The graph with significant outlier tendencies belongs to AA1.2, and was omitted from the calculations of mean.

D Experimental Protocols

D.1 Agarose Gel Electrophoresis

Make an agarose gel solution by dissolving 1.0 % agarose in 0.5x TAE buffer and heating to boiling point, and thereafter adding 5 μL Midori Green Advance (Nippon Genetics catalogue number MG04) per 100 mL gel for DNA staining. Pour the gel in an appropriately sized and completely level gel tray fixed in a casting chamber, with well combs placed in the gel while drying (20-30 minutes). After the gel has solidified, transfer the gel slab with the casting tray to an electrophoresis chamber filled with 0.5x TAE buffer. Mix samples with a loading dye and deposit in the wells. Then, subject the gel to 90 V current until the separation of samples is satisfactory (30-45 minutes). The gel slab can be visualized in a UV chamber.

D.2 Golden Gate Restriction and Ligation

For a 15 μL plasmid assembly reaction by restriction and ligation, combine the following elements, where X should be calculated considering equimolarity of DNA fragments. Temperature cycles are used to optimize for restriction enzymes and ligation enzymes in turn, as shown by the thermocycler input parameters on the right. The steps are 1) initial restriction, 2) restriction, 3) ligation, 4) final restriction, 5) heat inactivation and 6) storage.

$X_1 \mu\text{L}$	Insert 1	}	1) 37 °C for 4 min
$X_2 \mu\text{L}$	Insert 2		2) 37 °C for 5 min
...			3) 16 °C for 5 min
$X_n \mu\text{L}$	Insert n		(Repeat steps 2-3 for 50 cycles)
$X_D \mu\text{L}$	Destination vector		4) 37 °C for 4 min
1.0 μL	T4 ligase		5) 80 °C for 10 min
1.0 μL	Restriction enzyme		6) 12 °C for ∞
1.5 μL	Ligase buffer		
$\rightarrow 15 \mu\text{L}$	MQ-H ₂ O		

(If fast-digest enzymes are available, the protocol can be sped up by lowering the restriction time to 1 min and the ligation time to 2 min, and only completing the cycles 20 times.)

D.3 DNA Polymerase Protocols

D.3.1 KAPA HiFi HotStart Polymerase

For a 15 μL PCR amplification reaction, combine the following volumes, mix well and spin down. Thermocycler input parameters are shown on the right, where the steps are 1) initial denaturation, 2) denaturation, 3) annealing, 4) elongation, 5) final elongation and 6) storage.

7.5 μL	2x KAPA HiFi HotStart ReadyMix	}	1) 95 °C for 5 min
7.5-X μL	MQ-H ₂ O		2) 98 °C for 20 s
0.1 μL	Forward primer (100 μM)		3) 67 °C for 15 s
0.1 μL	Reverse primer (100 μM)		4) 68 °C for 30 s + 30 s/kb
$X \mu\text{L}$	Template DNA: (25 ng plasmid, 90 ng genomic)		(Repeat steps 2-4 for 35 cycles)
			5) 72 °C for 10 min
		6) 12 °C for ∞	

D.3.2 Phire Green HotStart II DNA Polymerase

For colony PCR reactions of 10 μL , multiply the following volumes by the number of desired reactions, combine in a master mix, mix well and distribute to required number of tubes. Template DNA can be added directly from a picked *E. coli* colony. Thermocycler input parameters are shown on the right, where the steps are 1) initial denaturation, 2) denaturation, 3) annealing, 4) elongation, 5) final elongation and 6) storage.

5.0 μL	2x Phire Green HotStart II DNA Polymerase Mix	} 1) 95 °C for 5 min 2) 95 °C for 10 s 3) 57 °C for 10 s 4) 72 °C for 30 s + 20 s/kb (Repeat steps 2-4 for 30 cycles) 5) 72 °C for 10 min 6) 12 °C for ∞
4.8 μL	MQ-H ₂ O	
0.1 μL	Forward primer (100 μM)	
0.1 μL	Reverse primer (100 μM)	
-	Template DNA	

D.3.3 Phire Plant Direct PCR

For colony PCR reactions of 20 μL , multiply the following volumes (except template DNA) by the number of desired reactions, combine in a master mix, mix well and distribute to the number of reaction tubes. Template DNA can be prepared from raw material by dissolving some mycelium in 20 μL DNA dilution buffer and spinning residual biomass down, so that the supernatant can be added to the reaction. Thermocycler input parameters are shown on the right, where the steps are 1) initial denaturation, 2) denaturation, 3) annealing, 4) elongation, 5) final elongation and 6) storage.

10.0 μL	2x Phire Plant PCR Buffer	} 1) 98 °C for 5 min 2) 98 °C for 10 s 3) 62 °C for 10 s 4) 72 °C for 30 s + 30 s/kb (Repeat steps 2-4 for 30 cycles) 5) 72 °C for 10 min 6) 12 °C for ∞
0.4 μL	Phire HotStart II DNA Polymerase	
9.4 μL	MQ-H ₂ O	
0.15 μL	Forward primer (100 μM)	
0.15 μL	Reverse primer (100 μM)	
0.5 μL	Template DNA	

D.3.4 Biozym Blue S'Green qPCR Kit

For qPCR reactions of 10 μL , multiply the following volumes (except template DNA) by the number of desired reactions, combine in a master mix, mix well and distribute to the number of reaction tubes. Template DNA should be genomic DNA extracted from strains of interest, diluted 1:1000. Thermocycler input parameters are shown on the right, where the steps are 1) initial denaturation, 2) denaturation, 3) annealing and extension 4) melt curve analysis and 5) storage.

5.0 μL	2x Blue S'Green qPCR	} 1) 98 °C for 5 min 2) 95 °C for 15 s 3) 60 °C for 20 s (Repeat steps 2-3 for 40 cycles) 4) 55 °C to 95 °C, increasing 0.5 °C per 5 s 5) 12 °C for ∞
2.9 μL	MQ-H ₂ O	
0.05 μL	Forward primer (100 μM)	
0.05 μL	Reverse primer (100 μM)	
2.0 μL	Template DNA	

D.4 Kit Manuals

D.4.1 EZNA High Performance (HP) Fungal DNA Kit

The following protocol is copied directly from the kit manual of Omega Bio-Tek product number D3195-01, found at: <https://www.omegabiotek.com/product/e-z-n-a-hp-fungal-dna-kit/>.

Protocol for Dried Samples

1. Transfer 10-50 mg powdered dried tissue to a 2 mL microcentrifuge tube.
2. Add 600 μ L CSPL Buffer. Vortex to mix thoroughly. If necessary, add 2 μ L RNase A to the lysate before Step 3 (incubation step) to remove the RNA.
3. Incubate at 65 °C for 30 min. Invert the tube twice during incubation to mix the sample.
4. Add 600 μ L chloroform:isoamyl alcohol (24:1). Vortex to mix thoroughly.
5. Centrifuge at $\geq 10,000\times g$ for 10 min.
6. Carefully aspirate 300 μ L aqueous phase (top) to a new 1.5 mL microcentrifuge tube making sure not to disturb the organic phase or transfer any debris.
7. Add 150 μ L CXD Buffer and 300 μ L 100 % ethanol. Vortex to obtain a homogeneous mixture.
8. Insert a HiBind DNA Mini Column into a 2 mL Collection Tube.
9. Transfer the entire sample (including any precipitate that may have formed) to the HiBind DNA Mini Column.
10. Centrifuge at 10,000 $\times g$ for 1 min.
11. Discard the filtrate and the collection tube.
12. Insert the HiBind DNA Mini Column into a new 2 mL Collection Tube.
13. Add 650 μ L DNA Wash Buffer.
14. Centrifuge at 10,000 $\times g$ for 1 min.
15. Discard the filtrate and reuse the collection tube.
16. Repeat Steps 13-15 for a second DNA Wash Buffer wash step.
17. Centrifuge the empty column at maximum speed for 2 min.
18. Transfer the HiBind DNA Mini Column to a clean 1.5 mL microcentrifuge tube.
19. Add 50-100 μ L Elution Buffer or sterile deionized water heated to 65 °C.
20. Centrifuge at maximum speed for 1 min.
21. Repeat Steps 19-20 for a second elution step.
22. Store DNA at -20 °C.

D.4.2 innuPREP DOUBLEpure Kit

The following protocol is copied directly from the kit manual of Analytic Jena product number 845-KS-5050250, found at: https://www.analytik-jena.com/fileadmin/content/products/02_Kits/innuPREP_DOUBLEpure_Kit/Manual_innuPREP_DOUBLEpure_Kit.pdf.

Standard protocol: DNA extraction from agarose gel slices

1. Excise the DNA fragment from the agarose gel with a sharp scalpel.
2. Transfer the gel slice into a 1.5 mL or 2.0 mL reaction tube and add 650 μ L Gel Solubilizer.
3. Incubate for 10 min at 50 °C until the agarose gel slice is completely dissolved.
4. Add 50 μ L Binding Optimizer and mix the suspension by vortexing or pipetting sometimes up and down.
5. Apply the sample onto the Spin Filter located in a 2.0 mL Receiver Tube. Close the cap and centrifuge at 11,000 $\times g$ (~11,000 rpm) for 1 min. Discard the filtrate and re-use the Receiver Tube. Place the Spin Filter back into the 2.0 mL Receiver Tube.
6. Open the Spin Filter and add 700 μ L Washing Solution LS, close the cap and centrifuge at 11,000 $\times g$ (~11,000 rpm) for 1 min. Discard the filtrate and re-use the Receiver Tube. Place the Spin Filter back into the 2.0 mL Receiver Tube.
7. Repeat step 6 completely.
8. Centrifuge at max. speed for 2 min to remove all traces of ethanol. Discard the 2.0 mL Receiver Tube.
9. Place the Spin Filter into a 1.5 mL Elution Tube. Carefully open the cap of the Spin Filter and add 30-50 μ L Elution Buffer (optionally pre-warmed to 50 °C). Incubate at room temperature for 1 min. Centrifuge at 11,000 $\times g$ (~11,000 rpm) for 1 min. A second elution step will increase the yield of extracted DNA.

Standard protocol: Purification and concentration of PCR products from reactions up to 50 μ L

A: Binding of the PCR fragments

1. Add 500 μ L Binding Buffer to the Spin Filter.
2. Add up to 50 μ L of your PCR reaction mixture to the Spin Filter which is already pre-filled with the Binding Buffer.
3. Mix Binding Buffer and PCR reaction mixture by pipetting three times up and down. Don't destroy the filter membrane! Alternatively, mix 500 μ L Binding Buffer with up to 50 μ L of the PCR reaction mixture very well by pipetting or vortexing outside the Spin Filter in a separate reaction tube. After this, transfer the mixed sample completely onto the Spin Filter.
4. Centrifuge for 3 min at 11,000 \times g (\sim 11,000 rpm). Discard the Receiver Tube.

B: Elution of the PCR fragments

1. Place the Spin Filter into an Elution Tube.
2. Pipette at least 20-50 μ L Elution Buffer or RNase-free water directly onto the center of the Spin Filter.
3. Incubate for 1 minute at room temperature.
4. Centrifuge for 1 minute at 11,000 \times g (\sim 11,000 rpm). The Elution Tube now contains the purified PCR fragments.

D.4.3 innuPREP Plasmid Mini Kit

This protocol is copied directly from the manual of Analytik Jena product number 845-KS-5040250, found at https://www.analytik-jena.com/fileadmin/content/products/02_Kits/innuPREP_Plasmid_Mini_Kit_2_0/Manual_innuPREP_Plasmid_Mini_Kit_2.0.pdf

Protocol 1: Isolation of plasmid DNA from 0.5-5 mL bacterial culture

1. Transfer 0.5 mL up to 5 mL of the overnight E. coli culture into a 1.5 mL, 2.0 mL or 15 mL reaction tube. Centrifuge for 1 min at maximum speed to pellet the bacteria; remove the supernatant as completely as possible.
2. Resuspend the bacterial cell pellet in 250 μ L Resuspension Buffer completely by vortexing or by pipetting up and down.
3. Add 250 μ L Lysis Buffer, close the tube and mix carefully by inverting the tube 6–8 times. Do not perform the lysis step longer than 5 min.
4. Add 350 μ L Neutralization Buffer and mix gently, but thoroughly by inverting the tube 6–8 times. Centrifuge for 8 min at full speed (12,000–14,000 rpm). During centrifugation place the needed amounts of Spin Filters into 2.0 mL Receiver Tubes.
5. Apply the clarified supernatant onto the Spin Filter located in a 2.0 mL Receiver Tube. Centrifuge at 11,000 \times g (\sim 11,000 rpm) for 1 min. Discard the filtrate and re-use the 2.0 mL Receiver Tube. Place the Spin Filter back into the 2.0 mL Receiver Tube.
6. Add 500 μ L Washing Solution A to the Spin Filter and centrifuge at 11,000 \times g (\sim 11,000 rpm) for 1 min. Discard the filtrate and re-use the 2.0 mL Receiver Tube. Place the Spin Filter back into the 2.0 mL Receiver Tube.
7. Add 700 μ L Washing Solution B to the Spin Filter and centrifuge at 11,000 \times g (\sim 11,000 rpm) for 1 min.
8. Discard the filtrate after the washing step and re-use the 2.0 mL Receiver Tube. Place the Spin Filter back into the 2.0 mL Receiver Tube. Centrifuge at full speed (12,000–14,000 rpm) for for 2 min to remove all traces of ethanol. Discard the 2.0 mL Receiver Tube.
9. Place the Spin Filter into a 1.5 mL reaction tube (not provided) and add 50–100 μ L Elution Buffer P onto the center of the Spin Filter. Incubate at room temperature for 1 min. Centrifuge at 11,000 \times g (\sim 11,000 rpm) for 1 min. Dividing the final elution volume in two equal volumes of Elution Buffer P increases the final concentration of pDNA in the first elution step, but not the yield of eluted pDNA.

D.4.4 PureYield Plasmid Midiprep System

The following is copied directly from the quick protocol of Promega product number A2496, for bacterial cell cultures of 50-100 mL.

Prepare Lysate

1. Pellet cells at 5,000×g for 10 min.
2. Suspend pellet in 3 mL Cell Resuspension Solution.
3. Add 3 mL Cell Lysis Solution. Invert 3-5 times to mix. Incubate 3 min at room temperature.
4. Add 5 mL Neutralization Solution. Invert 5-10 times to mix.
5. Centrifuge lysate at 15,000×g for 15 min at room temperature.

DNA Purification

6. Assemble a column stack by placing a blue PureYield™ Clearing Column on top of a white PureYield™ Binding Column. Place the column stack onto a vacuum manifold.
7. Carefully pour supernatant into column stack. Apply vacuum, continuing until all liquid has passed through both the clearing and binding columns.
8. Slowly release the vacuum from the filtration device. Remove the blue clearing column, leaving the binding column on the manifold.
9. Add 5 mL of Endotoxin Removal Wash to the binding column, and allow the vacuum to pull the solution through the binding column.
10. Add 20 mL of Column Wash Solution to the binding column, and allow the vacuum to pull the solution through the binding column.
11. Dry the membrane by applying a vacuum for 30-60 s. Repeat if the tops of the DNA binding membranes appear wet or there is detectable ethanol odor.
12. Remove the binding column from the vacuum manifold, and tap it on a paper towel to remove excess ethanol.

Elute by vacuum

13. Place a 1.5 mL microcentrifuge tube into the base of the Eluator™ Vacuum Elution Device (Cat. number A1071), securing the tube cap.
14. Assemble the Eluator™ Vacuum Elution Device, and insert the DNA binding column into the device, making sure that the column is fully seated on the collar.
15. Place the elution device assembly, including the binding column, onto a vacuum manifold.
16. Add 400-600 µL of Nuclease-Free Water to the DNA binding membrane in the binding column. Wait for 1 min. Apply maximum vacuum for 1 min or until all liquid has passed through the column.
17. Remove the microcentrifuge tube and save for DNA quantitation and gel analysis.

E Buffers and Media

E.1 Buffers

Tables E.1, E.2, E.3 and E.4 show the compositions of buffers used in this project.

Table E.1: $1\times$ TAE buffer.

Component	Conc.
Tris base	40 mM
Acetate	20 mM
EDTA	1 mM

Table E.2: (S)TC buffer.

Component	Conc.
Tris	10 mM
CaCl ₂	50 mM
(Sorbitol)	1.33 M

Table E.3: SMC buffer.

Component	Conc.
Sorbitol	1.33 M
CaCl ₂	50 mM
MES buffer (pH 5.8)	20 mM

Table E.4: DNA extraction buffer.

Component	Conc.
SDS	0.5 %
Tris HCl (pH 8.0)	0.2 M
EDTA (pH 8.0)	0.025 M

E.2 LB: Lysogeny Broth

Table E.5 shows the composition of lysogeny/Lennox broth medium (LB). For solid plate medium, agar was added.

Table E.5: LB medium, supplied by Sigma-Aldrich.

Component	Conc. [g L ⁻¹]
Tryptone	10
Yeast extract	5
NaCl	5

E.3 SOC: Super-Optimal Broth with Catabolite Repression

Super-optimal broth (SOB) is commonly used for plasmid transformations, and SOC is a derivative of this medium with added glucose for catabolite repression. Its composition is shown in Table E.6.

Table E.6: SOC medium.

Component	Conc. [g L ⁻¹]
Tryptone	20.0
Yeast extract	5.0
NaCl	0.50
KCl	0.186
MgSO ₄ · 7H ₂ O	2.47
Glucose	3.60

E.4 Stock Solutions for *A. niger* Media

Media used for *A. niger* are created from a set of defined stock solutions. The components of these are presented in Tables E.7 and E.8.

Table E.7: Asp+N solution (50x).

Component	Conc. [M]
KH ₂ PO ₄	0.55
KCl	0.35
NaNO ₃	3.5
5 M KOH	(until pH 5.5)

Table E.8: Vishniac trace element solution (1000x).

Component	Conc. [g L ⁻¹]
EDTA	10.0
ZnSO ₄ ·7H ₂ O	4.4
MnCl ₂ ·4H ₂ O	1.01
CoCl ₂ ·6H ₂ O	0.32
CuSO ₄ ·5H ₂ O	0.31
(NH ₄) ₆ Mo ₇ O ₂₄ ·4H ₂ O	0.22
CaCl ₂ ·2H ₂ O	1.47
FeSO ₄ ·7H ₂ O	1.0
1 M HCl	(until pH 4.0)

E.5 MM: Minimal Medium

Minimal medium's composition is shown in Table E.9.

Table E.9: Minimal medium.

Component	Stock Conc.	Final Conc.
Asp+N	50x	1x
Glucose	50 % (w/v)	1 % (v/v)
MgSO ₄	1 M	2 mM
Vishniac solution	1000x	1x

E.6 CM: Complete Medium

Complete medium's composition is shown in Table E.10.

Table E.10: Complete medium.

Component	Stock Conc.	Final Conc.
Asp+N	50x	1x
Glucose	50 % (w/v)	1 % (v/v)
MgSO ₄	1 M	2 mM
Vishniac solution	1000x	1x
Casamino acids	10 %	0.1 %
Yeast extract	10 %	0.5 %

E.7 TM: Transformation Medium

Transformation medium's composition is shown in Table E.11.

Table E.11: Medium for making transformation plates.

Component	Stock Conc.	Final Conc.
Sucrose	50 % (w/v)	1 % (v/v)
Asp+N	50x	1x
Vishniac solution	1000x	1x
MgSO ₄	1 M	2 mM

